Assessing the effects of dike protection systems on rice cropping patterns and water quality in An Giang province, Vietnam

2019.9

Graduate School of Environmental Science

Hokkaido University

Huynh Vuong Thu Minh

(フイン・ヴォーントゥミン)

Assessing the effects of dike protection systems on rice cropping patterns and water quality in An Giang province, Vietnam

by

Huynh Vuong Thu Minh

A dissertation submitted in partial fulfilment

of the requirement for the degree of

DOCTOR OF PHILOSOPHY

in

Graduate School of Environmental Science

of the

Hokkaido University

2019

Assessing the effects of dike protection systems on rice cropping patterns and water quality in An Giang province, Vietnam

by

Huynh Vuong Thu Minh

B.S. degree in Civil Engineering, Can Tho University, Vietnam

M.E. degree in Water Engineering and Management, AIT, Thailand

APPROVED BY SUPERVISORY COMMITTEE:

Chairperson: Professor Masaaki KURASAKI

Co-Supervisor: Professor Ram AVTAR

Member: Professor Mitsuru OSAKI

Member: Professor Tatsufumi OKINO

Member: Professor Teiji WATANABE

Sapporo - 2019

Abstract

The Vietnamese Mekong Delta (VMD) is one of the largest rice-growing areas in Vietnam, and exports a huge amount of rice products to destinations around the world. Rice is grown under the irrigated triple and double-rice cropping systems, and also under the rain-fed single-rice cropping system in the Vietnamese Mekong Delta (VMD). These rice cropping systems are adopted according to the geographical location and water infrastructure in place. Dike-protection systems have been built to prevent flooding in order to support agricultural intensification since the early 1990s. Thus, double and triple-rice cropping systems have been dependent on the semi- and full-dike systems. However, only a small number of studies have been conducted to evaluate the effects of rice cropping system on water quality in the context of dike development. This study aimed to value the impact of dike system on spatio-temporal variation of surface and ground water quality. We used multivariate statistical analyses and groundwater quality index based on Fuzzy-AHP with the Triangular Fuzzy Number method. The LULC was generated using Support Vector Machine (SVM) classification of Sentinel-1A data. We conducted fieldwork in An Giang province of the VMD, from March 2017 to March 2018. The overall accuracy of the classification was 80.7% with 0.78 Kappa coefficient. Therefore, Sentinel-1A can be used to understand rice phenological changes as well as rice cropping system distribution using radar backscattering. The assessment of surface water quality results show the mean concentrations of COD, NH_4^+, NO_3^-, PO_4^{3-}, EC, and turbidity in surface water inside full-dike as compared to outside full-dike and inside semi-dike in both seasons. Moreover,

surface water located in secondary canal inside full-dike system was considered as “hotspot” surface water quality with low GQWI unit. Besides, the high concentrations of PO_4^{3-} were detected in most of the primary canals where residential areas and local markets settled leading to increase PO_4^{3-} concentration; However, NO_3^- was mainly found to be higher in secondary canals where chemical fertilizers used for rice intensification inside dike-system were increased. The effect of dike system on groundwater quality was not very clear in this study since groundwater quality depends on characteristics of aquifers and unused well management. Dike infrastructures are useful for preventing flooding; however, changes in cropping system have resulted which adversely affect maintenance and surface water quality and challenging task for the protection of groundwater quality in the long-term in the study area.

Keywords: Water quality parameters, multivariate analysis, rice phenology; water infrastructure; rice cropping pattern mapping; SAR backscattering

Acknowledgments

I would like to express my deep sincere gratitude to my advisor, Professor Masaaki KURASAKI of the Graduate school of Environmental Science - Hokkaido University, for the never-ending kind support he provided for my Ph.D study. His patience, altruism, and immense knowledge have enabled me to overcome the entire problem during the last three years. I owe a deep sense of gratitude to my co-advisor, Professor Ram AVTAR, Faculty of Environmental Earth Science - Hokkaido University, for his sincere guidance. His insightful comments, encouragement, the timely suggestion with dynamics have enabled me to become confident in widening research from various perspectives.

I am deeply grateful to Professor Shunitz TANAKA for his kind guidance in the laboratory. I also express my sincere thanks to Professor Mitsuru OSAKI for introducing me to Professor Masaaki KURASAKI's laboratory, thus providing me a valuable opportunity to conduct my research at Hokkaido University.

I thank profusely the Vietnamese Ministry of Education and Training (MOET), Japan International Cooperation Center (JICE), Can Tho University, and Hokkaido University for providing both the Ph.D. scholarship and supporting equipment to complete this research.

I am deeply thankful to my family, colleagues, and friends I have met for their love.

Table of contents

List of Figures

List of Tables

Chapter 1. General Introduction

1.1 Back ground

The Mekong Delta in Vietnam is known as the largest agriculture producer which is one of the largest exporters of rice in the world. Most rice production in Vietnam takes place in the Vietnamese Mekong Delta (VMD), feeds a population of nearly 95 million, and provides food security in Southeast Asia [1–3]. Agricultural intensification has been applied for nearly 40 years to adapt to the food security situation and for economic development in Vietnam. Rice is grown under irrigated and non-irrigated systems in which triple and double-rice crops come under dike-system protection, while rain-fed single rice is a traditional rice cropping system often found outside the dike system.

Mekong Delta was vulnerable to water regime changes and seawater intrusion [4,5]. In the past, flooding was a common phenomenon in the upper Vietnamese Mekong Delta (VMD) where 22 flood events with high frequency occurred during 1926-2006 [6], in which about 65% of the high floods occurred from August to October [7]. At that time, the single-rice crop such as floating rice and landrace rice was dominant. However, its rice production could not ensure food-security for the whole country and for economic development. Besides, the rice cropping system heavily depended on geographical location, freshwater availability, and sediment supplied from the Bassac and Mekong Rivers [3]. Moreover, in 1986, the Renovation policies[1] were issued by the Vietnamese government resulting in the VMD becoming one of the largest rice exporting regions in the world since the 2010s [8–12] and in Vietnam becoming the second-

[1] A set of economic reforms aim at moving the Vietnamese economy towards the socialist-oriented market economy, and transitioning to a more industrial and market-based economy.

largest rice exporting country in the world in 2012 [13]. To this end, the Vietnamese government and local communities in the flood-prone areas of the VMD also decided to construct hydraulic infrastructure to support rice intensification and cope with the natural disasters. Vietnam expanded dike and irrigation systems to control annual short-term flooding [14–16]. The rapid intensification of agriculture mainly in irrigated areas has been explained by the renovation policy, which turned the delta into a rice bowl of Vietnam by the mid-1990s [9,11,17,18].

The dike-protection systems have been built to prevent flooding and to support agricultural intensification since the early 1990s. Thus, double and triple-rice cropping systems have appeared due to the semi and full-dike systems. The development of sluice-gate and canal systems together to manage water irrigation by water infrastructure turn the Mekong Delta in Vietnam under hydraulics landscape. A prominent area in the VMD with a long inundation period exists and sufficient impact of farming and renovation policy in An Giang province.

Typically, rice irrigation often takes place within a rectangular dike-protection system [19–21]. An Giang province has been well-known for having the largest dike system area in the VMD since 1996 [22]. The traditional-rice crop has been replaced by a double-rice crop. Since 2009, the double-rice crop has gradually been replaced by the triple-rice crop to increase rice production for food security and economic development [23]. However, the impact of rice intensification on the triple-rice crop has increased heavily on soil and water quality in the last 10 years [24–26]. Thus, An Giang government has recommended adopting the three-three-two cropping cycle to restore soil quality in recent years. Adequate

research on water quality at canals near the rice fields in An Giang is still lacking. There are signs that declining water quality and water regimes are threatening the sustainability of the agriculture system. Surface water quality in An Giang province in Vietnam is based on the hydrological regime and existing pollution sources. Moreover, it also varies between different rivers and canals. Besides the changes in land cover/land use, there are also changes in dams and hydraulic infrastructure protecting from flooding that are causing the water regime [27].

Along with rapid population growth in Vietnam, there is an increasing dependency on groundwater for various activities. Besides the source of rainwater, groundwater is an important source of water to supply mainly for rural and mountainous areas mainly allocation along main rivers. The exploitation of groundwater is 45.93% potential groundwater resources in 2013. Although surface water provides 97% and 98% for domestic supply and irrigation while groundwater resources provides 3% and 2% for domestic usage and irrigation [28]. However, the groundwater in An Giang is not a high amount of resources but infected with arsenic especially. The clear understanding of groundwater quality pattern can help policymakers to protect and effectively manage limited water resource for the long-term.

1.2 Study area

An Giang, a province located in the Mekong Delta in Vietnam (Figure 1.1) where the water source is mainly taken from the Mekong and Bassac River. The VMD is belongs to the Lower Mekong river basin, where the wet season occurs from May to November, and the dry season occurs from December to April. April and May are usually hotter months, while December and January are

cooler (Figure 1.2). The mean annual rainfall is about 1,400 mm accounting for 90% of the total annual rainfall. Water is mostly transported from the upstream of the Mekong river, whereas rainfall runoff in An Giang has minimal effect on river flow [28]. However, the two main rivers of the Mekong River system, i.e., the Mekong and Bassac rivers, along with 280 primary rivers and dense main canals are responsible for flood flow released in An Giang. And now An Giang is facing water pollution due to agricultural activities mainly.

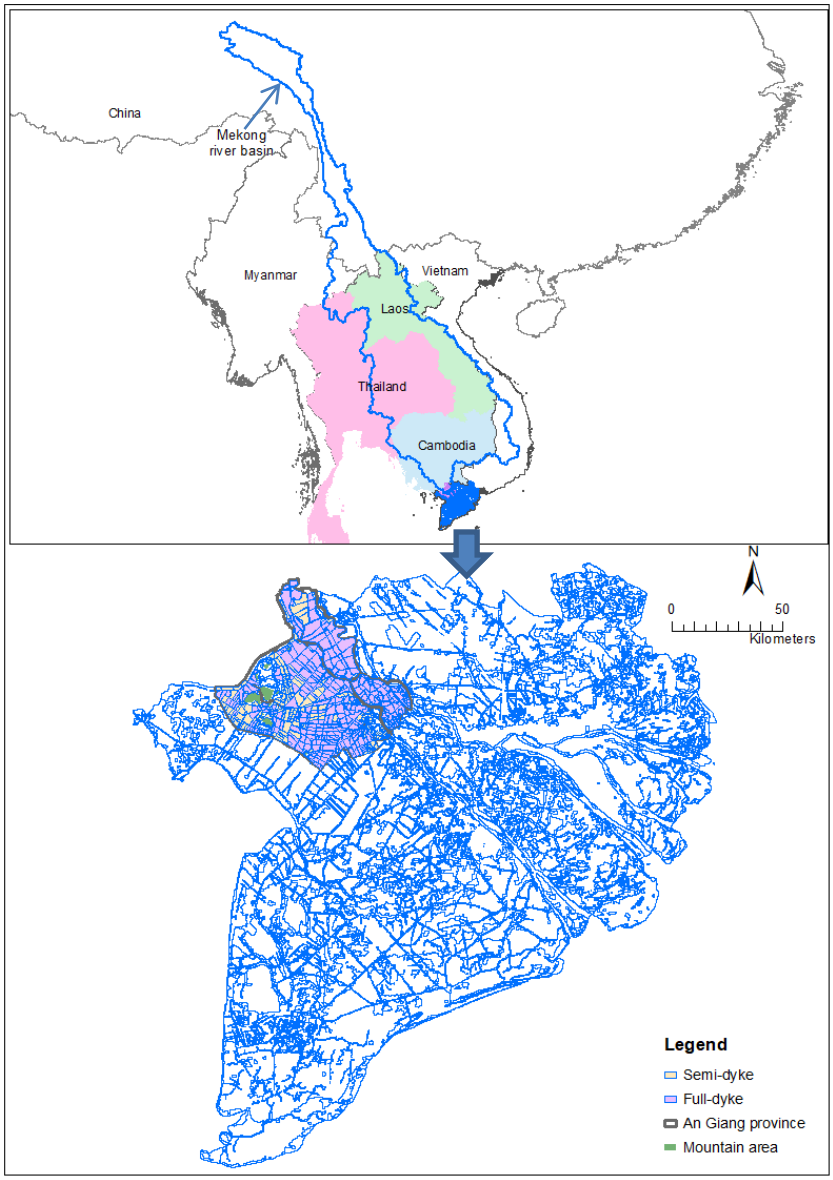

Figure 1.1 Location of the Mekong River Basin and the Mekong Delta in Viet Nam

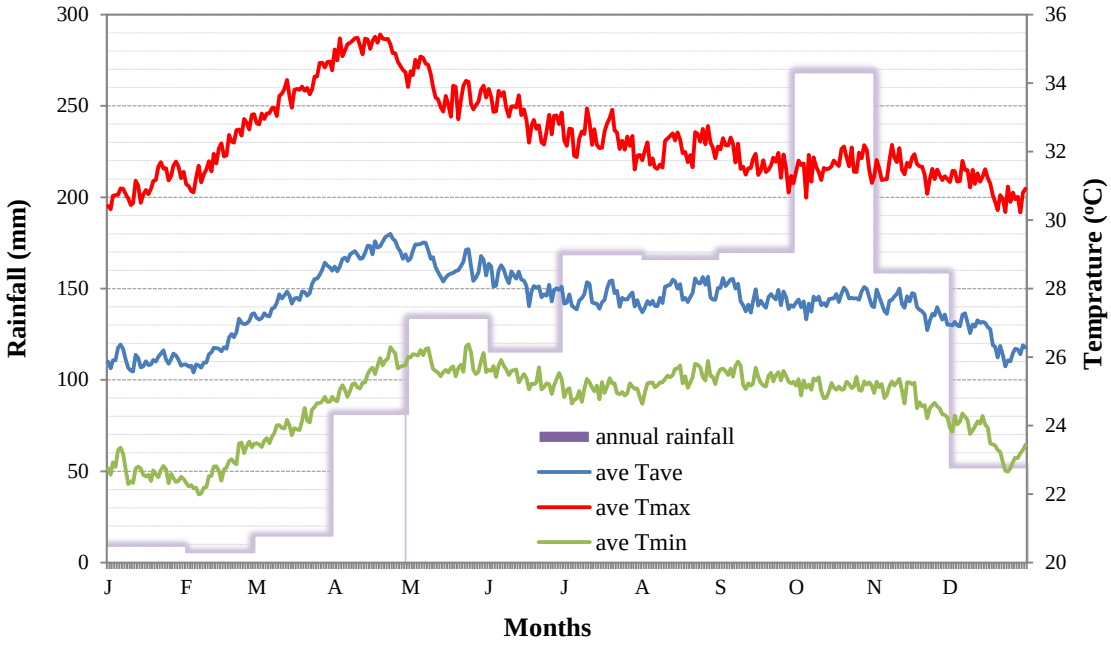

Figure 1.2 Average monthly rainfall, daily mean temperature (Tave), daily maximum temperature (Tmax), and daily minimum temperature (Tmin) during the period 1978-2016, collected from Southern Regional Hydro-meteorology Center in Vietnam.

1.3 Objectives

- To understand the behaviors of crop phenology based on the radar backscattering of Sentinel-1A data;

- To assess rice cropping system distribution under dike development in An Giang province;

- To evaluate the changes in surface and ground water quality inside and outside dike system links the changes to LULC.

Chapter 2. Monitoring and mapping Rice Cropping Pattern in An Giang Province Using Sentinel-1 Data under the Water Infrastructure

2.1 Introduction

Rice (*Oryza. sativa* L.) is one of the major crops and the primary daily grain consumption in Asia countries [29–31]. The increasing population in this region leads to an increased demand for rice production [31,32]. Previous studies revealed that rice demand is rising by about 1.8% per year [31,33]. It is challenging to increase rice production with limited land and water resources [33,34], specifically, under the extreme floods and weather driven by climate change [35–38]. Mekong Delta was vulnerable to water regime changes and seawater intrusion [4,5]. Most rice production in Vietnam takes place in the Vietnamese Mekong Delta (VMD), and feeds a population of nearly 95 million and provides food security in Southeast Asia [1–3]. Rice is grown under the irrigated triple and double-rice cropping systems, and rain-fed single rice, a traditional rice cropping system. In the VMD, these rice cropping systems have adopted according to the geographical location and water infrastructure [39]. Typically, irrigated rice often takes place within a rectangular dike-protection system [19–21]. The rapid intensification of agriculture mainly in irrigated areas has been explained by the renovation policy, which turned the delta into a rice bowl of Vietnam by the mid-1990s [9,11,17,18]. Since then, Vietnam has increased rice production continually and became the second-largest rice exporting country in the world in 2012 [13]. Vietnam expanded dike and irrigation systems to control annual short-term flooding [14–16]. An Giang province has been well known as having the largest dike system area in the VMD since 1996 [22]. The

traditional-rice crop has been replaced by a double-rice crop. Since 2009, the double-rice crop has gradually been replaced by the triple-rice crop to increase rice production for food security and economic development [23].

Understanding the dynamics of the rice crop is critical for stabilizing and sustaining rice production. Location and phenological stages of rice crops are utility for policymakers to protect crops and minimize productivity loss. The strategy for sustainable cropping systems is key for long-term development in the region. For example, An Giang has been facing dike-break several times. In October 2011, about 4,000 hectares of rice were lost in Chau Phu district and Chau Doc city. On August 29, 2018, dike-break resulted in submerging of 700 hectares of ready-for-harvest rice in Tri Ton district. Also, rice prices have recently declined due to sustained oversupply of rice. Typically, the local farmers have been gradually shifting from rice to non-rice crops based on market prices. Therefore, systematic rice crop mapping and monitoring in the VMD could play an essential role in economic planning. Remote sensing data might provide a quick, high-quality, consistent, and timely information about spatial and temporal changes in the rice cropping area in different seasons on regional and global scales [40–42].

Previous studies have used optical imageries such as Moderate Resolution Imaging Spectroradiometer (MODIS) and Landsat to monitor rice paddy growth [23,43–46]. However, it is difficult to achieve high accuracy due to moderate spatial resolution of images produced by MODIS and Landsat satellites. The low resolution leads to the inability to detect small rice fields [23,43]. The optical sensors have a high temporal resolution but, as passive sensors, they are frequently contaminated by clouds in the monsoon region [23,44,47]. Besides,

crop distribution has been mapped by just using time series of vegetation and water indices (e.g., normalized difference vegetation index, enhanced vegetation index and normalized difference water index) [43,48,49]. Thus, these studies showed relatively high errors in detection of rice patterns because the flood patterns disturbed the rice detection and led to confusion with other vegetation types. Advancements in the Synthetic Aperture Radar (SAR) (Figure 2.1) system have increased the ability to penetrate clouds and create own energy, leading to its radar signal being independent of the illumination condition. Moreover, SAR antenna can record elapsed time, receive energy of return pulse, and provides high-resolution. Thus, SAR is a better choice for timely mapping of crops, plantation, water bodies, and flooding by specific backscattering properties [33,41,42,50].

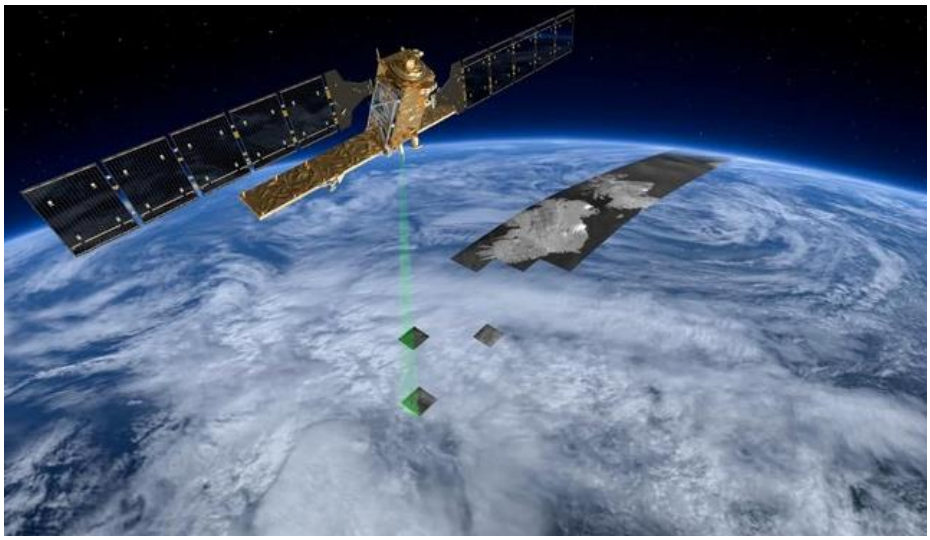

Figure 2.1 Sentinel-1 Radar modes (source: European space agency website https://www.esa.int/ESA)

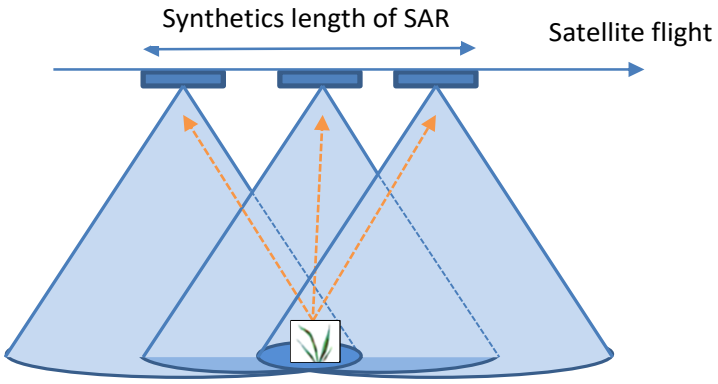

Figure 2.2 Synthetics Aperture Radar (SAR)

Recently, SAR data was utilized to map the rice crop [51,52]. Choudhury et al. [52] revealed the potential of RADARSAT-1 data for rice monitoring since RADARSAT-1 carries a SAR sensor. Its radar signal is independent of solar illumination and cloud condition producing high-quality satellite images (Figure 2.2). Nelson et al. [53] used a TerraSAR-X band to detect the rice map in Southern Asia, and achieved a relative accuracy of 85%. However, the shorter wavelength microwave radiation of X-band detects only the canopy. Also, the longer wavelength microwave radiation of L-band can penetrate targets like leaves and canopy and only return energy from the stem of the plant. Thus, the use of only X-band or L-band is hard to separate plant and other objects [54,55]. Also, studies found that the C-band was able to distinguish rice from non-rice, particularly in Japan, China, India, and Vietnam [50,56–60]. The SAR data availability has increased with the launch of Sentinel-1A C-band SAR on April 3, 2014, under the European Commission's Copernicus program [61,62]. Continuous, near-real-time land monitoring, providing dual-polarized, i.e., Vertical-Vertical (VV) and Vertical-Horizontal (VH) SAR images are contributed by Sentinel-1A. Depending on the geographic location revisit cycles are up to 6 days due to the Sentinel-1B. Even though Sentinel-1A has a moderate time series (12 days revisit cycle), it is still suitable for monitoring rice stages and the seasonal calendar. Each rice stage

takes at least 30 days, and sowing time also varies at least a month in the VMD. Sentinel-1A with single SAR C-band at a high spatial resolution (10 m pixel) is sensitive to water and crop geometry [50,61]. Thus, Sentinel-1A is particularly valuable for monitoring rice cropping patterns and can improve rice mapping accuracy.

In Vietnam, Sentinel-1 data has been successfully applied in various fields such as estimation of rice production and area, aquaculture production, and rice cropping pattern based on Earth observation. Clauss, K. et al. [63] has conducted the estimation of rice production and rice area in Viet Nam for the whole the Me Kong Delta in 2015 and revealed that Sentinel-1 could be used for estimation of rice production and area at regional and global scales. Ottinger, M. [64] has observed aquaculture ponds by using more than 500 Sentinel-1 scenes and the object-based analysis method, and has revealed that Sentinel-1 SAR with high spatial resolution can be used for monitoring aquaculture ponds in some regions such as Viet Nam and China. The author showed that this approach has great potential for global production projections. Interesting, Arai et al. [65] predicted methane emissions based on remote sensing data and found that PALSAR-2 could distinguish inundation-rice fields and non-inundation rice fields in Viet Nam. Also, studies of Bouvet et al. [40], Nguyen et al. [50], and Phan et al. [54] used SAR sensor from COSMO-SkyMed X-band, Sentinel-1A, and ENVISAT/ASAR satellite images, respectively, for monitoring rice in the VMD and An Giang. However, those studies were focused on specific seasons such as: Nguyen [50] paid attention to winter-spring season in 2017 and Phan et al. [54] concentrated on summer-autumn in 2018. Also, Bouvet et al. [40] focused on main seasons (winter-spring and autumn-winter). Little work has been done on analyzing the temporal pattern of three rice cropping patterns using the response

of the radar signal of Sentinel-1A. The study aimed to understand the behaviors of crop phenology based on the radar backscattering of Sentinel-1A data at different rice growth stages and at different rice cropping system. Also, we assessed the rice cropping system distribution under water infrastructure in this study. To address this, we analyzed temporal variation in backscattering and rice growth with dual-polarization and classified the rice extents at three cropping patterns by using Sentinel-1A data. The three cropping patterns throughout the entire rice growth stages by time-series backscatter data of VV and VH polarizations were considered. This study concentrated on rice mapping and monitoring in An Giang from March 2017 to March 2018.

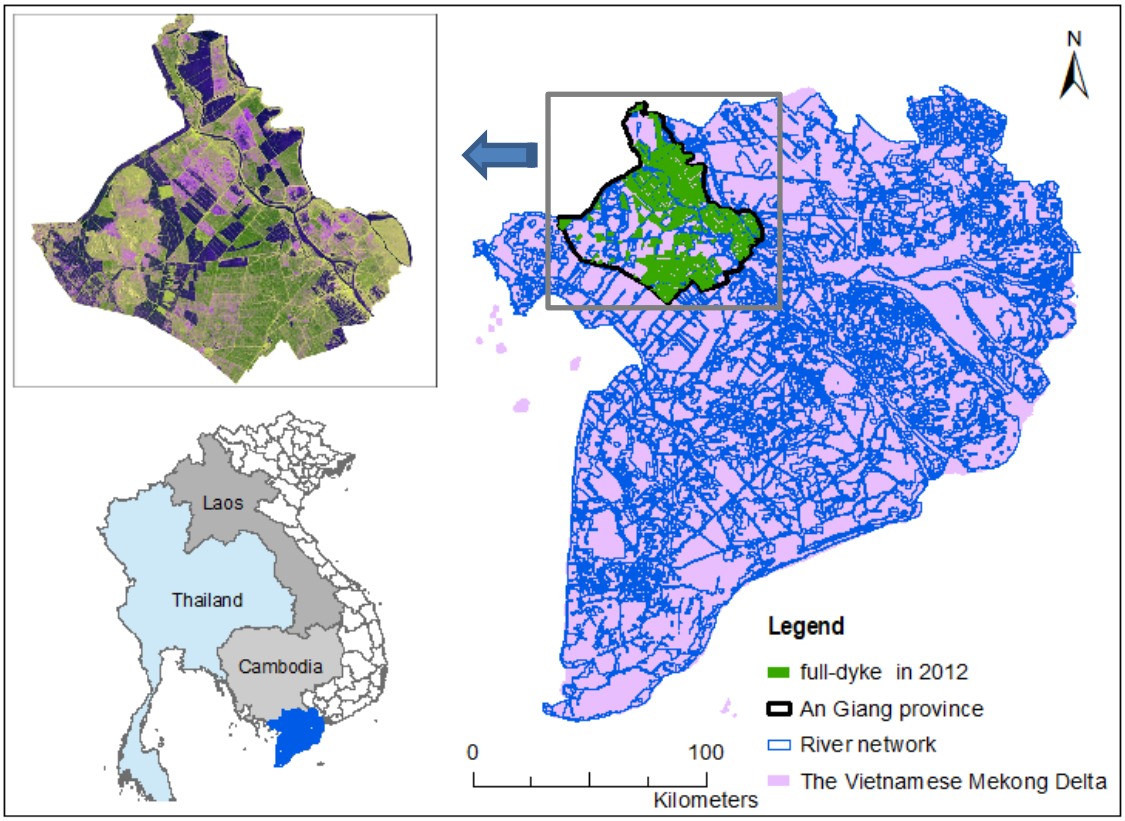

Figure 2.3 Location of An Giang province in the Vietnamese Mekong Delta. The display of An Giang province in composite image R:G:B by bands (VV:VH:VV/VH) (date: 2017.10.15).

2.2 Materials and Methods

2.2.1 Study area

The study site is located in An Giang province which belongs to the upstream of the Lower Mekong river basin in Vietnam (Figure 2.3). Flooding is a common phenomenon in this area, and has been controlled by hydraulic infrastructures. Also, farmers construct minor-canals and dikes to manage water for their small rice fields [6]. Most rice production produced by An Giang which accounts for about 80% of the total rice production in the VMD. The rice production depends heavily on the freshwater availability and sediment supplied from the Bassac and Mekong Rivers [3]. An Giang has an area of 3,406 km^2 and borders with Cambodia in the Northwest. The province falls within tropical climate and within dry and monsoon seasons annually with the average temperature at 27.6^oC, maximum temperature at 32.4^oC, and minimum temperature at 24.6^oC. For the last 40 years, the annual mean rainfall is about 1,400mm, in which the highest rainfall occurs in October (270mm). Around 90% of the rainfall occurred during the monsoon season, between May and October. An Giang receives slightly lower average annual rainfall compared to the VMD in 2,000mm per year because the province is located in the inland delta with minimal effect of the southwest monsoon.

The flooding season often starts a month after the start of the rainy season and ends at the same time as rainy season (Figure 2.4). Daily average discharge shows a decrease in the discharge pattern from 2000 to 2014 due to partial effect of the hydropower plants in the upstream of the Mekong river basin. The partial impact of the hydropower plants on changing the natural flow regimes of the

Mekong River in the VMD has been noticed before [66]. Also, the peaks of discharge move slightly from September to October and have been decreasing.

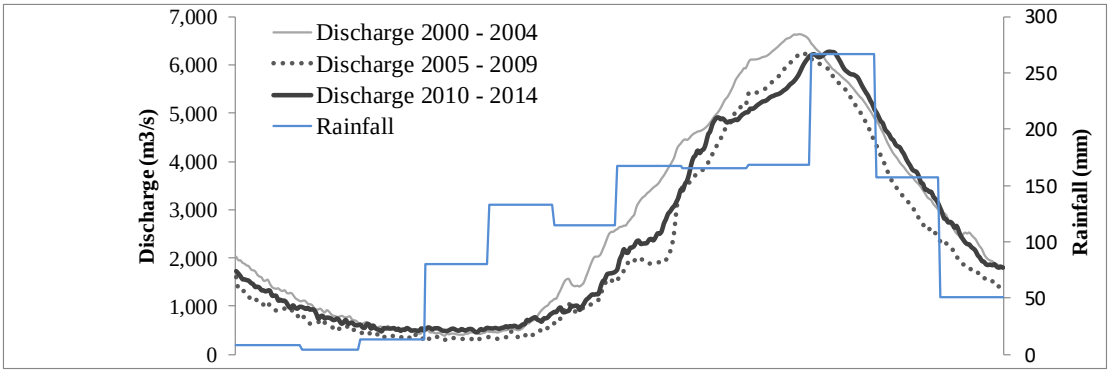

Month	1	2	3	4	5	6	7	8	9	10	11	12
Crop pattern/season	winter-spring			summer-autumn				autumn-winter				
Triple-rice crop												
Double-rice crop												
Single-rice crop												
Traditional-rice crop												

Rice
Vegetable

Figure 2.4 Average monthly discharge at Chau Doc station in Bassac River, during 2000-2014, and average monthly rainfall, and crop calendar. Discharge and rainfall data were obtained from Southern Regional Hydro-meteorological Center (SRHMC), Vietnam.

Rice is grown in three distinct cropping seasons such as winter-spring from December to March, summer-autumn from mid-April to mid-August. In the autumn-winter, either irrigated or non-irrigated field is usually sowed from the mid-July to the end of August in Figure 2.4 [50]. In An Giang, rice crop is cultivated in single, double and triple-rice-cropping systems. The double-rice crop is often found within the semi-dike system with an elevation lower than 3-m above sea level. In such dike systems, flooding can take place because water overflows into the fields. It causes sediment deposition during the monsoon season [15]. Traditionally, farmers employed the double-rice crop, and seeking extra income fishing or small-scale livestock husbandry practices are also common in the fallow rice field. The triple-rice crop is found within the full-dike

system (above 3-m above sea level) with operational sluice gates, which can bring less sediment during flooding. Farmers adopted triple-rice cropping by upgrading from semi-dike system to full-dike system to fulfill the government targets.

2.2.2 Sentinel-1A data and preprocessing

Sentinel-1A data with C-band (5.4 GHz) SAR were acquired from March 2017 to March 2018. Sentinel-1A data supports operation in dual polarization (HH+HV, VV+VH) implemented through one transmit chain (switchable to H or V) and two parallel receive chains for H and V polarization [61]. The four acquisition modes are Interferometric Wide swath (IW), Stripmap (SM), Extra-Wide swath (EW), and Wave Mode (WV). These products are available in single (HH or VV) or dual polarization (HH+HV or VV+VH) [62,67]. The main operational mode features are Interferometric Wide Swath mode (IW) with 10m x 10-m pixel size and a swath width of about 250m. We used the IW model dual-polarization data acquired in Ground Range Detected (GRD) Level-1. The repeat cycle of Sentinel-1A data is 12 days with dual-polarization (VV+VH) [68]. To cover the whole An Giang, satellite track in ascending pass was used. Thirty-two images are available from March 2017 to March 2018 (Figure A1). Table 2.1 shows the specification of Sentinel-1A data with the dates of acquisition.

Figure 2.5 shows the general flowchart of the methodology. Sentinel-1A data were processed using the free and open source Sentinel-1 toolbox in the Sentinel Application Platform (SNAP) software. The GRD images were processed including restituted orbit files. Radiometric calibration was performed to output σ° bands. Orthorectification and terrain correction were done using SRTM 30m DEM data. The biggest speckle noise was often found in SAR data [69,70]. We

used Enhance Lee filter to reduce SAR speckle noise since Enhance Lee has more advantages compared to Lee filter, median filter, Kuan filter, Frost filters, and mean filter. Because they degraded the spatial resolution of images and smooth details, while also decreasing the speckle noise level due to without considering the pixels homogeneity level [71,72]. We used the Enhance Lee filter to reduce SAR speckle noise since Enhance Lee has more advantages compared to other filters. The Enhance Lee filter might keep edges and present the details preserved while filtering images in both homogeneous and heterogeneous regions [71,72]. The backscattering coefficient in decibel (dB) was acquired for analysis and classification according to the equation $10\,x\,log_{10}(\sigma^0)$. Plant phenological characteristics were identified following Jonsson et al. [73]. The mapping algorithm was used which introduced by Nguyen et al. [50,74]. Later, backscattering information was used to identify single, double and triple-rice crops and other land covers were classed.

Table 2.1 Multi-temporal Sentinel-1A data with specification and date of acquisition.

Sensor	**SAR C – band**
Product level	Level 1 Ground Range Detected (GRD)
Date acquisition (YYYY.MM.DD)	2017.03.13; 2017.03.25; 2017.04.06; 2017.04.18; 2017.04.30; 2017.05.12; 2017.05.24; 2017.06.05; 2017.06.17; 2017.06.29; 2017.07.11; 2017.07.23; 2017.08.04; 2017.08.16; 2017.08.28; 2017.09.09; 2017.09.21; 2017.10.03; 2017.10.15; 2017.10.27; 2017.11.08; 2017.11.20; 2017.12.02; 2017.12.14; 2017.12.26; 2018.01.07; 2018.01.19; 2018.01.31; 2018.02.12; 2018.02.24; 2018.03.08; 2018.03.20
Frequency (GHz)	5.405
Image mode	Interferometric Wide swath (IW)
Swath with	250km
Look direction	right
Incidence angle range	29.10 – 460
Antenna size	12.3m x 0.721m
Sub-swaths	3

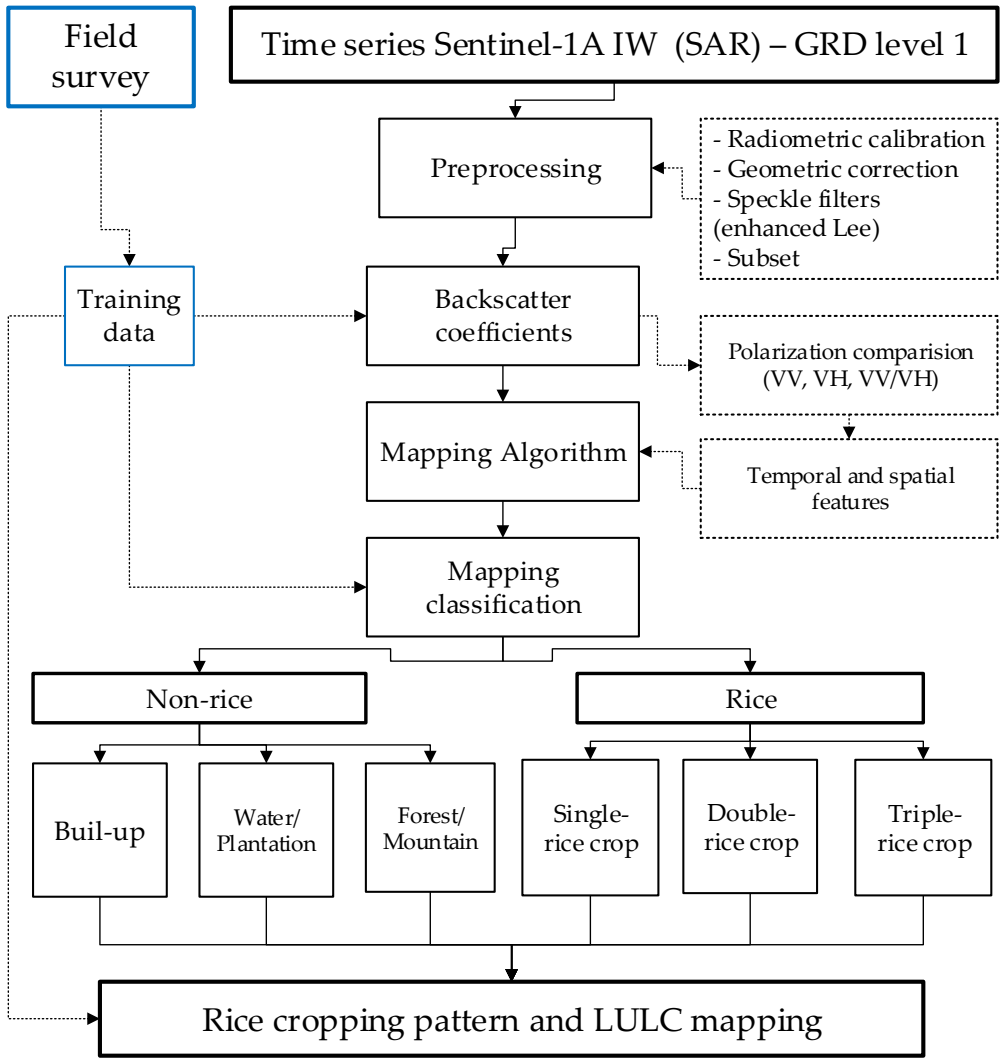

Figure 2.5 Flowchart of Sentinel-1A processing and rice cropping classification.

2.2.3 Field survey and secondary data collection

We conducted fieldwork throughout the study area between March 2017 and March 2018. The data included surveys on the crop practices calendar and field condition. We collected Geotagged photos about rice growing stages in different locations. The locations of single, double and triple-rice crops were marked in the Global Positioning System (GPS) (using Garmin 60x device). These locations were used as a training and validation of the Sentinel-1A processing. Figure 2.6 shows the multi-temporal composite of SAR data overlaid with the field data.

We divided the data into training and test datasets. For the time series observation, we selected 34 ground-truth points randomly distributed in single, double and triple-rice cropping areas for classification. The fieldwork was carried out on the dates close to Sentinel-1A acquisition in An Giang. Besides, we also measured rice height at three distinct rice cropping patterns during rice growth stages (Figure 2.7). The fieldwork was carried out on the dates close to Sentinel-1A acquisition in An Giang. The rice height was only conducted in summer-autumn for double and triple-rice crops, and in autumn-winter for single-rice crop. The average rice height is 104cm, 102cm, and 87cm in triple, double, and single-rice crops, respectively. There was no significance difference in the management practices of water and fertilizer usage in triple and double-rice crops. The single-rice crop was grown naturally without fertilizer and pesticides usages.

Land use/land cover mapping was validated by 140 ground-truth points. Photos of rice growth stages showed various growing stages of different crops and were found in Figure 2.8, Figure 2.9, and Figure 2.10. The rice growth stages at triple and double-rice crops located inside full and semi-dike protection, respectively in Figure 2.8 and Figure 2.8. Also, these photos of rice growth stages at single-rice crop located outside of dike system. Single-rice cropping area has also been used to produce vegetables during the non-rice season by local farmers were found in Figure 2.10.

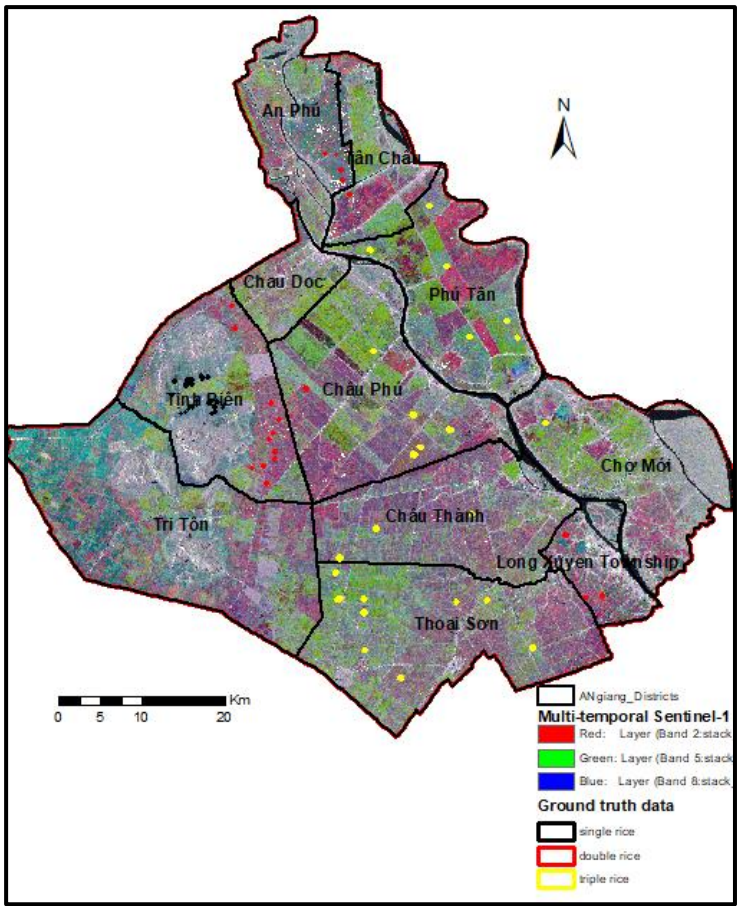

Figure 2.6 Multitemporal Sentinel-1A data color composite with training polygons overlaid. R:G:B = HV2017.03.13: HV2017.03.25: HV 2017.04.06.

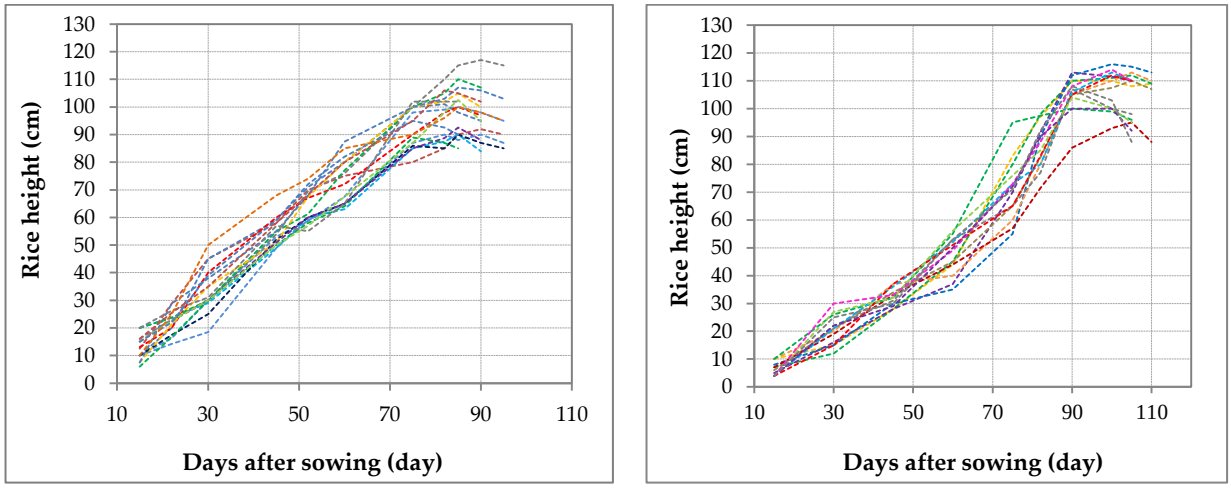

(a) (b)

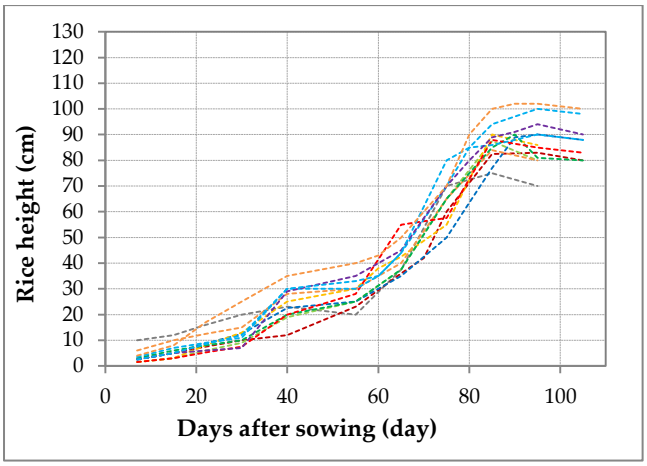

(c)

Figure 2.7 Temporal changes in rice height at 43 locations for different growth stages: (a) triple-rice crop, (b) double-rice crop, (c) single-rice crop.

The daily mean temperature (Tave), daily maximum temperature (Tmax), daily minimum temperature (Tmin), and daily rainfall at Chau Doc station were collected from Southern Regional Hydro-meteorology Center in Vietnam, during 1978-2016. Rice yield and rice production data at the district level in An Giang were obtained from IRRI and the yearly statistical book of An Giang, 1975-2016. The areas of full- and semi-dike were collected from DARD and Construction department of An Giang, 1995-2017.

Rice development can be defined in three main growth stages such as vegetative stage, reproductive stage and maturity stage [75]. Vegetative stage usually takes from sowing to 35-55 days depending on rice varieties while reproductive and maturity stages take about 30 days for each phase of all rice varieties [75]. Rice growth can be affected by various natural factors (e.g., rainfall, irrigation water supply, and air temperature) and artificial factors (e.g., fertilizers and pesticides) [76–78].

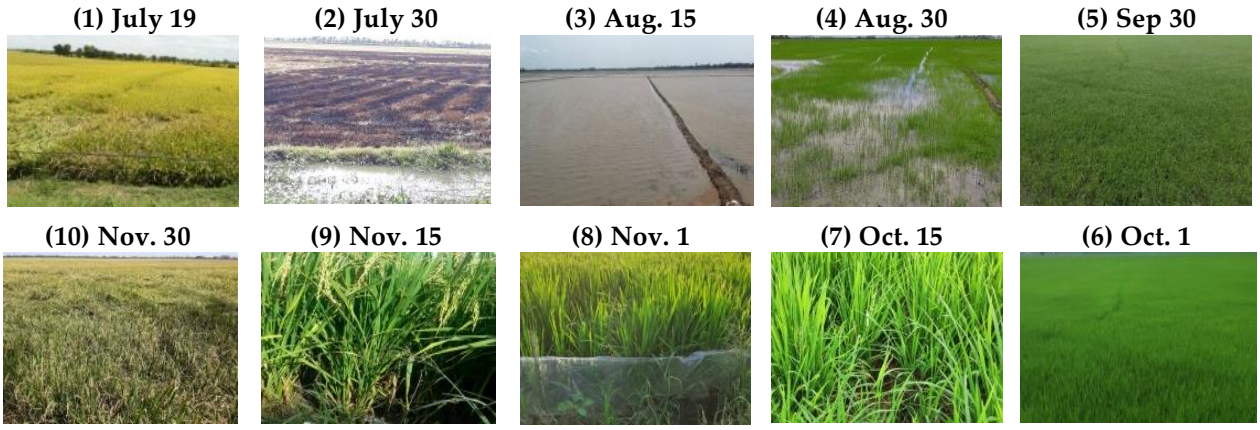

Figure 2.8 Rice growth stages for triple-rice crop, (b) double-rice crop, (c) single-rice crop. Notes: (1) harvesting time, (2) soil reparation; from (3) to (10): summer-autumn season in triple-rice system and fallow period in double–rice system; in single-rice crop: (1) to (4) is vegetable season; from (5) to (10): autumn-winter season.

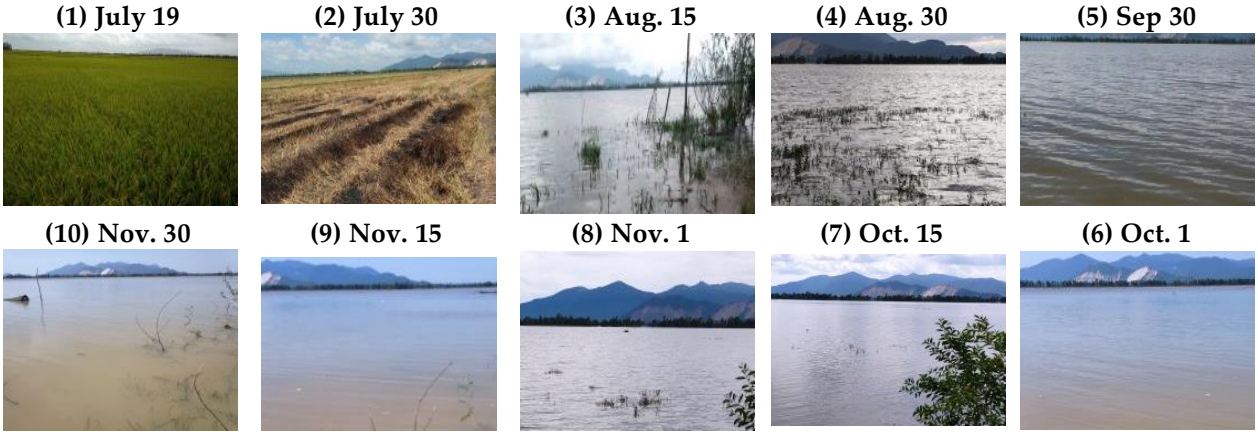

Figure 2.9 Rice growth stages for double-rice crop. Notes: (1) harvesting time, (2) soil reparation; from (3) to (10): fallow period in double–rice system

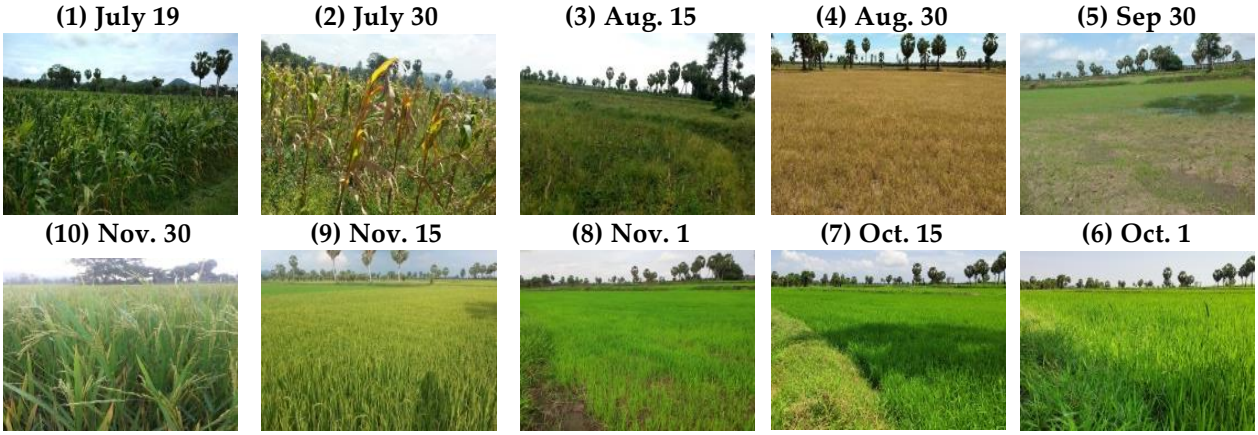

Figure 2.10 Rice growth stages for single-rice crop. Notes: single-rice crop: (1) to (4) is vegetable season; from (5) to (10): autumn-winter season.

The majority of rice varieties in the study area are short duration varieties (average 85-95 days), and a few rice varieties are grown with a duration of 95-105 days. The various growth stages of rice in different cropping pattern from the summer-autumn season to autumn-winter season, in the study sites and vacant time in the double-rice crop and vegetable-crop in the single-rice crop Figure 2.10.

2.2.4 Data analysis and accuracy assessment

Training polygons were digitized over the triple-rice, double-rice, and single-rice cropping areas using field-based GPS location and fine-resolution Google Earth imagery. Backscattering information of multi-temporal Sentinel-1A data at σ^oVH and σ^oVV polarization has been analyzed to investigate backscattering characteristics of triple, double and single-rice crops. Also, dual-polarization Sentinel-1A data were analyzed to detect rice phenological changes in the rice cultivation from sowing to harvesting and finally to delineate rice cultivation area and different land use/land cover. Besides, the local maxima and minima of VH backscattering and crop duration were utilized to consider cropping intensity and cropping season.

The scattering mechanism depends on various properties of objects such as dielectric properties, surface roughness, soil moisture, plant growth, orientation, etc. [79]. The σ^oVV and σ^oVH polarization can detect variation in scattering behaviors of targets such as volume scattering, and double-bounce scattering in the agricultural area. Previous studies noted that the σ^oVV polarization is more sensitive to water bodies while the σ^oVH polarization is able to delineate various rice growth stages [33,50,54]. The observed σ^oVV is generally higher than σ^oVH polarization because of the higher double-bounce. Support Vector Machine (SVM) with Kernel function [80–82] was used to LULC mapping. The RBF

parameters were optimal based on classification results by polarimetric SAR data [81–86]. The optimal parameters were grid-search along with cross-validation, which was introduced by previous studies [87,88]. The supervised classification proves highly solving regression and classification tasks [89,90]. Confusion matrix and Kappa coefficient were used to assess the accuracy of classification in this study. Although the kappa coefficient was used in many studies' fields, kappa has been noted to be have weaknesses as an accuracy metric [75–80] . For example, the kappa coefficient is dependent on the proportion of objects in each category and number of categories [96], and the kappa fails in case measurements have been made in ordered [97]. Thus, in this study, we presented all object proportion features and number of categories via confusion matrix which provides clear information for the users. Moreover, since land use categories were unordered in this study so that the kappa coefficient can be used [97]. We performed accuracy assessments of the resulting rice maps by selecting the remaining sampling points.

2.3 Results

2.3.1 Rice cultivation systems in An Giang province

The impact of rice intensification on the triple-rice crop has been increasingly felt on soil and water quality in the last ten years [24–26]. Thus, An Giang government has recommended adopting the three-three-two cropping cycle[2] to restore soil quality in recent years. Figure 2.11 shows ternary plots of triple, double, and single-rice cropping areas. A strong non-linear regression (R-squared of 0.9) was noted between rice production and full-dike area during

[2] Three-three-two cropping cycle refers to a three-year crop rotation that triple rice cropping is cultivated in the first two-year and a double-rice cropping system in which the paddy field is left fallow during a full flooding season in the third year.

1975-2017 (Figure 2.12). Besides, the major modern high-yielding varieties such as IR 50404, Sticky rice, OM 6979, OM 4218, and Jasmine were applied [98]. We have noticed that the full-dike area has increased from 1995-2017, and has mostly shifted from the semi-dike area. For example, during 1995-2010, the semi-dike areas had been upgraded to the full-dike area while outside-dike area did not change (Figure 2.11). In the short period from 2011 to 2013, the outside-dike area was replaced by full-dike area. From 2015-2017, the semi-dike area was continuously replaced by full-dike area (Figure 2.11).

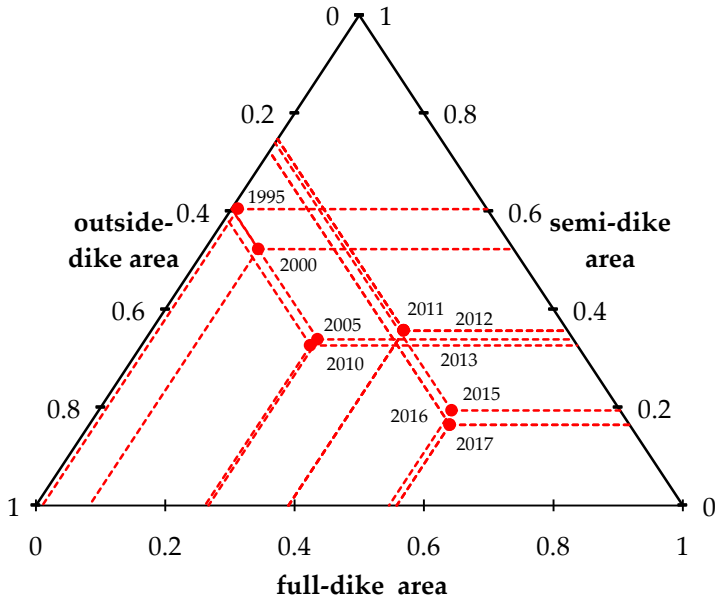

Figure 2.11 Ternary plots the increasing trend of full-dike area, and decrease trend area of semi-dike and outside of dike system, 1995-2017; dike system area data were collected from DARD and the Construction Department of An Giang, 1995-2017.

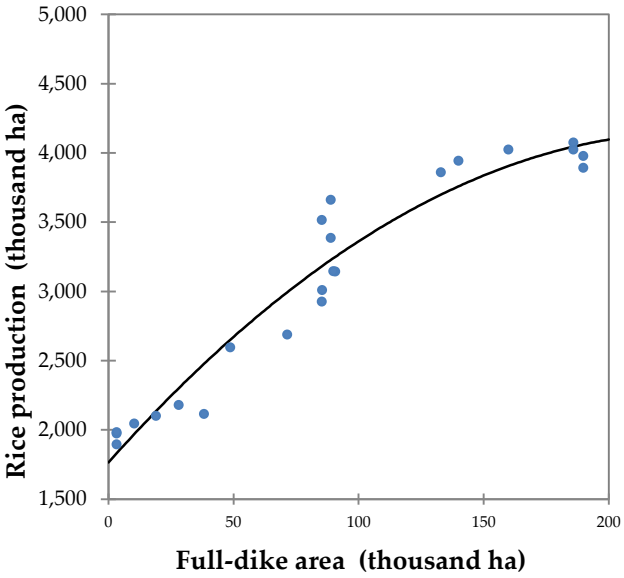

Figure 2.12 Non-linear regression between rice production and full-dike area, 1995-2016. Rice production data was obtained from IRRI;

Figure 2.13 shows principal component analysis (PCA) for variation of rice yield in three rice seasons. F1 explained 82.87% and F2 performed 11.06% of the total variance of rice yield. PCA shows less variation of rice yields in winter-spring compared to both summer-autumn and autumn-winter seasons at district level. Also, the highest rice yield was detected in winter-spring season (Figure 2.14

In winter-spring, the weather is optimum for planting and water carries abundant sediments and nutrients from upstream during the monsoon season to enhance productivity (Figure 2.14). Besides, the sudden changes in water discharge from the upper Mekong river basin damage the productivity in summer-autumn and autumn-winter [66]. An incident of dam-break occurred at the Xepian-Xe Nam Noy hydropower dam in Laos on July 23, 2018, as an evidence of productivity losses in An Giang. The lowest rice yield and the highest variation in the yield were found in the autumn-winter season (Figure 2.13). The lost rice production in early rice stage due to early flood damages was

found in some rice plots in autumn-winter season. Moreover, early harvested rice to avoid pest attacks also caused low rice yield (Figure 2.13).

In the summer-autumn season, (hot summer months) the high air temperature led to the growth of insects that affect rice productivity. In three crop seasons, the district of Tan Chau and Phu Tan have high rice yield, which is located in alluvial soil whereas Tri Ton and Tinh Bien have the lower yields because of acid sulphate soil and limited irrigation water supply (Figure 2.13). Differences in rice yields between Long Xuyen with other districts were found in Figure 2.14. Long Xuyen has the highest rice yield in summer-autumn season, followed by winter-spring, and the least in autumn-winter season.

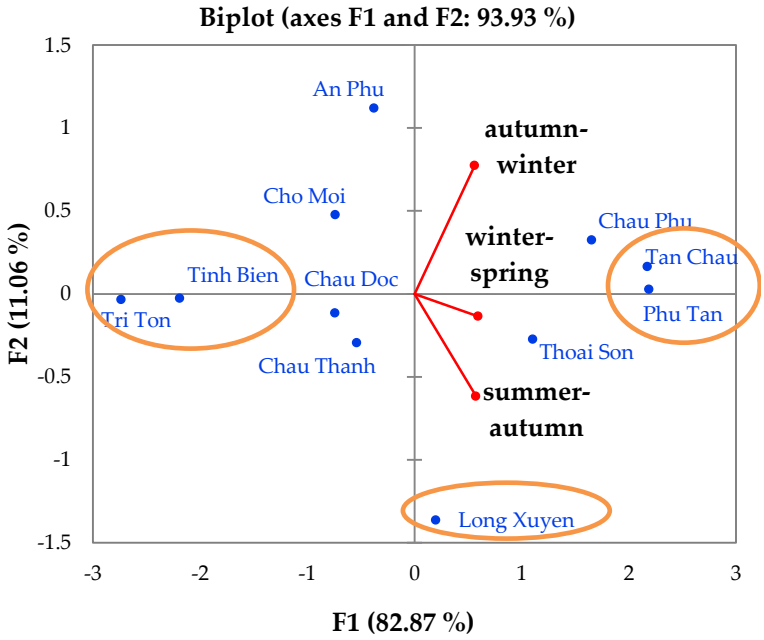

Figure 2.13 Principal component analysis for variation of rice yield in three rice seasons at the district level in An Giang. Rice yield data was obtained from IRRI, 1975-2016.

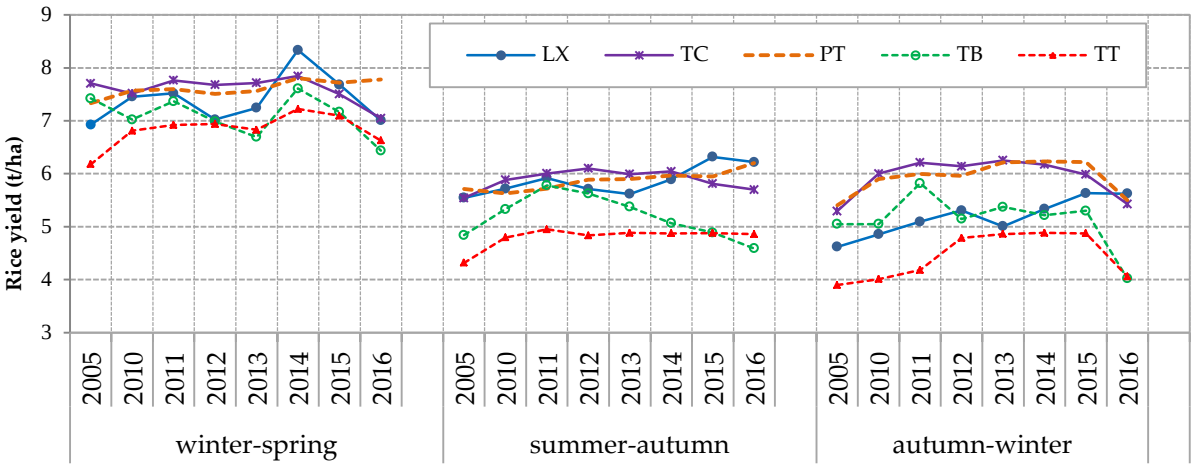

Figure 2.14 Rice yield at district level in winter-spring, summer-autumn and autumn-winter seasons in 2005 and 2010-2016. Rice yield data was obtained from IRRI. Note: LX – Long Xuyen, PT – Phu Tan, TT – Tri Ton, TC – Tan Chau and TB – Tinh Bien.

2.3.2 Polarization analysis of triple, double and single-rice crops

Figure 2.15 shows the rice growth stages in the summer-autumn season for double-rice cropping area. Low backscattering was noticed in the VV and VH polarizations at the vegetative stage in April 2017. It can be explained that the rice seedling is small, short and sparse. Thus, only surface scattering is dominant. During the vegetative phase, σ^{o}VH gradually increased with the rice growth stage. From vegetative to maturity stage, σ^{o}VV and σ^{o}VH reached maximum value at rice maturity stage in July 2017. In the reproductive period, σ^{o}VH and σ^{o}VV increased with the growth of rice height and canopy (Figure 5). The σ^{o}VV and σ^{o}VH values had a strong correlation with rice development during the reproductive phase. In the maturity stage, σ^{o}VV and σ^{o}VH continued to increase until they reached a maximal value on July 11, 2017. A decrease in backscattering was noticed near harvesting period because plants started drying up. Also, water in the agricultural field was drained out causing a soil moisture reduction in August 2017. Moreover, we can see the maximal values of σ^{o}VV and σ^{o}VH appearing at maturity stage after the maximum of greenness index are consistent

with the study of He et al. [99]. Previous studies showed that σ°VH correlated with rice development stage [33,50,54]. Thus, we used local maxima of σ°VH to consider rice cropping intensity and cropping season.

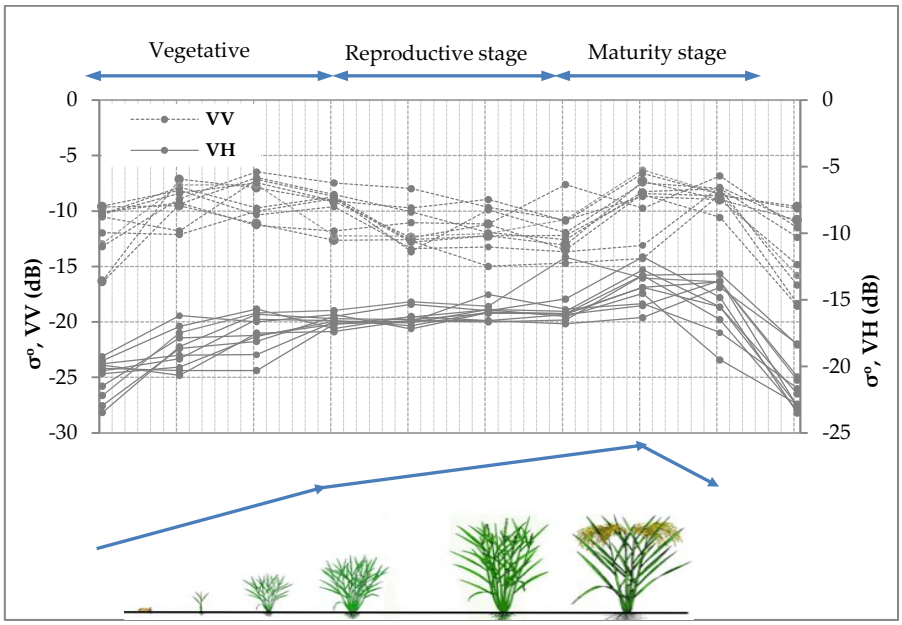

Figure 2.15 Growth cycle of rice in summer-autumn in double-rice crop. The primary vertical axis is σ°VV and the secondary vertical axis is σ°VH. Growth cycle of a rice plant was collected from International Rice Research Institute (IRRI) (source: http://knowledgebank.irri.org).

Figure 2.16 shows σ°VV and σ°VH during the entire period of the triple-rice crop. Low backscatters were noticed in the σ°VV and σ°VH due to the sowing of rice time at the early stage in April 2017, September 2017 and January 2018. During the vegetative phase, σ°VH increased gradually whereas the σ°VV increased rapidly because of high soil moisture or high water level in the fields. In the reproductive phase, the moderate backscatters of σ°VV and σ°VH were found and gradually increase with the growth of rice plants. In the maturity stage, σ°VV and σ°VH continued to rise until they reached a maximal value before having a sharp fall during harvesting time in August, December 2017 and March 2018, respectively.

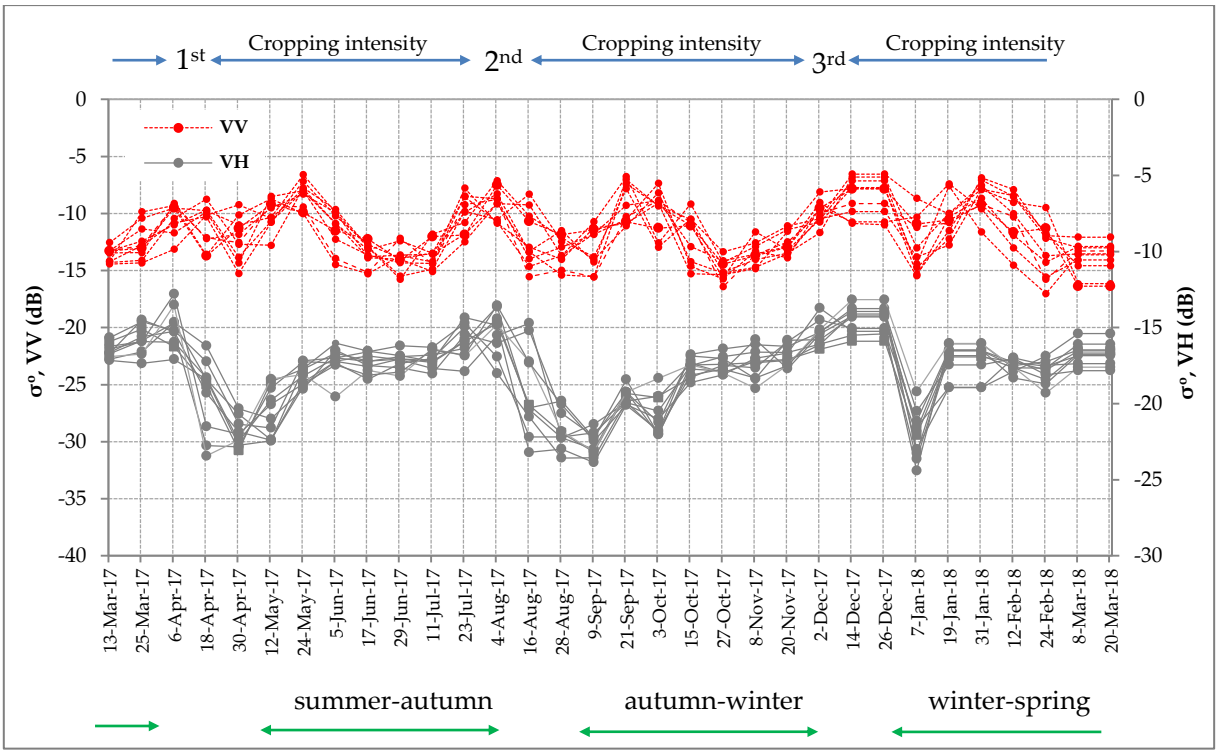

Figure 2.16 Graph represents the multitemporal Sentinel-1A backscattering in triple rice cropping area. The first vertical axis is σ°VV and the second vertical axis is σ°VH.

Figure 2.17 illustrates the behavior of σ°VV and σ°VH during the entire period of the double-rice crop. The observed σ°VH and σ°VV showed an increase after sowing because of the increase in volume and double-bounce scattering with the plant growth (Figure 2.17). Before sowing rice, the field soil was bare and thus lower values of σ°VH and σ°VV were obtained in April 2017. A gradual increase in the σ°VH was observed when rice grew from vegetative stage to maturity stage. The highest values of σ°VH and σ°VV were noticed in July 2017 during the second cropping season of the double-rice crop. There is a fallow period in the double-rice crop from August to November. During the fallow period, the rice cropping area can accumulate nutrients, enhance productivity and remove toxic substances from pesticides and pathogens during the monsoon season [100]. We also found the lowest value of σ°VV and σ°VH during August-November, which shows the fellow period to prepare the soil for next planting of

rice. The next sowing period starts at the end of December 2017 when low backscattering has been noticed in the σ°VV and σ°VH polarization (Figure 2.17). The σ°VV and σ°VH gradually increase with the growth stage from vegetative to the maturity stage and reached to a maximum value near harvesting time in March 2018. When the winter-spring season is considered, the σ°VH clearly had two peaks in July 2017 and March 2018. The peaks matched well with the crop calendar (Figure 2.4). Thus, multi-temporal Sentinel-1A data is a promising approach to identify the double-rice crop, rice growth stages, and standing water during fallow period were indicated at -23 dB of σ°VH.

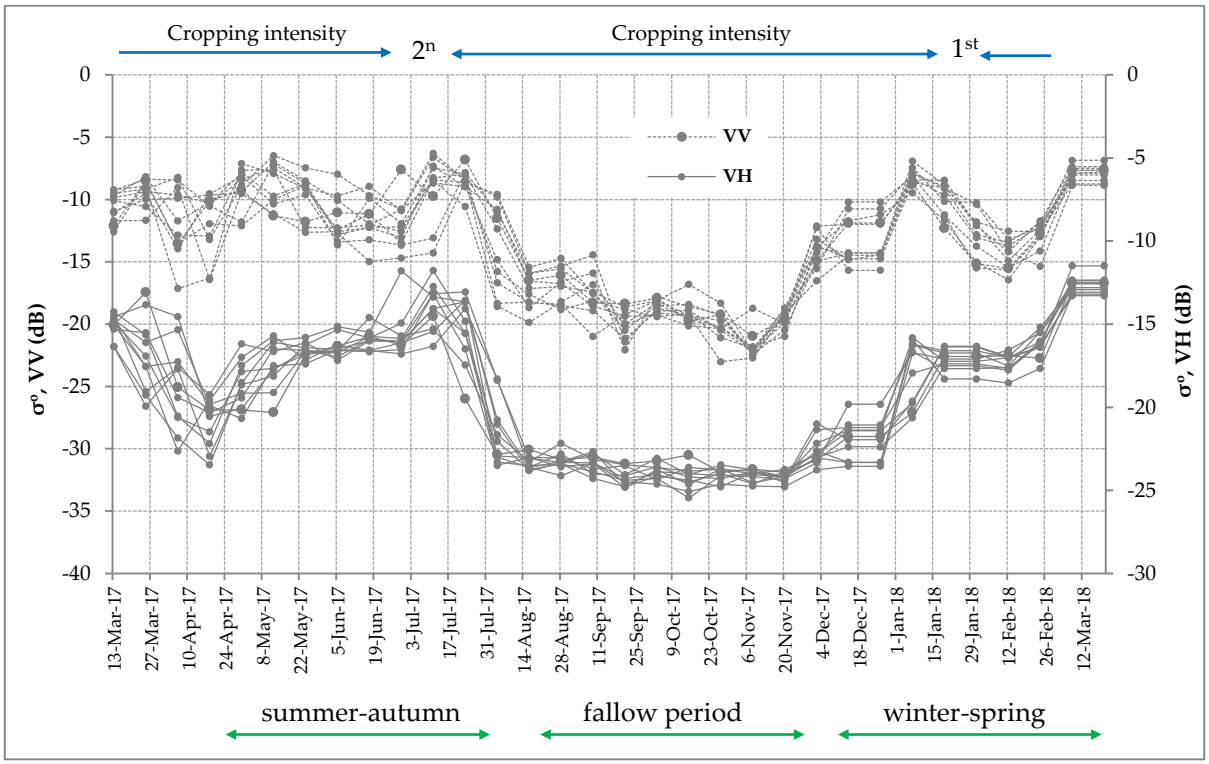

Figure 2.17 Graph represents the multitemporal Sentinel-1 A backscattering in double rice cropping area. The first vertical axis is σ°VV and the second vertical axis is σ°VH.

The minima and maxima of VH backscatter for each rice crop were also identified. The minima average of VH polarizations were -22dB in triple and double-rice crops, and -18dB for the single-rice crop. These values were consistent with previous studies [50,101]. Oyoshi et al. [101] also found -20.5dB (±3dB) of minima VH polarizations. The mean of VH backscatter thresholds

varied from -13 to -15dB in triple-rice crop, from -13 to -14dB in the double-rice crop, and -15dB for the single-rice crop. The mean maximal values of σ^oVH in three cropping patterns were not much different from each other. In this study, we also compared the maxima of σ^oVH among rice cropping seasons in double and triple-rice crops. The results showed that the mean values of σ^oVH in the winter-spring season were usually higher than in summer-autumn and autumn-winter seasons; In triple-rice crop, the mean values of σ^oVH -15dB and -15.2dB were found in winter-spring and autumn-winter, respectively. In double-rice crop, the mean values of σ^oVH were -12.5dB and -14dB, found in winter-spring and autumn-winter, respectively. Moreover, the σ^oVH was often higher in the double-rice crop than in triple-rice crop [102].

Figure 2.18 shows the increase in the observed σ^oVH and σ^oVV after sowing of rice in September 2017 because of the increase in volume and double-bounce scattering with the plant growth. Before sowing rice, vegetable was planted between March and July 2017. There was a gradual increase in the σ^oVH with the growth of the rice plant during the vegetative-reproductive stages. The highest value of σ^oVH was noticed in December 2017. There was a fallow period after December 2017, thus, farmers started growing vegetables for extra income. The σ^oVH and σ^oVV showed the changes in the backscattering properties with the difference in the objects in the agriculture field. The changes in σ^oVH and σ^oVV matched well with the crop calendar shown in Figure 2.4. Single-rice cropping system includes rice-vegetable-vegetable and rice-fallow period models. In the rice-fallow model, farmers can grow traditional rice crop (landrace rice and floating rice) almost anytime during July and December. Floating rice is often cultivated in Luong An Tra Commune, Tri Ton district during August-

September and harvested in December or January. The single-rice crop is mostly grown in Tinh Bien and Tri Ton districts with low annual yield.

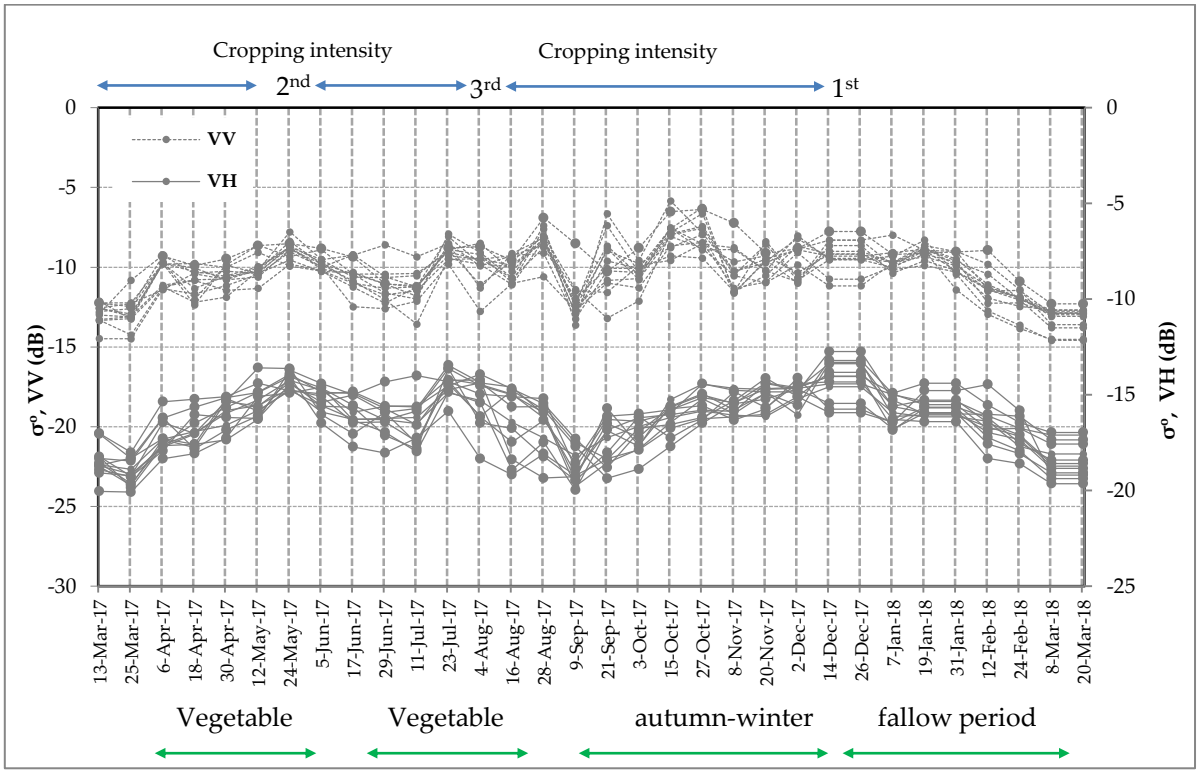

Figure 2.18 Graph represents the multitemporal Sentinel-1 A backscattering in single rice cropping area. The first vertical axis is σ^o VV and the second vertical axis is σ^o VH.

2.3.3 Delineation of rice cropping area

The study area of LULC was classified into eight categories, i.e. single-rice crop, double-rice crop, triple-rice crop, forest, plantation, mountains, built-up, and water bodies. Figure 2.19 shows the results of the classification that rice crops at all seasons were distinguished and represents the statistical distribution of various LULC classes in An Giang. The estimated LULC for An Giang was as following: (46.6%) in triple-rice cropping area, 870.4 sq.km (24.7%) for double-cropping area, 258.5 sq.km (7.3%) for single-cropping area, and 21.4% for others. The total rice planted area from March 2017 to March 2018 was 2770.8 km^2. Table 2.2 shows the distribution of various LULC classes at the district level. The three

largest triple-rice cropping areas are Thoai Son, followed by Chau Thanh and Chau Phu. The three largest double-rice cropping areas are Tri Ton, Chau Phu, and Tinh Bien.

The most common method to assess the accuracy of classification is the confusion matrix [64-65]. We used SVM classification with radial basis function kernel to classify Sentinel-1A data and Kappa coefficient for accuracy assessment of rice cropping patterns in the study area. Table 2.3 illustrates the confusion matrix of the SVM classification. The producer's accuracy is derived by dividing the number of correct pixels in one class divided by the total number of pixels as derived from reference data. It measures how well a certain area is classified. The user's accuracy is a measure of reliability of the map [103]. In this study there is no significant difference in the user's and producer's accuracy. Therefore, we focused on overall accuracy and Kappa coefficient. The overall accuracy of the classification was 80.7% with 0.78 Kappa coefficient. Triple-rice crop, water, and mountain area showed some misclassification. Figure 2.20 shows the dike system overlaid on the classified map. Most of the triple-rice cropping area comes under the full-dike system whereas, double-rice cropping area comes under the semi-dike system.

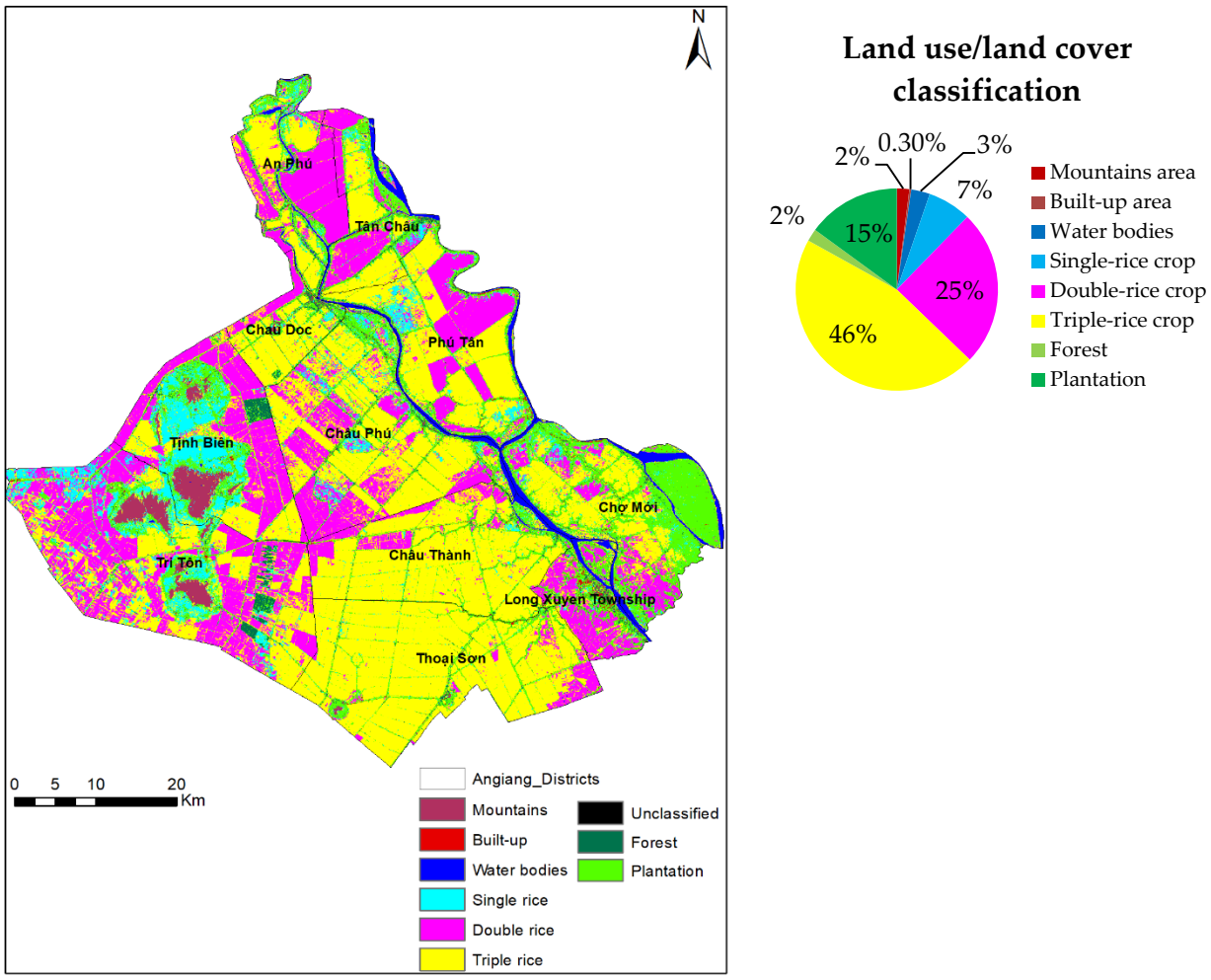

(a) (b)

Figure 2.19 **(a)** Sentinel-1A based land cover classification of An Giang province and **(b)** Distribution of land use/land cover classes in An Giang.

Table 2.2 District level distribution of various land use/land cover classes.

District	Single-rice cropping area (sq km)	Double-rice cropping area (sq km)	Triple-rice cropping area (sq km)	Plantation area (sq km)	Others area (sq km)
An Phu	11.1	88.3	72.1	34.0	14.4
Chau Phu	28.2	119.3	235.5	48.0	20.4
Chau Thanh	5.9	38.1	266.1	34.7	9.9
Cho Moi	17.0	46.2	118.0	150.4	38.1
Chau Doc	4.0	14.9	63.0	13.7	7.0
Long Xuyen	3.0	48.2	14.6	31.3	17.1
Phu Tan	20.3	88.2	159.0	37.6	21.5
Tan Chau	9.4	51.0	61.6	31.2	16.7
Tinh Bien	74.1	114.0	70.9	51.9	40.9
Thoai Son	5.0	23.6	392.9	39.1	7.5
Tri Ton	80.5	238.7	188.1	45.4	45.6
Total	258.5	870.4	1641.9	517.2	239.1

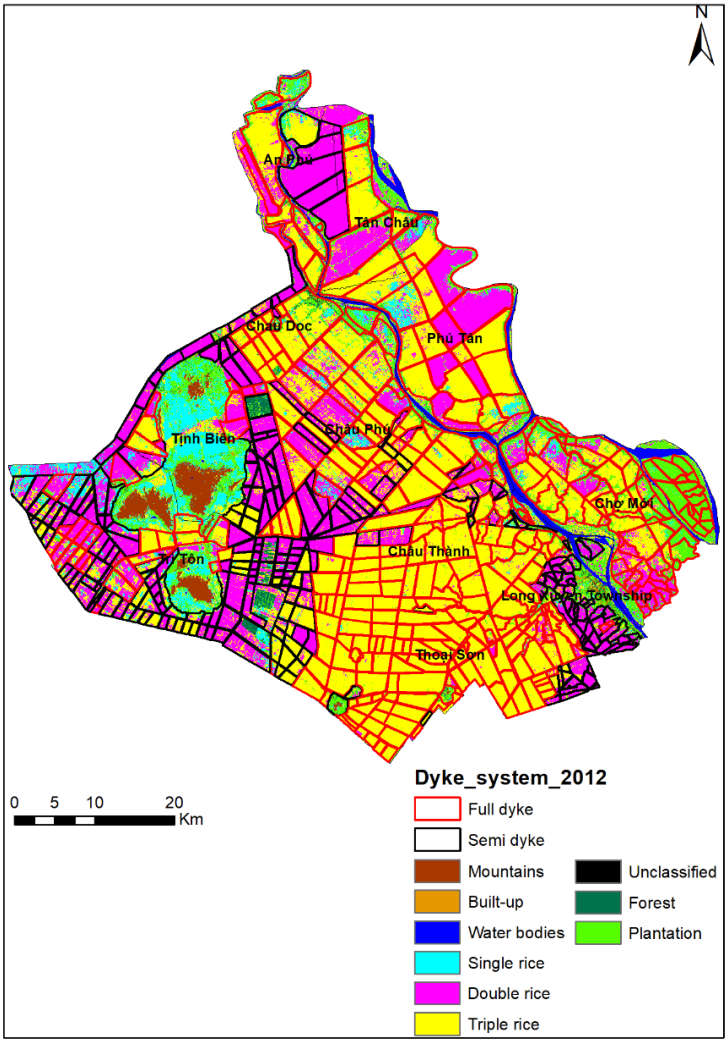

Figure 2.20 Distribution of various land cover classes and dike system.

Table 2.3 Confusion matrix for accuracy assessment.

Classified	**Ground survey**									
	Mountain	Built-up	Water	Single-rice crop	Double-rice crop	Triple-rice crop	Forest	Plantation	Total	User's accuracy (%)
Mountain	**11**	0	0	0	0	0	1	1	13	84.6
Built-up	0	**9**	0	2	0	0	0	0	11	81.8
Water	0	0	**18**	0	0	2	0	0	20	90.0
Single-rice crop	0	2	0	**12**	1	0	0	0	15	80.0
Double-rice crop	0	0	1	0	**18**	3	0	0	22	81.8
Triple-rice crop	0	0	2	0	3	**20**	0	1	26	76.9
Forest	2	0	0	0	0	0	**15**	2	19	78.9
Plantation	1	0	0	1	0	0	2	**10**	14	71.4
Total	14	11	21	15	22	25	18	14	**140**	
Producer's accuracy (%)	78.6	81.8	85.7	80.0	81.8	80.0	83.3	71.4		

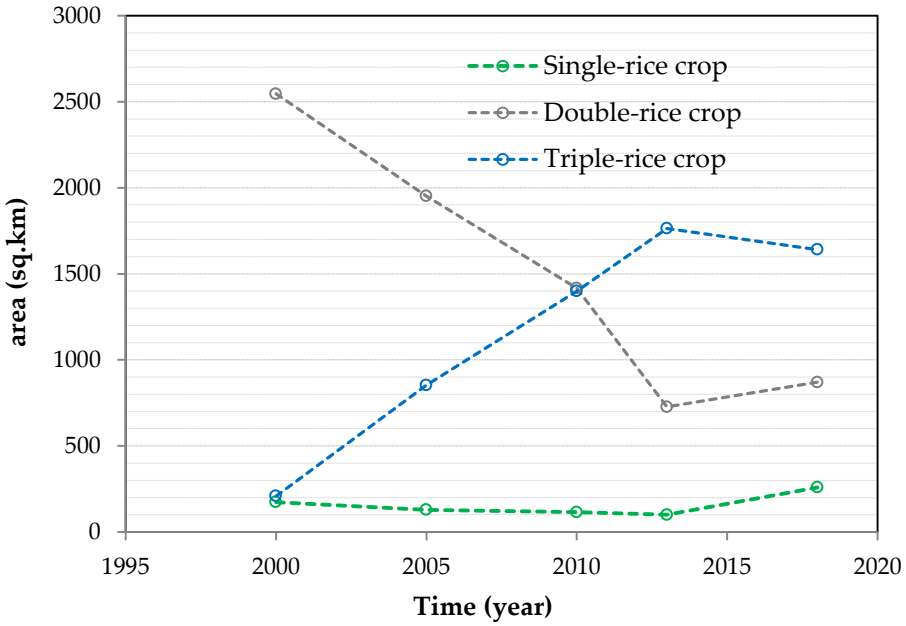

Figure 2.21 Yearly change area of rice cropping pattern.

2.4 Discussion

We presented a study of rice cropping pattern monitoring and mapping in An Giang based on Sentinel-1A SAR data, during March 2017 and March 2018. The backscattering behavior of Sentinel-1A SAR shows a good relationship with rice phenological changes at three rice cropping patterns. The σ^{o}VH polarization showed better information about rice growth than σ^{o}VV.

The Sentinel-1A data showed the trajectory of rice growth stages, and the trajectory also matched well with the crop calendar in the area (Figure 2.4). For example, the behavior of σ^{o}VH and σ^{o}VV during the entire period of triple, double, and single –rice crops were greatly correlated with rice growth stages especially in mature stages due to less effect of standing water in rice fields. The σ^{o}VV had two peaks in each growing season except the vegetable crop in single-rice crop. The result has agreed with Nguyen et al. [50] that σ^{o}VV got maximal values 30 days after sowing. In this study, we found that the first peak appeared 30 days after the sowing date and the second occurred about 12 days after the

reproductive stage. These two peaks were approximately equal to each other. The first peak in the σ^oVV polarization is probably related to the appearance of water level in the agriculture fields, which causes double-bounce scattering right after the sowing. Although Sentinel-1A data with σ^oVH and σ^oVV polarization can be used to identify various growth stages of the rice crop, the responses of σ^oVH polarization were more consistent with rice growth stages than the σ^oVV polarization responses. Moreover, both σ^oVH and σ^oVV is not sufficient to distinguish backscattering from surface, steam, and canopy; however, use of full polarimetric data can be useful to distinguish surface, stem and canopy scattering. σ^oVV polarization also holds signals from volume or double-bounce (e.g., water-stem, and water-canopy). The σ^oVH backscatter is less affected from standing water conditions [50] and is thus expected to better represent the actual rice growth cycle.

Regarding rice phenology, the low values of backscattering of σ^oVV and σ^oVH were found in the early stages such as sowing days and soil preparation, and the fallow periods in the semi-dike area. Lasko et al., Torbick et al., and Bayro-Corrochano [51,57,90] also agreed that there was low backscattering during sowing dates . Moreover, Oyoshi et al. [101] noticed that there low backscattering occurred during the sowing stage and high backscattering occurred during the maturity stage based on the unique phenological changes of rice crop using SAR data. Thus, this feature of SAR data can be utilized for discriminating between the rice crop and other objects. Interestingly, the mean of maximal values of σ^oVH were found to be higher in the winter-spring season than in other seasons.

Based on the mapping of LULC, we detected that most of the triple-rice crop was distributed close to the main rivers (Bassac and Mekong rivers) as compared to double-rice crop. However, we also noticed some double-rice cropping close to the main river during the study period as farmers had applied the three-three-two cropping cycle model. The single rice cropping pattern was dominant in Tinh Bien and Tri Ton districts that are far away from Bassac River since most of the single-rice cropping is near mountains and usually faces a shortage of water supply. Nguyen et al. [50] also detected that rain-fed single rice has less optimum growing conditions in the VMD. We have noticed a decreasing trend of triple rice cultivation area after 2013 (Figure 2.21). This change has been detected in recent years; however, we expect that An Giang will be able to retrieve single-rice crop to enhance water and soil quality and to keep traditional rice culture in the future.

The accuracy assessment was applied to quantify how good the LULC mapping was. Overall accuracy and kappa coefficient were popularly used to assess the accuracy of rice mapping in many studies [50,83,105]. In this study, the confusion matrix showed a classification error in triple-rice cropping which was affected mainly by double-rice crop and water bodies. In the scatter double-rice plots in inside the semi-dike, farmers increased one more rice crop in autumn-winter. The farmers temporarily upgraded to full-dike from semi-dike to boost rice production; however, the risk of dike-break would increase. Also, in some triple-rice plots in full-dike area was commission by double-rice crop. Some local farmers have converted the third rice crop to vegetable or to the fallow period since farmers need to diversify crops. Land degradation was also one of the factors that led to conversion of rice crop to other uses. The water bodies had little effect on misclassification in triple and double-rice classes. The standing

water often appeared in rice fields leading to inundated areas, especially during August and November in the semi-dike area. Some single-rice plots were misclassified by built-up or double-rice due to some of them not yet having any cultivation or vegetable-rice model application, respectively. Thus, the use of PALSAR-2 data can improve the accuracy as introduced by Arai et al. [65] to distinguish between the inundated-rice fields and non-inundated-rice fields.

Chapter 3. Effect of dike-protection systems on surface water quality in the Vietnamese Mekong Delta

3.1 Introduction

Water quality has become a major concern in environmental debates [106–109] with about 80% of the world population in facing the threat of water scarcity [2]. The complex and diffuse contaminated pollutants get transferred from multiple land use to surface water, thus making the maintenance of water quality a challenge [110–117]. Discharge from agricultural catchments were found to have higher amounts of nutrients than forested ones, and agricultural activities have been identified as major contributors to water pollution [115,118]. Agriculture is considered a primary source of livelihood for 40% of the population and feeds for more than seven billion people in the world [119]. The intensification of agriculture has been practiced to meet the rising food demand in the limited amount of land under the context of urban development [116,120]. Therefore, fertilizers and pesticides have been utilized to increase productivity; however, they heavily impact the environment [25,121,122]. In addition, most governments in developing countries are often forced to focus on economic development rather than environmental protection [27]. For example, some developing countries in Africa, the Middle East, and Asia have been identified as hot-spots of water pollution with an average monthly concentration of Biochemical Oxygen Demand (BOD) above 8 mgL^{-1} in surface water [123].

In Southeast Asia, the irrigated rice system area accounts for more than 50% of the total agricultural area in Indonesia, the Philippines, and Vietnam [124]. Intensification of rice often comes with more than one crop per year and accounts for 79.4% of the total area under rice cultivation [124]. Also, the increase

in fertilizer use in irrigated rice fields compared to rain-fed rice crop was found [125]. In the Vietnamese Mekong Delta (VMD), agricultural intensification has been applied for nearly 40 years to adapt to economic development and population growth. In 1986, the Renovation policies [3] were issued by the Vietnamese government which has led the VMD to become one of the largest rice exporting country in the world since the 2010s [8–12]. To this end, many dike-protection systems, canals, and sluice-gates were built in parts of the upper VMD such as An Giang, Dong Thap, and Long An provinces to prevent flooding and to provide irrigation and drainage. Therefore, the VMD had been transformed into a hydraulic landscape under human control since the 1990s [19–21]. The use of pesticide and herbicide chemicals has swelled to wasteful levels in many parts of the region, where the local government is now seeking to reduce the use of the chemicals to improve water quality, especially in areas inside the dike systems. A prominent area in the VMD with sufficient impact of farming and renovation policy is An Giang province in the upper VMD.

An Giang province, where periods of long inundation exist, was selected to assess surface water quality under flood-protection-dike development (Figure 3.1). The province is located inland in the VMD where the wet season occurs during the period May-November, and the dry season occurs from December to April. The mean annual rainfall is about 1,400 m accounting for 90% of the total annual rainfall. Water volume is mostly transported from the upstream of Mekong river, whereas rainfall runoff in An Giang has minimal effect on river flow [28]. However, the two main rivers of the Mekong River system, i.e., the Mekong and Bassac Rivers, along with 280 primary rivers and dense main canals

[3] A set of economic reforms aim at moving the Vietnam economy towards the socialist-oriented market economy, and transitioning to a more industrial and market-based economy.

are responsible for flood flow release in the An Giang. The province is a flood-prone area where 22 flood events with high frequency occurred during 1926-2006 [6] in which about 65% of the high floods occurred from August to October [7].

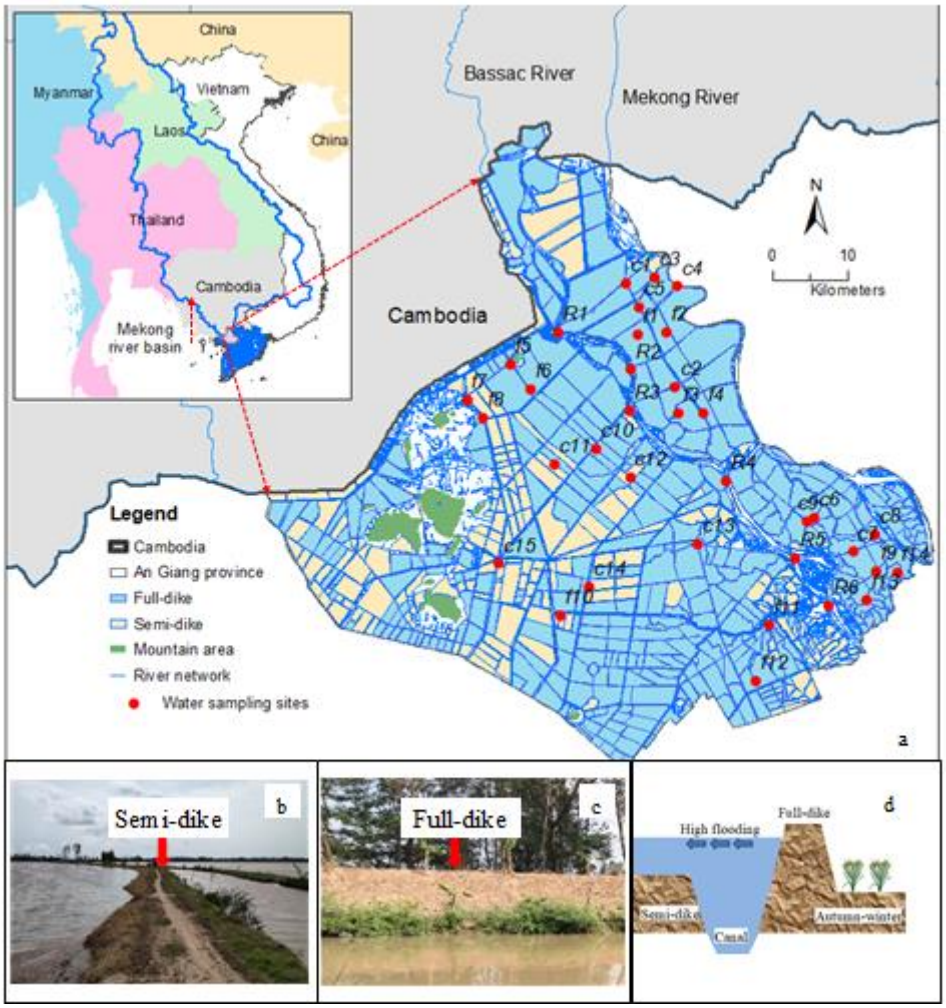

Figure 3.1 Map of the study area and surface water quality monitoring sites in An Giang province, Viet Nam. These photos were taken by the authors during field work in the Mekong Delta in 2017. Note: R: Main river, c: primary canal, f: secondary canal (field canal).

In response to these natural disasters, the Vietnamese government and local communities in the flood-prone areas of the VMD decided to construct dike systems to cope with the flooding situation and also to support agricultural intensification. An Giang covers an area of 3,406km^2 in which the rice land area accounts for 75% of the total area [126]. The dike protection area accounted for

over 80% of the total area of An Giang in 2017 (Table 3.2). These farmers might practice triple-rice intensification in full-dike-protection systems even during flooding season. The full-dike system protected triple-rice crops with an elevation variation from 4 to 6m above sea level [127,128]. Meanwhile, the double-rice crops often come under the semi-dike-protection system with elevation ranging from 2 to 3m above sea level. In this dike system, water flow enters the fallow field periodically in monsoon season, during August and November. Table 3.2 also shows the increased and decreased trend of full-dike and semi-dike areas, respectively, during 1995 to 2017. The local farmers have shifted to triple-rice crop from double-rice crop along with an increase in area covered with full-dike system since 1995. Triple-rice crops were dominant since the 2000s and rice production had a strong positive correlation with the full-dike area during 1995-2017 [43,127]. This rice intensification puts pressure on soil and water quality [78]. Previous studies found that intensive rice cultivation caused changing ecosystem, rising pest infestation, decreasing water quality and potential toxicity, especially for the area inside the dike system [18,23–25,129]. In recent years, groundwater is the main resource supplied for domestic use, while surface water resources mainly contribute to raising fish and irrigation. Surface water quality indices often exceed permission of the Vietnamese standards for domestic water supply [130]. For example, in October 2016, the concentrations of dissolved oxygen (DO), total suspended solids (TSS), Chemical Oxygen Demand (COD), BOD_5 and Total coliforms (TC) exceeded permitted values by 1.5 to 5 times, 1.5 to 10 times in the main river and canal compared to the Vietnamese standard [130,131]. Moreover, surface water was recommended not to be used for drinking and cooking without treatment techniques in An Giang [130].

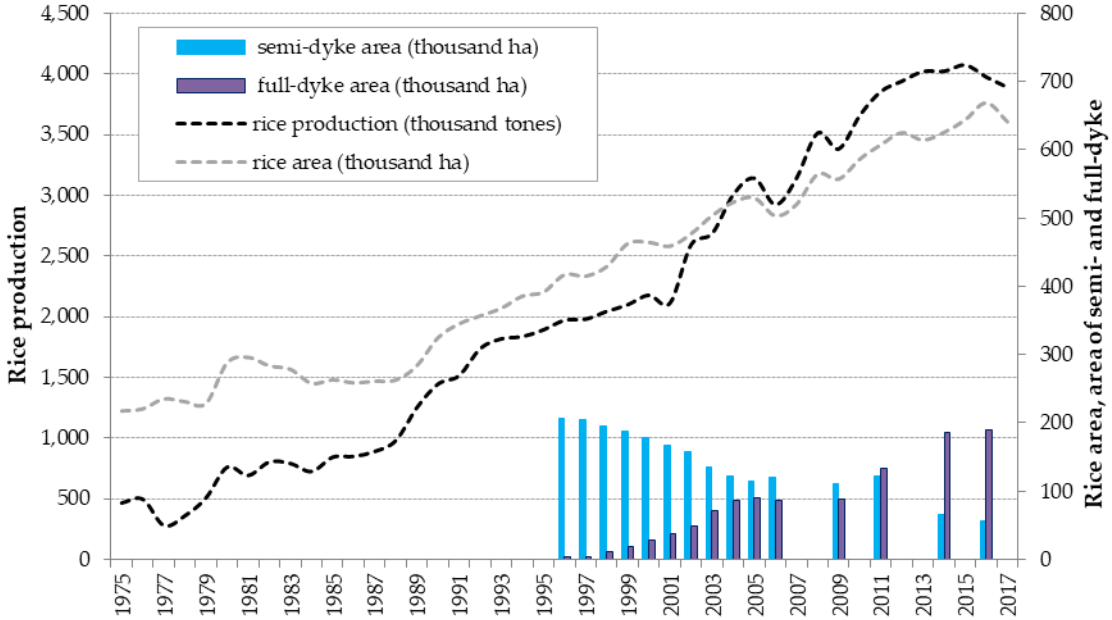

Figure 3.2 Rice area and production graph in dike protection system. Rice production was increased by double from 2 million tons to 4 million tons, 1997-2017. Rice area and production data were collected from IRRI, during 1975 to 2017; dike area data were collected from DARD and Construction department of An Giang, during 1995 to 2016.

Recently, [132] found that the concentrations of nutrients (P and N) often exceeded guideline standards in the border dike. Dike systems supported intensive pastoral agriculture in southern New Zealand. In Viet Nam, however, [133] revealed that the dike system caused changes in water regime in the VMD. However, they did not examine the effects of dike systems on water quality. Recently, Chea et al. [2] revealed that surface water quality in the main branches of the Mekong river was poor compared to the water quality in the Mekong river. The authors focused mainly on primary canals and also did not link with dike system protection. To the best of our knowledge, a short study focused on water quality inside the dike system in flood-prone areas in the VMD such as An Giang province. Due to water variation in quality depending on its location, time, season and existing pollution sources, this study aims to analyze surface water pollution levels in both spatial and temporal canals inside the dike system, and compare to the water quality outside the dike system area to identify the impact

of land use change on hotspots of water quality. In this study, we applied multivariate statistical analysis to assess the changes in surface water quality to find out the level of discriminant water quality parameters to distinguish between the inside and outside of dikes as well as between two seasons. This information might provide a picture about the water quality situation in An Giang which will be useful information for the AG government and for further researches.

3.2 Materials and Methods

3.2.1 Water quality sampling and analysis

Water quality samples were taken during the dry season (April 22-28, 2017) for the first time and the wet season (October 6-13, 2017) in the second time. A total of 35 surface water samples per season were measured at different rivers and canals inside and outside of the dike system in An Giang. We also conducted geotagged photos of site water samples which were marked in Global Positioning System (GPS) (Table 3.1). Stratified random sampling was used to select sampling sites in which the 6, 15, and 14 sites were selected in Bassac River (a branch of the Mekong River), primary canals, and secondary canals, respectively (Figure 3.1). Physical parameters were measured in-situ using a HORIBA multi-parameter meter (Kyoto, Japan) and a handheld meter (Oaklom; Tokyo, Japan). Chemical parameters such as phosphorus, nitrate, nitrite, ammonium, and chemical oxygen demand (COD) were measured by using the pack test listed in Table 3.2.

The secondary data of rice production, rice yield, and dike system area in An Giang were collected from the Department of Agriculture and Rural development (DARD) and the Construction Department of An Giang, 1995-2017.

Table 3.1 Location of 35 water-sampling sites in the dry and wet seasons in An Giang.

No.	Sites	Log.	Lat.	No.	Sites	Log.	Lat.
1	c1	105°12'25.20"	10°46'7.78"N	18	f3	105°16'9.83"E	10°36'44.98"N
2	c2	105°15'56.86"E	10°38'38.50"N	19	f4	105°17'55.17"E	10°36'46.66"N
3	c3	105°14'28.43"E	10°46'32.38"N	20	f5	105° 4'5.78"E	10°40'17.92"N
4	c4	105°16'2.69"E	10°45'53.35"N	21	f6	105° 5'30.06"E	10°38'30.42"N
5	c5	105°13'19.60"E	10°44'24.37"N	22	f7	105° 1'0.07"E	10°37'44.03"N
6	c6	105°25'56.10"E	10°29'15.79"N	23	f8	105° 2'5.19"E	10°36'29.09"N
7	c7	105°28'43.62"E	10°26'47.58"N	24	f9	105°30'23.99"E	10°25'22.07"N
8	c8	105°30'15.60"E	10°28'1.67"N	25	f10	105° 7'40.93"E	10°22'11.83"N
9	c9	105°30'23.99"E	10°25'22.07"N	26	f11	105°22'37.45"E	10°21'30.16"N
10	c10	105°10'16.02"E	10°34'10.30"N	27	f12	105°21'44.71"E	10°17'29.98"N
11	c11	105° 7'17.33"E	10°33'6.65"N	28	f13	105°29'39.51"E	10°23'18.24"N
12	c12	105°12'42.17"E	10°32'8.37"N	29	f14	105°31'52.81"E	10°25'16.97"N
13	c13	105°17'34.29"E	10°27'19.16"N	30	R1	105° 7'35.16"E	10°42'41.14"N
14	c14	105° 9'44.70"E	10°24'17.39"N	31	R2	105°12'43.56"E	10°39'53.83"N
15	c15	105° 3'16.39"E	10°25'56.12"N	32	R3	105°12'41.23"E	10°36'58.64"N
16	f1	105°13'15.39"E	10°42'27.56"N	33	R4	105°19'33.59"E	10°31'52.72"N
17	f2	105°15'19.71"E	10°42'36.67"N	34	R5	105°24'34.59"E	10°26'21.35"N
				35	R6	105°26'58.50"E	10°22'56.02"N

Table 3.2 Water quality parameters, units, and methods of analysis.

Parameters	**Abbreviations**	**Units**	**Method of analysis/Equipment**
pH	pH		In situ, Handheld pH meter I-1000
Electrical Conductivity	EC	$S.cm^{-1}$	In situ, Handheld conductivity meter I-1200
Total coliforms	TC	MPN/100mL	Shibata science (Tokyo, Japan)
Dissolved Oxygen	DO	mgL^{-1}	In situ, HORIBA Multi-parameter Meter
Turbidity	Turb	NTU	In situ, Turbidity Meter Lutron TU-2016
Orthophosphate	$PO_4^{(3-)}$	mgL^{-1}	In situ, Pack test Kyoritsu Chemical-Check Lab., Corp; Tokyo, Japan
Nitrite	$NO_2^{(-)}$	mgL^{-1}	In situ, Pack test Kyoritsu Chemical-Check Lab., Corp; Tokyo, Japan
Nitrate	$NO_3^{(-)}$	mgL^{-1}	In situ, Pack test Kyoritsu Chemical-Check Lab., Corp; Tokyo, Japan
Ammonium	$NH_4^{(+)}$	mgL^{-1}	In situ, Pack test Kyoritsu Chemical-Check Lab., Corp; Tokyo, Japan
Chemical Oxygen Demand	COD	mgL^{-1}	In situ, Pack test Kyoritsu Chemical-Check Lab., Corp; Tokyo, Japan

The multivariate approaches for the matrix for water quality parameters offer a better understanding of the characteristics of water quality, which was found in previous studies [134–137]. First, we assessed temporal variation of water quality between the dry and wet season by using the Spearman correlation coefficient (Spearman R) and discriminant analysis (DA) technique. Second, cluster analysis (CA) and principal component analysis (PCA) were then applied for spatial pattern assessment parameters for each season to detect the differences in water quality between inside and outside the dike. Finally, we calculated the water quality index based cluster obtained in the CA step. The statistical software and data analysis add-on for Excel (XLSTAT) version 2018, a statistical program and Inverse Distance Weighting (IDW) interpolation were chosen for display results.

The DA technique was used to perform characteristics changes in water quality linked seasons. It can also determine the most significant parameters and separate two or three clusters in terms of data sets [138–141]. In this study, we conducted three different modes approaches, i.e. standard, forward stepwise and backward stepwise that was applied successfully in previous studies [142,143]. In forward stepwise mode, variables are included step-by-step beginning with the most significant until no change is obtained. In backward stepwise mode, variables are removed step-by-step beginning with the least significant until significant changes, as expressed in equation 1 [138,144].

$$f(G_i) = k_i + \sum_{i=1}^{n} w_{ij} p_{ij} \quad (1)$$

F test of Wilks' lambda where i is a number of clusters (G), k_i is the constant inherent to each cluster, n is the number of parameters, and w_j is the weight coefficient assigned by DA to a given selected parameter (p_j). Wilks' lambda determines the difference of the mean of identified clusters, i.e., a small value near 0 implies that clusters differ, and 1 means that all clusters are equal of mean values. The F test of Wilks' lambda identifies significantly contributed parameters, i.e., a decrease in the independent variable's lambda value means the increase of variable contribution. From there, significant contributor variables will be identified [144].

3.2.2 Spatial pattern water quality analysis

(i) Cluster analysis (CA) was applied to examine the data for spatial and temporal differences which previous researches have applied for water quality assessment [140,141,145–147]. In this study, CA, an unsupervised model, was chosen to divide the data set into clusters within 35 water sampling sites. The most common approach starts with each site being similar to others in the cluster according Dlink/Dmax ratio to a predetermined selection criterion. Then, in a separate cluster, the sites join together step by step until one cluster remains [139–141,148–151]. An example of CA, agglomerative hierarchical clustering (AHC) with bottom-up approach was applied, wherein each site starts in its own cluster, then pairs of clusters are merged as one moved up the hierarchy. Ward's method measures the distance-linked clusters, in which Dlink/Dmax represents linkage distances of ratio-identified cluster to maximal linkage distance [138,141,150,152,153].

(ii) Principal component analysis (PCA) was used to transform the original variables into new principal components performed along directions of maximum variance. Also, reducing the contribution of less significant variables with minimal information loss was identified. In this study, the principal component was applied to identify which factors will be the most important parameters of water quality, as expressed by the equation 2 [147,154–161].

$$Z_{ij} = a_{1i}x_{1j} + a_{2i}x_{2j} + \cdots + a_{im}x_{nj} \qquad (2)$$

Where Z is the component score, a is component loading, x is component number, j is sample number, and m is a total number of variables.

(iii) Factor analysis (FA): was used to reduce the contribution of less significant variables to simplify further the data structure produced from PCA. Factor analysis is expressed by equation 3.

$$Z_{ji} = a_{f1}f_{1i} + a_{f2}f_{2i} + \cdots + a_{fm}f_{mi} + e_{fi} \qquad (3)$$

Where Z is the measured variable, a is the factor loading, f is the factor score, e is the residual term accounting for errors or other sources of variation, i is the sample number, and m is the total of factor.

3.2.3 Water quality assessment

The water quality index (WQI) has been applied in many countries and in the Mekong River basin; with WQI being one of the pronounced methods to represent the level of water quality by using several physico-chemical and biological parameters into a single number [2,162–166]. An Giang belongs to the Mekong Delta basin, standard of water quality which applied for whole Mekong River basin was conducted. However, there is no specific water quality standard or guideline used as criteria in the Lower Mekong Delta basin [2,162,163]. Thus, we used a standard which was introduced by the Mekong River Commission (MRC) in 2012 [164]. These six indicators of water quality concerning aquatic life (pH, EC, ammonia (NH_3^+), nitrite and nitrate-nitrogen ($NO_{2,3}$_N), total phosphorus (T-P), and DO were conducted [163]. Thus, we used the water

quality index for aquatic life protection (WQI_{al}) to evaluate surface water quality in An Giang, as expressed in equation 4 [164].

$$WQI_{al} = \frac{\sum_{i=1}^{n} p_i}{M} \; x \; 10 \qquad (4)$$

Where p_i represents the points scored on the sample (when each of the parameters meets its target value, its corresponding weighting factor is scored; otherwise, the score is zero); n is the number of samples; M is the maximum possible score for the measured parameters. Table 3.3 shows the grade scale; i.e., 10-9 for high quality, 9.5-9 for good quality, 9-7 for moderate quality, and < 7 for poor quality [162,163].

Table 3.3 Water quality parameters used for calculating the rating score of the water quality Index for the protection of aquatic life.

Parameters	**Target value**
pH	6 - 9
EC ($S.cm^{-1}$)	< 150
$NH_3^{(+)}$ (mgL^{-1})	0.1
$NO_{2,3}$_N (mgL^{-1})	5
T_P (mgL^{-1})	0.13
DO (mgL^{-1})	> 5

Note: Total-PO_4 (mgL^{-1} as PO_4^{3-}) = PO_4^{3-}x0.3262, and NH_3^{+} = NH_4^{+}x0.944, and NO_2_N = NO_2^{-}/3.28442, NO_3_N = NO_3^{-}/4.42664 [167,168]

3.3 Results

3.3.1 Temporal variation of water quality parameters

Table 3.4 Correlation matrices in the dry season using Spearman rank-order.

Variables	DO	pH	EC	Turb	COD	NH4(+)	NO2(-)	NO3(-)	PO4(3-)	TC
DO	1									
pH	-0.001	1								
EC	-0.108	-0.664*	1							
Turb	-0.276	-0.463*	0.657*	1						
COD	0.076	-0.068	0.310	0.394	1					
$NH_4^{(+)}$	-0.234	-0.275	0.572*	0.495*	0.224	1				
$NO_2^{(-)}$	0.227	0.273	0.133	0.082	0.108	0.208	1			
$NO_3^{(-)}$	0.139	0.505*	-0.106	-0.115	0.101	0.095	0.795*	1		
$PO_4^{(3-)}$	-0.082	-0.454*	0.504*	0.662*	0.396	0.298	0.054	-0.030	1	
TC	-0.004	0.112	0.177	0.013	0.123	0.101	0.109	-0.012	-0.225	1

Note: * value is different from 0 at a significant level of 0.05.

Table 3.5 Correlation matrices in the wet season using Spearman rank-order.

Variables	DO	pH	EC	Turb	COD	NH4(+)	NO2(-)	NO3(-)	PO4(3-)	TC
DO	1									
pH	0.059	1								
EC	-0.016	-0.532*	1							
Turb	-0.193	0.261	-0.174	1						
COD	0.055	-0.387	0.486*	-0.098	1					
$NH_4^{(+)}$	-0.132	-0.229	0.508*	-0.176	0.380	1				
$NO_2^{(-)}$	-0.145	-0.139	0.223	0.168	0.237	0.371	1			
$NO_3^{(-)}$	-0.100	-0.336	0.149	0.001	0.202	0.016	0.506*	1		
$PO_4^{(3-)}$	0.039	-0.162	0.484*	0.021	0.284	0.382	-0.013	-0.244	1	
TC	-0.122	-0.117	0.045	-0.473	0.073	0.111	0.262	0.182	0.011	1

Note: * value is different from 0 at a significant level of 0.05.

Table 3.4 and Table 3.5 show the correlations among ten water quality parameters in dry and wet seasons, respectively. The results indicated that water quality in the dry season was significantly different from its quality in the wet season. There were higher correlations among parameters in the dry season compared to those in the wet season. For example, in the dry season, turbidity

had a statistically positive correlation with EC and $PO_4^{(3-)}$ concentrations ($p < 0.05$), but there was no statistically significant correlation with other parameters in the wet season.

The pH value was significantly correlated with four-parameters (i.e., EC, Turb, NO_3^- and PO_4^{3-}) in the dry season, whereas it was significantly correlated only with EC in the wet season. Only EC had a significant correlation with more than one variable, i.e., COD, NH_4^+, and PO_4^{3-} in the wet season. In contrast, we found that in the dry season, EC and pH were significantly correlated with three and four water quality parameters, respectively. Therefore, it can be expected that the water quality parameters varied widely in the two seasons (Table B1 for descriptive statistics of collected data).

Table 3.6 Unidimensional lamda test of equality of water quality parameters.

Variable	Standard mode	Backward stepwise	Forward stepwise
DO	0.808***	0.808***	0.808***
pH	0.992		
EC	0.812***	0.812***	0.812***
Turb	0.790***	0.790***	0.790***
COD	0.755***	0.755***	0.755***
$NH_4^{(+)}$	0.896**	0.896**	0.896**
$NO_2^{(-)}$	1.000		
$NO_3^{(-)}$	0.874**	0.874**	0.874**
$PO_4^{(3-)}$	0.975		
TC	0.961		
Percent correct	95.54%	92.68%	92.68%

Note: Seasonal variation in water quality was evaluated by discriminant analysis (DA). It was performed on raw data with $p<0.05$ to further explore temporal variation of water quality. A Lamda value of 1 indicates that the means of water quality parameters in dry season are not different from those in wet season. A Lamda value of 0 indicates that the means of water quality parameters in dry season are totally different from those in wet season. Significance is denoted as follows: $^{*}p < 0.05$ $^{**}p < 0.01$ $^{***}p < 0.001$.

Table 3.6 shows the discriminant factions (DFS) on the three modes used in DA (Table B2 for the classification matrices (CMs)). In the standard mode, there was an obtained DFS with six discriminant variables (COD, turbidity, EC, DO, NO_3^-, and NH_4^+) producing CMs with 95.54% correct. Similarly, both backward stepwise and forward stepwise modes gave 92.68% correct. Also, the test of Wilks Lambda in the standard mode provided a value of 0.301 ($P<0.0001$). The null hypothesis stated the means of vectors of the two groups (the dry and wet seasons) are equal. The alternative hypothesis, on the other hand, at least one of means of the vector is different from another. In this case, the computed P-value is lower than 0.01; the null hypothesis was rejected. Moreover, p-value being lower than 0.0001 indicates that the means of two groups were strongly different. Therefore, the results of DA showed the concentrations of DO, EC, turbidity, COD, NH_4^+, and NO_3^- were the most significant parameters to discriminate between these seasons in the study area.

Figure 3.3 shows the concentrations of 6 parameters in the dry and wet seasons. In general, these concentrations in both seasons did not meet the Vietnamese water quality standard for domestic water supply found in [131], and they are consistent with the findings of [2,78,102,130]. The concentrations of COD, and NH_4^+ in the wet season were higher in values and wider in ranges in comparison with those in the dry season. Also, some high outliers values of EC, COD, and NH_4^+ were found in the wet season; and most of the outliers were from sites located inside full-dike such as c7, f1, f3, f6, f9, and f14. The concentration of the water quality parameters inside the full-dike was higher than that in the semi-dike and outside the dike.

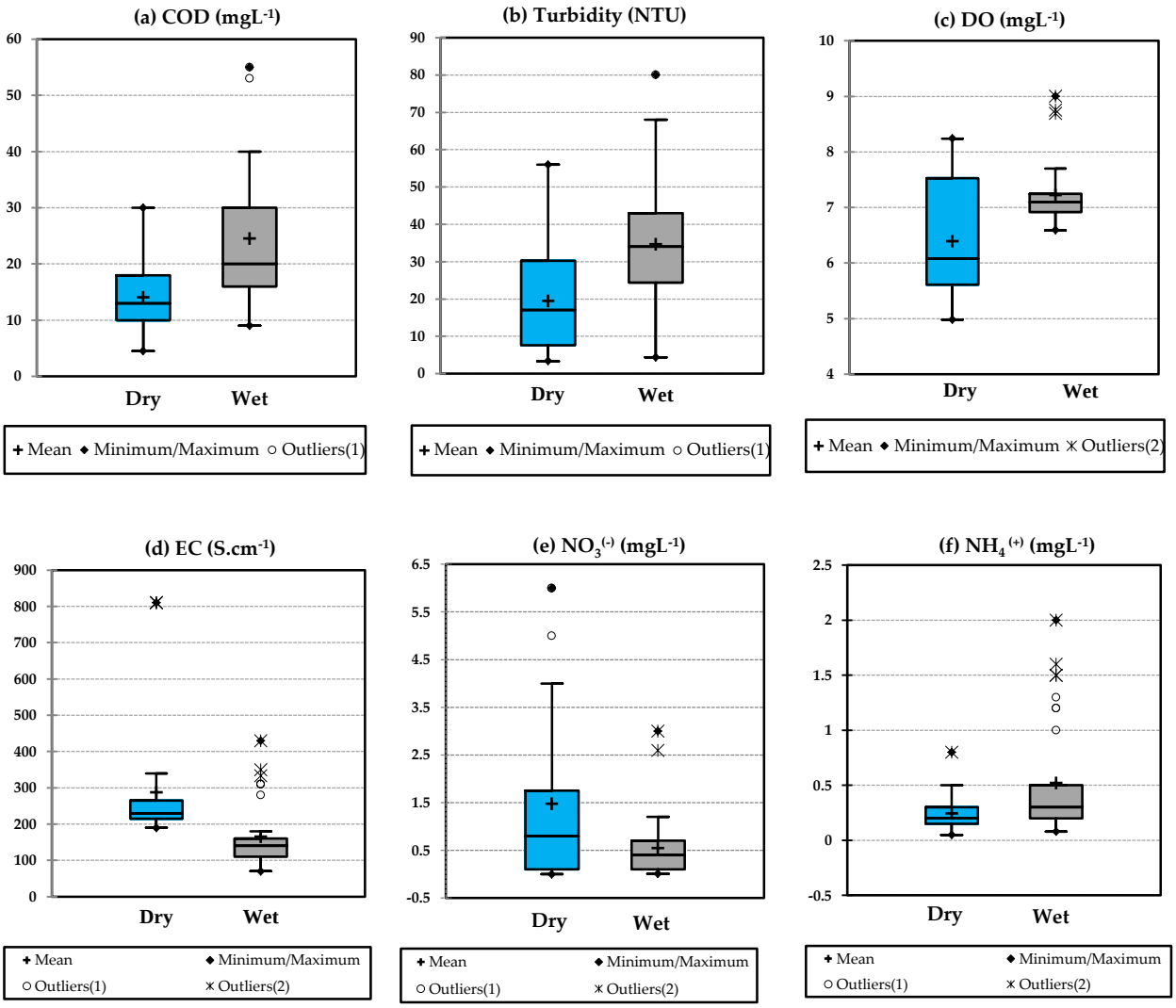

Figure 3.3 Box and whisker plot in discriminant parameters in dry and wet seasons: (a) COD, (b) turbidity, (c) DO, (d) EC, (e) NO_3^-, and (f) NH_4^+ in surface water quality. The outliers of NH_4^+ and EC in wet season were found inside full-dike (c7, f1, f3, f6, f9, and f14). Note: (R: river, c: primary canal, f: field canal; 1: inside full dike, 2: inside semi dike, 3: outside of dike).

3.3.2 Spatial variation of water quality parameters

Figure 3.4 and Figure 3.5 show dendrogram clusters in the dry and wet seasons in which three statistically significant clusters with linkage distance represented at (Dlink/Dmax)x100<60 (cluster 1, 2 and 3) and at (Dlink/Dmax)x 100<35 for sub-clusters (3a and 3b). The clusters still had a similar characteristic of water quality due to natural background source types. This finding agreed with findings from previous studies in Asia [142,143]. Figure 3.6 shows a large

discriminant between cluster 1 and the other clusters. The number of clusters was also decided by the practicality of the results such as an abundance of information main river (R), primary canal (c), secondary canal (f), and full-dike (1), semi-dike (2), outside dike (3)). The majority sites of cluster 1 were located inside the full-dike system in both the seasons (Table 3.5). Cluster 2, obtained from four out of nine sites inside the full-dike in the dry season and seven out of nine sites inside the full-dike during the wet season. Cluster 3a and 3b obtained mixing types such as inside the full-, semi-, and outside of dike systems except for cluster 3a in the dry season included most sites which were located inside the full-dike. We presented the water quality characteristic by clusters in Figure C1.

The cluster 1 was obtained in secondary canals which were close to rice fields (eight sites in the dry season: f1, f4, f7, f8, f9, f14, c1, and c11; and six sites in the wet season: f1, f3, f6, f9, f14, and c1). Cluster 2, in the dry season, included a majority of samples sites located in the main river, primary, and secondary rivers. However, in the wet season, most samples' sites (six out of nine) were located in the primary canals. Cluster 3a included sample sites located in secondary canals (five out of ten) such as f3, f5, f6, f10, f13, c4, c9, c10, R3, and R4; primary canals inside semi-dike (f5, f8, f13, c6, c10, c12, c13, and c14) in the dry season were also included in Cluster 3a. Cluster 3b included sites inside the full-dike in the dry season and mixing type of sample sites in the wet season.

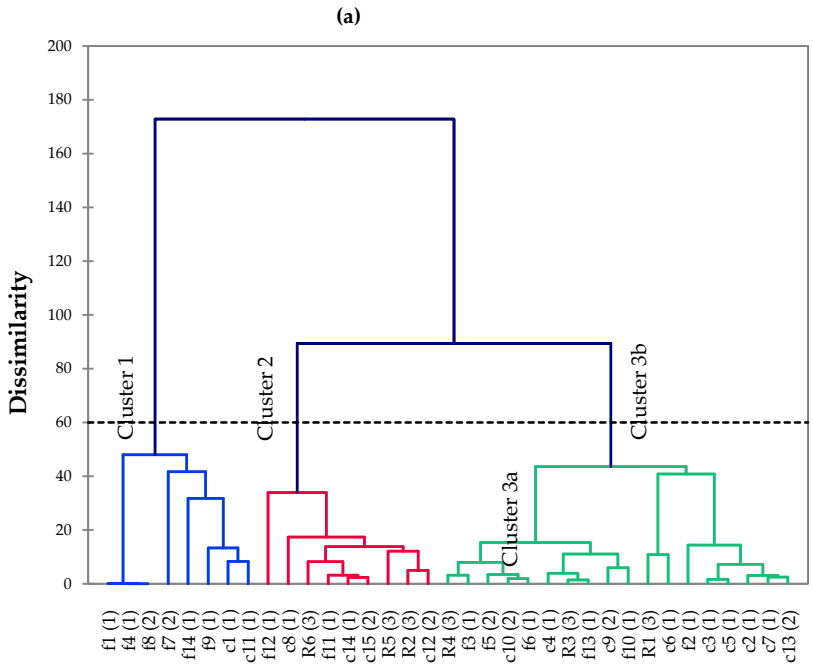

Figure 3.4 Dendrogam of clusters of sampling sites according to surface water qualities at (Dlink/Dmax)x100<60 and (Dlink/Dmax)x100<35 for sub-clusters (3a and 3b) in both the seasons. In dry season (cluster 1 obtained f1, f4, f7, f8, f9, f14, c1, and c11; cluster 2: f1, f12, c8, c12, c14, c15, R2, R5, and R6; cluster 3a: f3, f5, f6, f10, f13, c4, c9, c10, R3, and R4; cluster 3b: f2, c2, c3, c5, c6, c7, c13, and R1). Note: (R: river, c: primary canal, f: field canal; 1: inside full dike, 2: inside semi dike, 3: outside of dike).

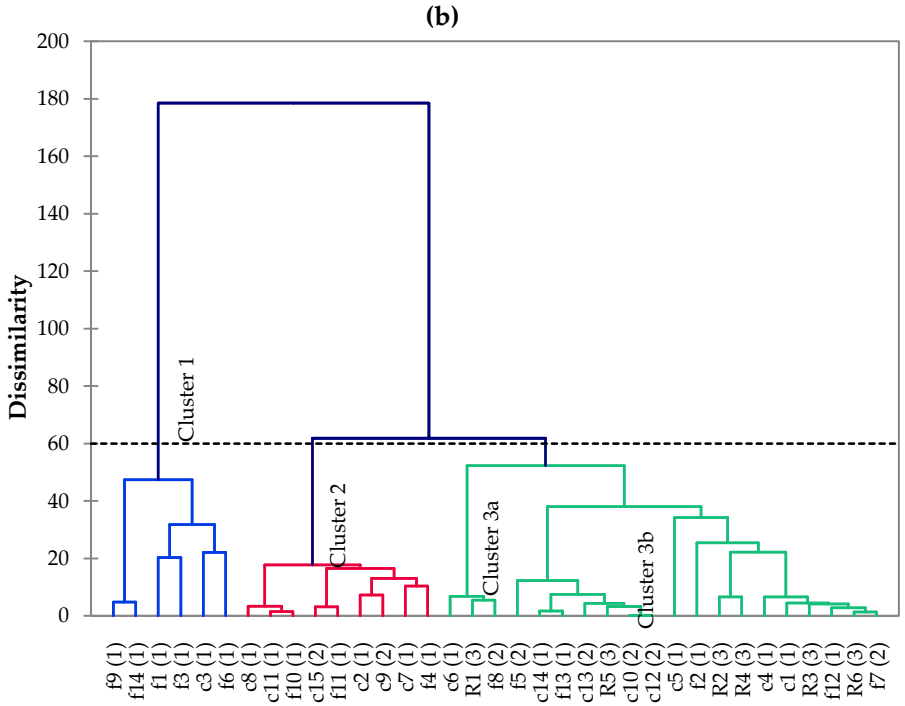

Figure 3.5 Dendrogam of clusters of sampling sites according to surface water qualities at (Dlink/Dmax)x100<60 and (Dlink/Dmax)x100<35 for sub-clusters (3a and 3b) in both

two seasons. In the wet season (cluster1:f1, f3, f6, f9, f14, and c1; cluster 2: f4, f10, f11, c2, c7, c8, c9, c11, and c15; cluster 3a: f5, f8, f13, c6, c10, c12, c13, c14, R1, and R5; cluster 3b: f2, f7, f12, c1, c4, c5, R2, R3, R4, and R6).

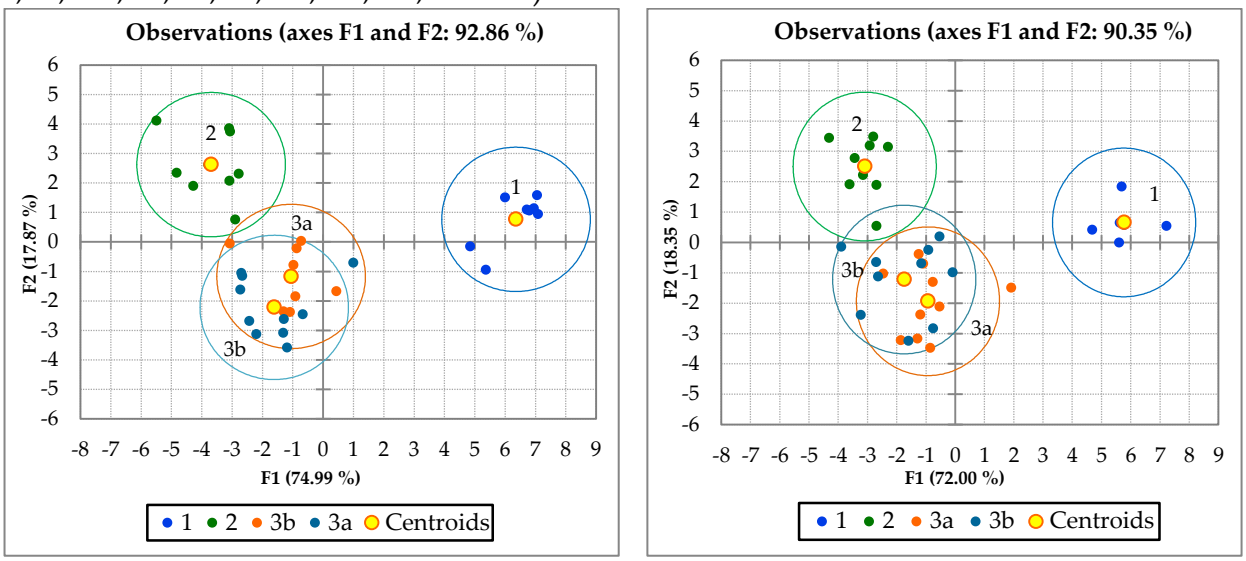

Figure 3.6 Results from DA among 4 groups in each season (1, 2, 3a, 3b): (a) dry season, (b) wet season. In both the dry and wet seasons, a large discriminant exists between cluster 1 and the other clusters while clusters 3a and 3b have less discriminant features. In the dry season, F1 and F2 explained 74.99% and 17.87% of total variation, respectively. In the wet season, F1 and F2 explained 72% and 18.35%, respectively.

3.3.3 Data structure determination and sources identification

In PCA, eigenvalues were used to identify principal components (PCs) which can be retained. An eigenvalue measured the significance of the factors. Screen plots were obtained from the pronounced change of slope after the third eigenvalue (Figure D1), in which eigenvalues greater than or equal to 1, were considered [147,169,170]. The first four eigenvalues in two seasons were used for further analysis. These PCs were selected with eigenvalues greater than 1 and explained 78.36 % and 70.70 % of total variances in the dry and wet seasons, respectively (Table D1).

Figure 3.7 shows that the PC1 explained 33.91% of the total variance in the dry season. This component was positively and largely contributed by mineral/physical parameters (EC and turbidity) and inorganic parameters (NO_2^-

and NO_3^-); but was negatively contributed by pH concentration. The 21.16% performed in PC2 was contributed by inorganic nutrient-related water quality parameters (NO_2^-, NO_3^-), and pH. The concentrations of DO and TC were considered as less important since the loading coefficients (eigenvector) were low in these two parameters in two seasons. These components revealed the importance of the effect of EC, Turb, PO_4^{3-} in the dry season. The high NO_2^- and NO_3^- indicated that high amounts of fertilizers had been used releasing toxins which harm aquatic life and human health. Wilbers et al. [171] mentioned the NO_3^- concentrations were still slightly higher after treatment while other parameters were reducing such as EC, NH_4^+, NO_2^- in surface water in the VMD. It was also found that most of these components appeared in cluster 1 in which most of the sampling sites were located in secondary canals inside the full-dike protection system.

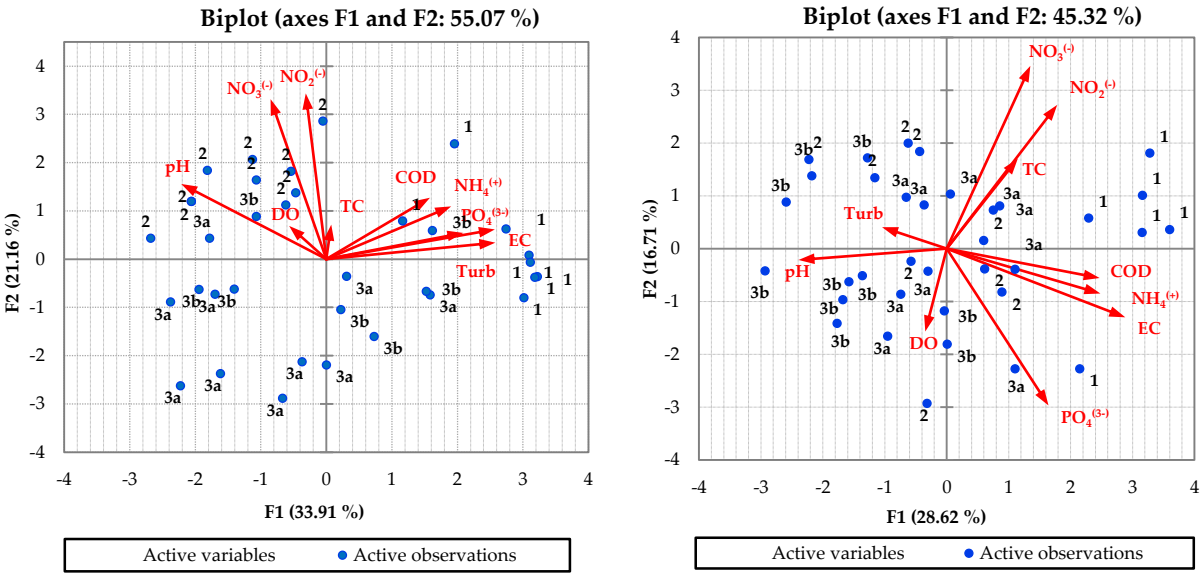

Figure 3.7 PC1 and PC2 loading of water parameters (a) in dry season and (b) in wet season. **(a)** shows a new coordinate axis in which F1 and explained 33.91% and 21.16%, respectively. The high variation of EC, Turb, PO_4^{3-} were found. Cluster 1 obtained high EC, Turb, COD, and NH_4^+. **(b)** shows a new coordinate axis in which F1 and explained 28.62% and 16.71%, respectively. The concentrations of EC, NH_4^+, COD, NO_2^-, and $NO_3^{(-)}$

were high variation in the wet. Cluster 1 has also high EC, NH_4^+, and COD in the wet season. DO and TC were low variation in two seasons.

In the wet season, PC1 explained 28.62% of the total variance and was mostly positively contributed by mineral (EC) and inorganic matters (COD, and NH_4^+), but negatively contributed by pH. This component revealed the importance of inorganic components over the physical-related water qualities except for pH. The PC2 in the wet season was explained by 16.71% of total variance and was highly positively contributed by inorganic nutrient-related water quality parameters (NO_2^-, and NO_3^-) and highly negatively contributed by PO_4^{3-}. These components demonstrated that DO, turbidity, and TC were less important in accounting for water quality variance. Also, these components showed the higher EC and inorganic components (COD, NH_4^+, NO_2^-, and NO_3^-) which were found in clusters 1 where most of the sampling sites were located in the secondary canal inside full-dike.

As shown in Figure 3.7, the first component (PC1) and the second component (PC2) were highly influenced by most of the variables in both seasons. However, this result explains the difficulty in identifying which parameters are more important than the others in influencing water quality variations in this study. Therefore, we conducted principal factor analysis (PFA) to circumvent the ambiguity in the data. Table D1 showed the correlations between variables and factors for each season. In this study area, we applied the 85% correlation coefficient value that indicates the importance of water quality parameters for seasonal variations. Thus, EC, turbidity, NO_2^-, and NO_3^- were identified as the most important parameters that positively contributed to water quality variations in the dry season. In the wet season, only EC was identified as the most important parameter to water quality variations. Therefore, this further

reveals that EC is always an important factor for water quality variations in the study area for both seasons. It should be noted that EC values in water inside full-dike were different compared to inside semi-dike and outside dike. Mean EC values were often extremely high compared to other sites. For example, Mean EC values inside full-dike were 480 S/cm and 330 S/cm in the dry and wet seasons, respectively, which highly exceed those of inside semi-dike and outside of dike (Table E1,E2).

3.3.4 Water quality assessment

Table 3.1, Figure 3.8, and Figure 3.8 show the water quality index for the protection of aquatic life, WQI_{al}. In the dry season, most clusters were identified as "poor" water quality level; an especially low-grade in cluster 1 was detected (WQI_{al} = 3.5 and 5.7-grades, respectively). Moreover, cluster 1 was identified as "poor" water quality with a very low-grade in both dry and wet seasons. Although cluster 2 was found to have slightly low values of NO_3^- and PO_4^{3-} in the wet season, cluster 2 was considered as a "poor" water quality level in two seasons. The WQI_{al} in cluster 3b was also considered as a "poor" level of water quality in dry and wet seasons even though the QWI_{al} was close to "moderate" threshold in the wet season. Only WQI_{al} in clusters 3a was approximately 7-grade in the wet season and was identified as a "moderate" water quality. The water quality of most sites in cluster 3a in the main river and the main canal and inside semi-dike was found to be of better quality compared to cluster 3b. In cluster 3b, high turbidity concentration in the wet season was found in most sites in primary canals. The poor water quality level is due to the increased use of chemical fertilizers and pesticides, as well as the discharge controlled by the sluice-gates operations calendar [133,172].

Table 3.7 Water Quality Index for aquatic life (WQIal) in An Giang.

Clusters	**Cluster 1**	**Cluster 2**	**Cluster 3a**	**Cluster 3b**
Dry season	3.7	4.2	5.4	4.8
Wet season	4.7	6.2	**7.1**	6.4

Note: 10 – 9 for high quality, 9.5 – 9 for good quality, 9 – 7 for moderate quality, and < 7 for poor quality

Cluster 1 is the most significant discriminant among clusters (Figure 3.8 and Figure 3.9) and was considered as a water quality hotspot for the protection of aquatic life. Majority of sampling sites in cluster 1 lie in the secondary canal (field canal) and inside the full-dike system. The poor water quality in this cluster is due to the increasing use of chemical fertilizers and pesticides in the area.

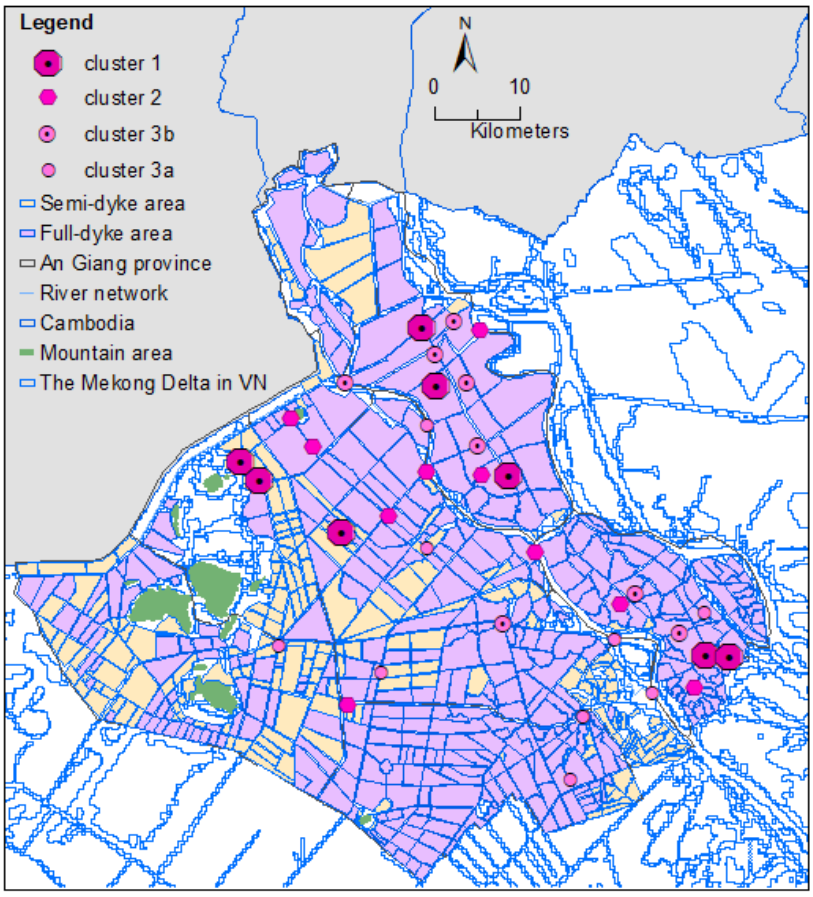

Figure 3.8 Distribution of surface water quality in dry season obtained by cluster.

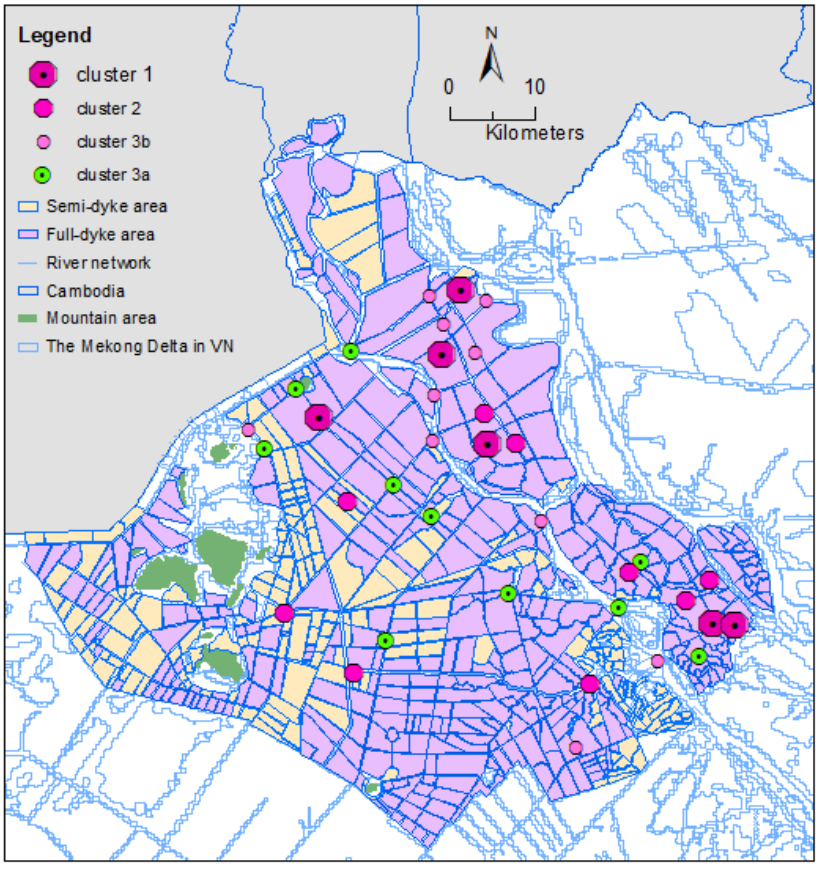

Figure 3.9 Distribution of surface water quality in wet season obtained by cluster

3.4 Discussion

Knowledge on water quality change inside dike protected area is important for further sustainable development in this study area. We used multivariate statistics on ten water quality parameters to examine their spatio-temporal variation in the study area during the dry and wet seasons in 2017. Overall, it was detected that water quality parameters varied widely between the wet and dry seasons. Also, the protected area inside the full-dike systemwas characterized with higher pollution load than that in semi- and outside dike systems, which is discussed in detail below.

The study area belongs to the Mekong River basin, and thus this study was affected by characteristics of water inflow and its quantity from the upper basin of the trans-boundary river system [165,173]. In this study, the concentrations of COD, NO_3^-, and NH_4^+ in the wet season are higher than in the dry season (Figure 8). It is possible due to the potential influence from inflow water quality in the upper Mekong river basin. Chea et al [2] revealed that in the upper part of the Lower Mekong Delta basin, the higher T-P and lower DO concentrations were found in the wet season compared to the dry season and the author explained that the low DO concentration in Cambodia was affected by agricultural, domestic, and industrial zones in Cambodia, during 1985-2010. Low DO, and high concentrations of T-P, NO_3^-, and NH_4^+ might affect aquatic life and human health, respectively [174]. Besides, the NH_4^+ concentration was quite similar in two seasons which was found for the whole Mekong river basin [2].

The PCA found that the EC seems more likely to be positively correlated with diversified water parameters in both the seasons compared to others. Thus, it might be the crucial parameter in both the wet season and dry season. This result

agreed with the result of Al-Mukhtar et al. [175]. They showed that EC and total dissolved solids (TDS) were important parameters. Moreover, [176] also detected that EC and TDS essentially influenced concentrations of DO and BOD. However, DO concentration was not found to have a significant correlation with any other water quality parameters in both seasons. It is possible that some other factors may have had effects on DO concentration such as water temperature, photosynthesis from aquatic plants, TSS, BOD, and river discharge although water level and river discharge may control the majority of water quality by the dilution of nutrient concentrations at a seasonal scale [177–179]. Also, Evtimova et al. [177] found that increased water level has a positive effect on the water quality in Lake Poyang, China. For example, water quality was best in summer, second best in autumn, and then in winter. However, in this study, the mean concentrations and standard deviations of COD and NH_4^+ were higher in the wet season compared to those in the dry season. The mean concentrations of COD and NH_4^+ in the wet season were higher than that in the dry season. It might be partly affected by other sources of pollution by the upstream of the Mekong River basin. For example, the mean of COD concentrations in cluster 1 were 18 mgL^{-1} (SD = 5.25 mgL^{-1}) and 39.67 mgL^{-1} (SD = 13.37 mgL^{-1}) in the dry and wet seasons, respectively (Table E1,E2). The NH_4^+ concentrations were 1.23 mgL^{-1} (SD = 0.5 mgL^{-1}) and 0.43 mgL^{-1} (SD = 0.18 mgL^{-1}) in the dry and wet seasons, respectively. Similar to cluster 1, high concentrations of COD and NH_4^+ were found in the wet season in clusters 2 and 3 (a, b). Moreover, rainfall runoff dissolves and washes downstream toxic wastes and pollutants from various sources in the rainy season, for example, agricultural fields. These wastes, in turn, affect the water quality and cause variation in water quality parameters between the wet and dry seasons. Chea et al. [2] also found that the concentration of T-P

slightly increased during the rainy season in the Lower Mekong river basin due to the combination effect from upstream flow and inside study area.

Based on the WQI_{al} result, the "poor" surface water quality level was detected inside the full-dike system in An Giang province. Cluster 1 was identified as a hot-spot region with sites located inside the full-dike area. Cluster 1 had high nutrient (N and P) in the dry season and NH_4^+, COD in the wet season. Furthermore, cluster 1 was identified as the most significant discriminant among clusters. The high nutrient in the dry season may be explained by wastewater discharged directly into the canal system from fishponds in the secondary canals, and households and markets in the primary canals. People often live along riverbanks of primary canals for their water livelihoods. And, farmers often construct minor canals (or ditches) for irrigation and drainage from their rice fields [6]. Thus, fresh water resources inside the dike system were not very suitable for aquatic life during the study period. Moreover, the water quality in the main rivers may have affected the spatial variations although other regions were considered as having "moderate" water quality level such as cluster 2 in the wet season. The impact of water quality could be associated with water level stability, and its discharge operation is often based on the sluice-gates operations calendar [133,172]. The minimum WQI_{al} value was found at cluster 1 with sampling sites in the secondary canals and inside the full-dike system protection area. These sites received large amounts of nutrients and chemical pollution from chemical fertilizers or pesticides from rice fields. The dike systems can protect productivity and provide support for rice intensification; however, they adversely affect the maintenance of water quality within the region.

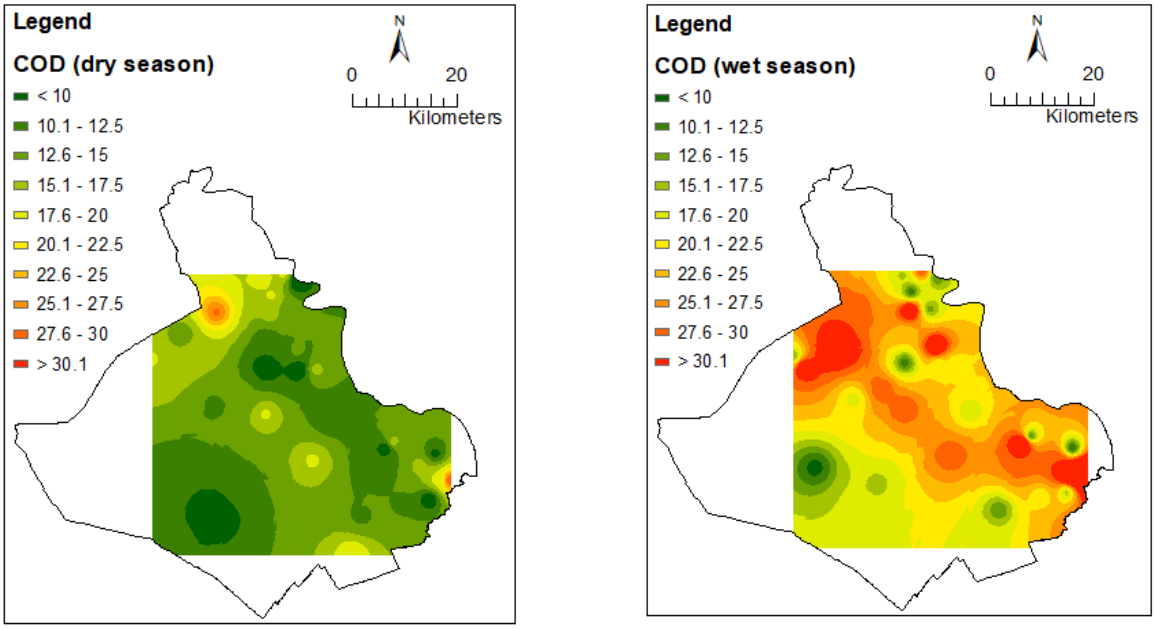

(a) (b)

Figure 3.10 Concentrations of COD were displayed by IDW: (a) in the dry, (b) and in wet seasons, An Giang province, 2017.

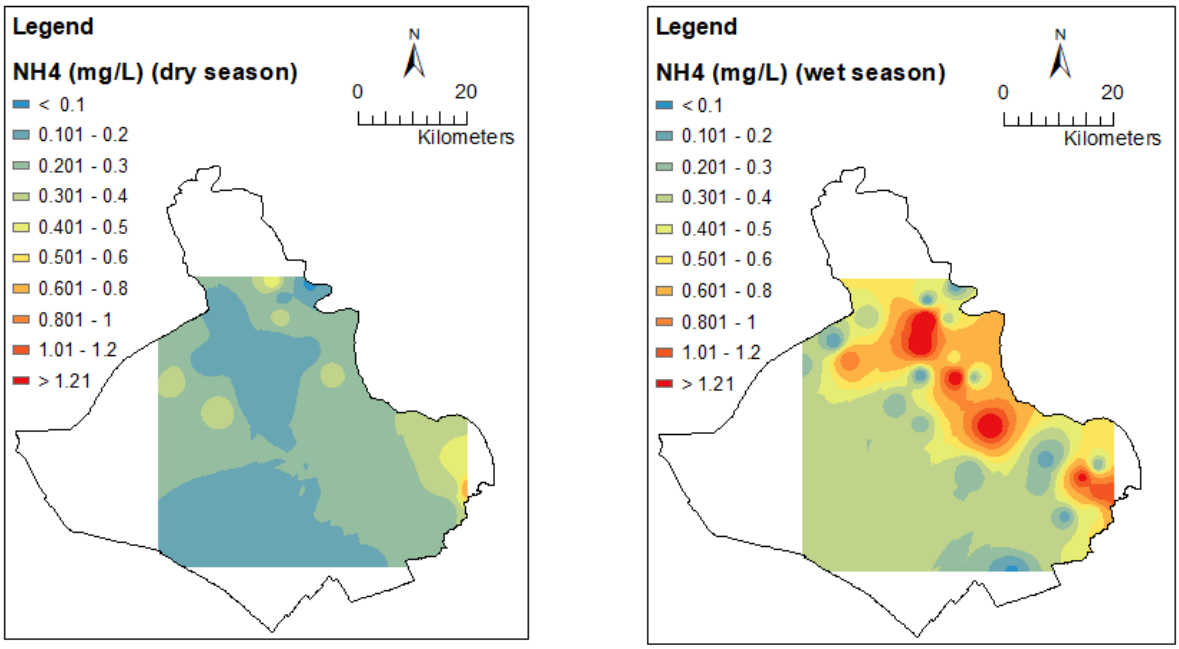

(a) (b)

Figure 3.11 Concentrations of NH_4^+ were displayed by IDW: (a) in the dry, (b) and in wet seasons, An Giang province, 2017.

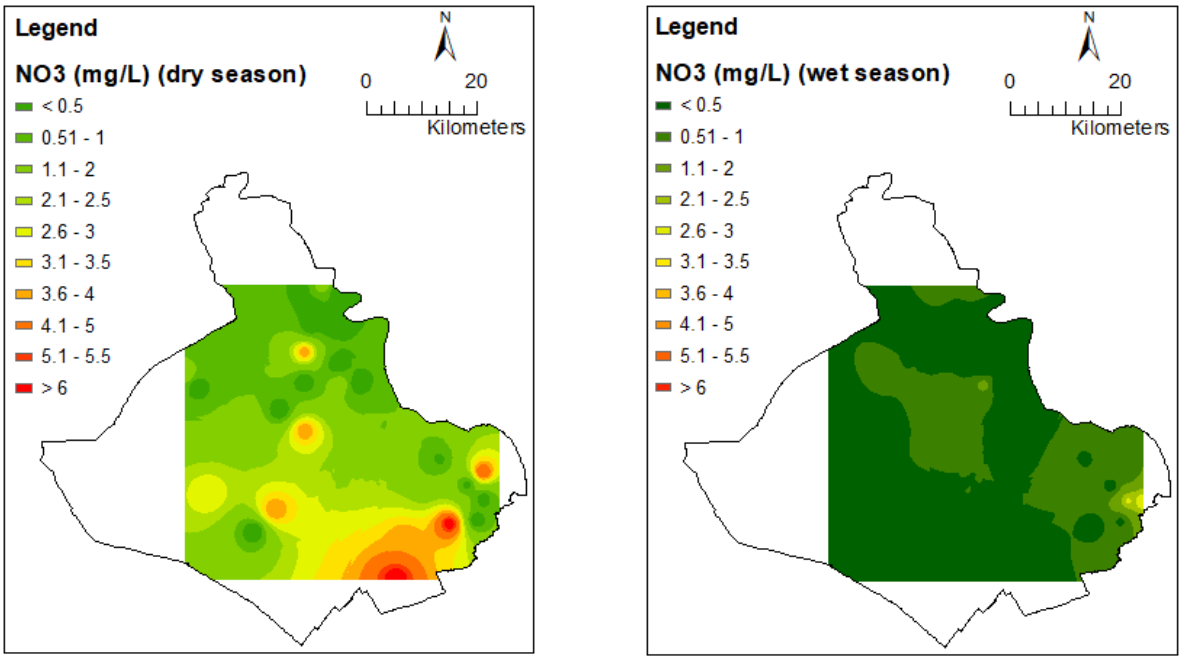

(a) (b)

Figure 3.12 Concentrations of NO_3^- were displayed by IDW: (a) in the dry, (b) and in wet seasons, An Giang province, 2017.

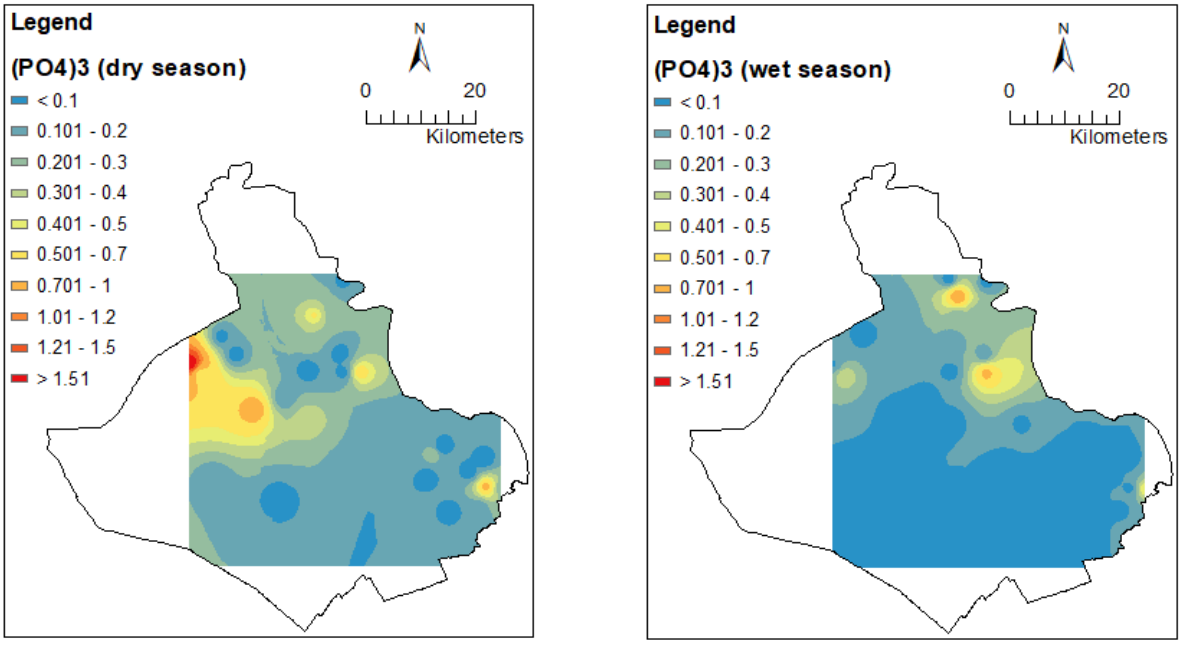

(a) (b)

Figure 3.13 Concentrations of PO_4^{3-} were displayed by IDW: (a) in the dry, (b) and in wet seasons, An Giang province, 2017.

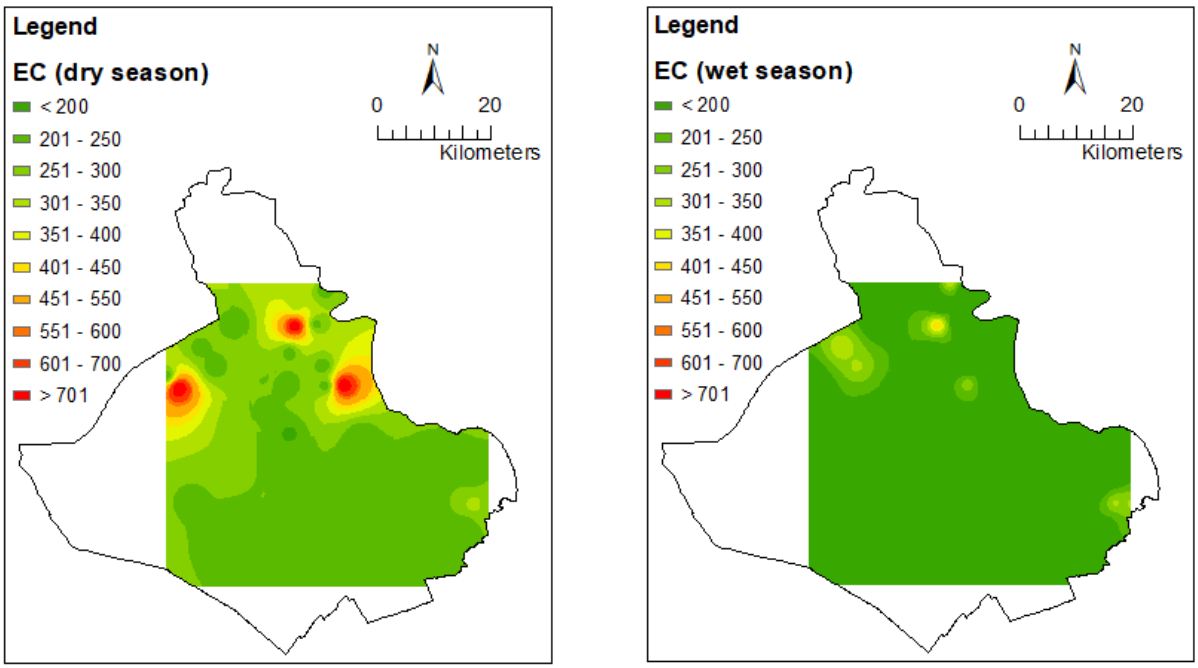

(a) (b)

Figure 3.14 Concentration of EC were displayed by IDW: (a) in the dry, (b) and in wet seasons, An Giang province, 2017.

Chapter 4. Groundwater quality assessment using Fuzzy-AHP in An Giang province of Vietnam

4.1 Introduction

Multiple criteria decision-making (MCDM) is a selective model used for evaluation of many complex decisions [180,181]. The Fuzzy Analytic Hierarchy Process (Fuzzy-AHP), based on AHP under fuzzy environment, is one of the most robust and flexible MCDM tools in the evaluation procedure [181,182]. In 1980, a simple AHP method was introduced based on a ratio scale [181,183,184]. The method was commonly applied in previous studies with advantages such as the simple and flexible model with a wide range of usage [185,186]. The disadvantages of the AHP method include the uncertainty and ambiguity in expressing opinions as the method depends on the decision maker's knowledge and experiences during the decision-making process. Moreover, among other factors, the AHP method does not contain feedback loops [187].

The fuzzy set was first developed by Zadeh in 1965 [184] and combined with Saaty's priority theory to reduce human ambiguity [188,189]. Later, the Fuzzy-AHP was developed in order to overcome the uncertainty and ambiguity of criteria weights in deterministic and inflexible classifications [190]. Using the Fuzzy-AHP can provide fuzzy number, interval judgment values rather than fixed or exactly values [181]. This approach reduces uncertainty in assigned relative weight and therefore, the Fuzzy-AHP was then successfully used in many actual decision situation sections such as energy alternatives selection [191,192], supplier selection [193], environmental sustainability evaluation [186], and water quality assessment [194–197]. Baghapour et al. [194] conducted the Fuzzy-AHP with Fuzzy ordered weighted averaging (FOWA) for developing of

the groundwater quality index (GWQI). They further revealed that it can be able to effectively calculate weights of groundwater quality parameters. Deng et al. [198] used Fuzzy number scales with pair-wise comparisons for solving decision problems involving qualitative data very effectively in Australia. Two of the fuzzy pair-wise comparison and FOWA were used for different water resource assessments such as prioritizing the restoration strategies for Lake Urmia, Iran to avoid shrinkage [197], evaporation estimation [199,200], water consumption prediction [176], rainfall-runoff forecasting and modelling [201–203], and evaluation of groundwater pollution using GWQI [204].

To assess water quality various multi-variate statistical analyses were successfully applied in many previous studies such as groundwater modelling using the principal component analysis (PCA) technique [205]. However, PCA can only reduce the dimensionality of large data sets based on the variation of variables in the new coordinate axis [135,206]. Whereas, the powerful WQI tool can be used to reduce a huge number of parameters into a single number [207]. The WQI method was first developed by Horton in 1965 [208] by using ten parameters of water quality. It has then been widely applied in Asian countries [209]. In 1970, Brown et al. [210] introduced a new WQI which is similar to the index of Horton. Later, many modifications were made for WQI such as the Weight Arithmetic Water Quality Index (WAWQI), National Sanitation Foundation Water Quality Index (NSFWQI), Oregon Water Quality Index (GWQI), and WQI_{al} for aquatic life recommended by Mekong River Commission (MRC) [164,209,211].

In the Vietnamese Mekong Delta (VMD), people rely both on surface and groundwater resources not only for irrigation and aquaculture but also for daily

domestic usage. However, the poor surface water quality (high concentrations of nutrients and metals) in primary and secondary canals due to the release of untreated agricultural runoff, domestic wastewater, and other sources from the upper stream of Mekong river basin [206]; which can pose serious health risks [78,212]. Therefore, groundwater sources serve as one of the main supply for domestic water use and partly for irrigation due to surface water quality often exceeding the permission of the Vietnamese standards for domestic water supply in An Giang in recent years [130]. Very few studies on groundwater quality assessment were conducted, which evaluate the impact of water quality on the health risks of children and adults in An Giang province, especially with regard to As concentration [213]. Furthermore, Thu et al. [214] investigated sources of As contamination in the groundwater in An Phu district of An Giang province. To the best of our knowledge, there are only few holistic studies that evaluate groundwater quality and its evolution process using the GWQI using fuzzy number.

Many studies used the top-down approach in which the fixed weight of groundwater quality is used to calculate the GWQI. For example, Asadi et al. [215] and Maheswaran et al. [216] used the weight of groundwater quality of WHO to calculate the GWQI in Hyderabad and Salem district of India. In this study, we used the bottom-up approach at the local level in terms of weighted values of water quality parameter to find out the locally important groundwater parameters in An Giang. Considering the above gaps, this study focuses on estimating the groundwater WQI (GWQI) by using Fuzzy-AHP to assess groundwater quality in An Giang. Fuzzy-AHP approach is used due to its computational effectiveness in weighted values of water quality selection and its ability to reduce uncertainty from experts' opinions [217,218]. The pair-wise

comparison with triangular fuzzy numbers, along with the weighted arithmetic index methods were used to calculate the GWQI. Inverse distance weighted (IDW) interpolation was used to display variation in spatial and temporal parameters. The findings of this study can provide the status of groundwater quality at a spatiotemporal scale, which would be useful for decision-makers to design timely management plans for water resources and thus minimize any further adverse effect on people's health.

4.2 Study area

An Giang province encompasses an area of about 3,406 sq.km with a total population of about 2 million people in 2017. The province is located at the upper region of VMD, which is comprised of the dense river network system (Figure 4.1). The wet season starts from May to November, and the dry season occurs during December and April. An Giang province is part of agricultural intensification region of VMD, where the water regime is mainly under human control through sluice gates, canals, and dike systems [6,38,66]. The LULC map of An Giang shows the percentage of various LULC classes in 2018 with triple, double, and single-rice crop and other classes cover 46.6%, 24.7%, 7.3%, and 21.4%, respectively [219]. The high irrigated triple and double rice crops occur inside the dike system using surface water, which has negative impacts on surface and groundwater quality especially in full-dike system [206,213,219]. Consequently, the health of two million people in An Giang may be at risk [213,214]. Moreover, the single rice cropping was dominant in the region that is far away from the main river with less river network system. The single-rice cropping area also includes cultivation of rainfed rice in wet season and vegetables in the dry season using groundwater. River discharge data shows a

decreasing trend in the wet season and a slightly increasing trend in the dry season from 2009 to 2017 (Figure 4.1).

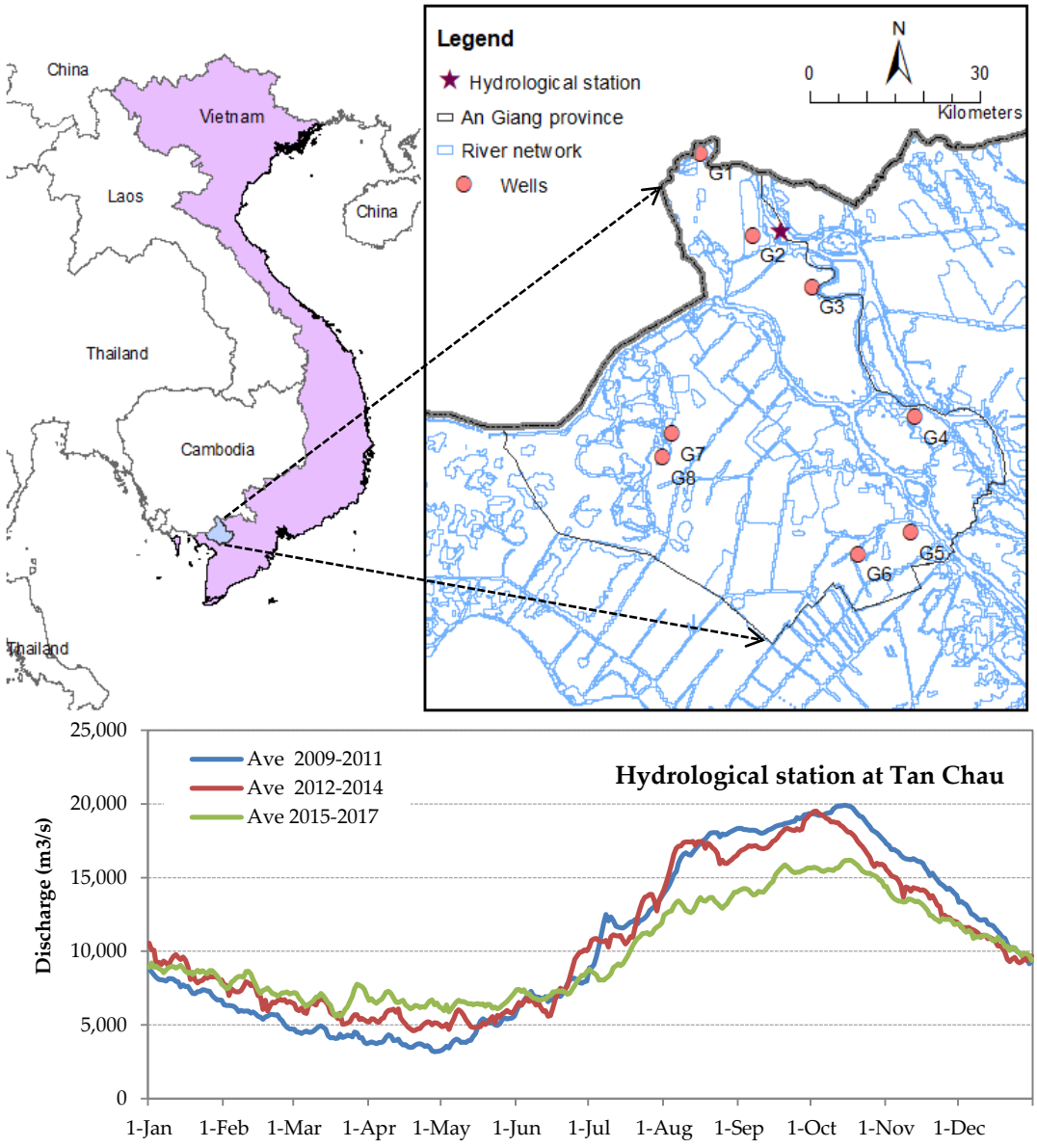

Figure 4.1 Study arae map with location of monitoring wells used in this study. Land cover map collected from Diva-GIS sources.

An Giang province belongs to the Southern part of Vietnam with five main aquifers, namely, the Upper Pleistocene aquifer (qp3), Middle-upper Pleistocene aquifer (qp2-3), lower Pleistocene aquifer (qp1), Medium Pliocene aquifer (n22), and lower Pliocene aquifer (n21) [220]. The groundwater was mostly extracted

water from the Pleistocene and Holocene aquifers supply to domestic and irrigation purposes. In 2014, the total number of existing groundwater wells was 4,746 which include 233 unused/discontinued wells. Out of 4,513 wells, there were 553 wells used for irrigation and 3,960 wells for the domestic water supply [28,221,222].

4.3 Data and Methodology

Groundwater quality data of eight wells were collected from 2009 to 2018 in the wet and dry season from the Department of Natural Resources and Environment of An Giang (DONRE) (Figure 4.1). The depth of G6 and G8 wells (deep well) ranges from 80-300m below ground level lies in the Pleistocene aquifer. Whereas, depth of G1, G2, G3, G4, G5, and G7 wells (shallow wells) are exploited at the average depth of 50m lies in Holocene aquifer. Furthermore, wells G5 and G6 were exploited mainly for industrial zones, while the other six wells supply was used for domestic uses and irrigation. Six groundwater quality parameters were collected viz. As, NO_3, NH_4, $CaCO_3$, total Fe and pH in March and September each year.

Figure 4.2 shows the process to determine the relative weight for each groundwater quality parameter in order to calculate the GWQI. We conducted Fuzzy-AHP, which was developed to weight criteria in decision-making by using the output of the experts' opinions. The weighted value was assigned by pair-wise comparison for each of the six-groundwater quality parameters, including As, NO_3, pH, NH_4, $CaCO_3$, and total Fe. Twenty experts were clustered in 4 groups and the experts in each group compared the parameters by pair-wise variables comparison using fuzzy triangular number scales and four scenarios of pair-wise were obtained. The Fuzzy-AHP process weighting was accomplished

in four steps and groundwater quality index (GWQI) was then calculated [195]. We used inverse distance weighting (IDW) interpolation to display the results of the GWQI.

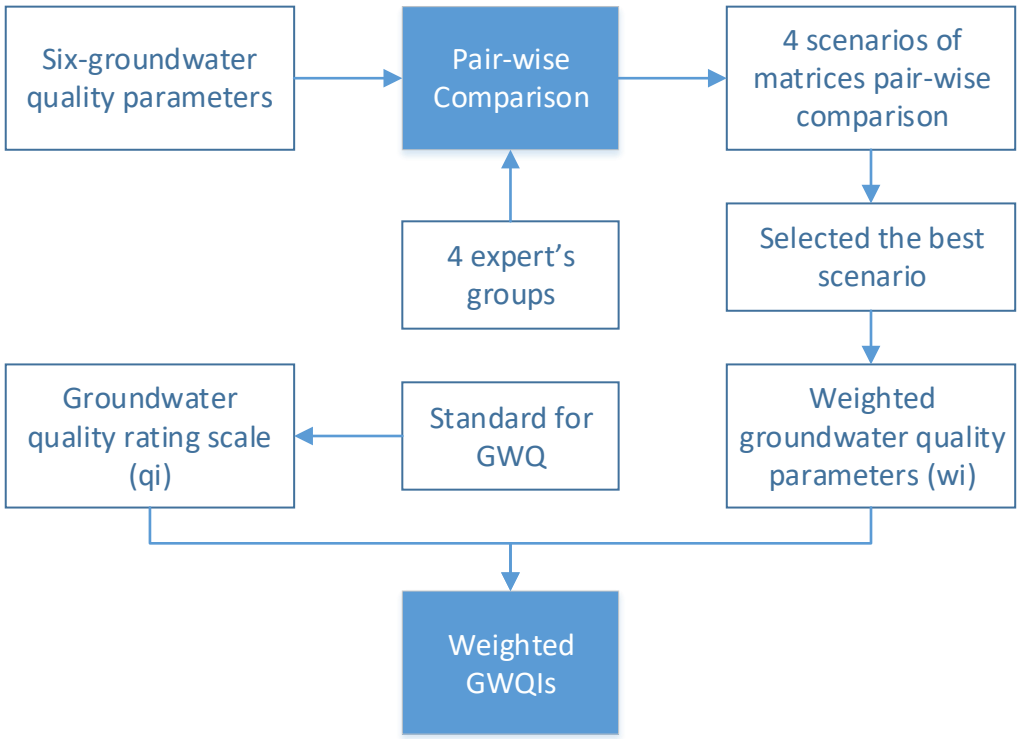

Figure 4.2 Flowchart of study progress of weighted groundwater quality indices by using Fuzyy-AHP.

4.3.1 The Fuzzy- AHP with pair-wise comparison approach

To achieve relative weights of groundwater quality parameters, in the Fuzzy-AHP process was divided into four steps (hierarchy construction development, pair-wise comparisons represented by fuzzy numbers, the fuzzy triangular number calculation, and normalized weights of parameters establishment).

Step1- Hierarchy construction development

We conducted the hierarchy structure composed of three levels as seen in Figure 4.3. The first level is the overall objective to determine the quantification the potential of groundwater resources; the second level is to comparison of

water quality parameters. We used fuzzy triangular number scale which was transferred from linguistic terms scale's Saaty (1980) in Table 4.1 through pair-wise comparisons matrices [183,223]; and finally, the groundwater quality classification is compared based on five-class classes of GQWI.

Table 4.1 Linguistic terms and the corresponding triangular fuzzy scale.

Saaty's scale	**Linguistic terms**	**Fuzzy Triangular Scale (TFN)**
1	Equal importance	(1,1,1)
3	Moderate importance of one over another	(2,3,4)
5	Essential or strong importance	(4,5,6)
7	Demonstrated importance	(6,7,8)
9	Extreme importance	(9,9,9)
2, 4, 6, 9	Intermediate values between two adjacent judgments	(1,2,3), (3,4,5), (5,6,7) and (7,8,9)

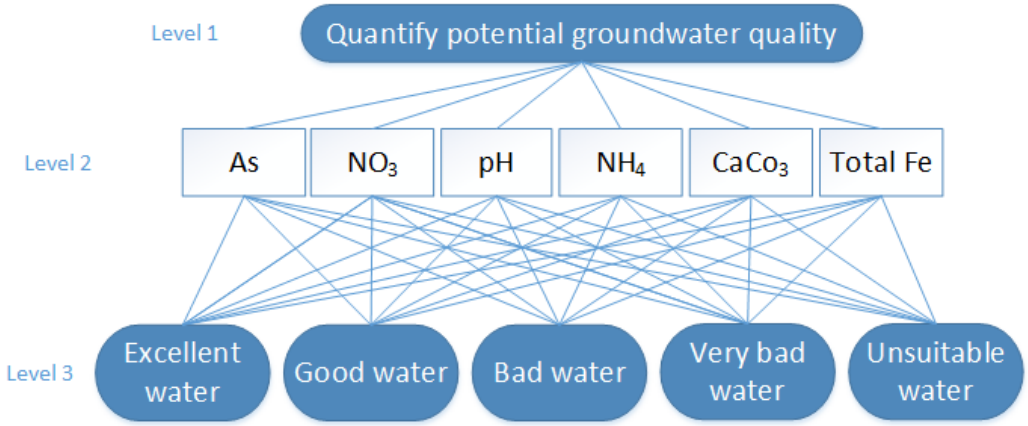

Figure 4.3 The proposed hierarchy structure for performance evaluation process of the groundwater quality assessment

Step 2 - The pair-wise comparisons represented by fuzzy numbers

The Decision Making, comparison of parameters based on the opinions of four experts groups (Professors in Universities, government experts, non-government experts, and water supply companies) [196]. The fuzzy triangular number scales were used to compare between two parameters and find out the more important parameter than another parameter. The parameters are

compared by transfer from linguistic terms to fuzzy number as shown in Table 4.1. The pair-wise contribution matrix is expressed in eq.1. The sensitivity assessment was conducted to reduce the uncertainty of expert's opinions by comparison of parameters' weights in four scenarios based on mean values and standard deviation (SD) and the least SD in the weight change was selected as the optimal relative weight.

$$\tilde{A}^k = \begin{bmatrix} \tilde{d}_{11}^k \tilde{d}_{12}^k \tilde{d}_{13}^k \tilde{d}_{1n}^k \\ \tilde{d}_{21}^k \tilde{d}_{22}^k \tilde{d}_{23}^k \tilde{d}_{2n}^k \\ \dots \quad \dots \quad \dots \quad \dots \\ \tilde{d}_{n1}^k \tilde{d}_{n2}^k \tilde{d}_{n3}^k \tilde{d}_{mn}^k \end{bmatrix} \qquad (1)$$

Where, Tilde (~): the triangular number; $\tilde{d}_{ij}^k$ presents the k[th] decision maker's preference of i[th] criterion over j[th] criterion;
$\tilde{d}_{ij} = \frac{\sum_{k=1}^{K} \tilde{d}_{ij}^k}{K}$ is average decision maker.

Step 3: The fuzzy triangular number determine

The geometric mean technique for computing the weights (W_i) is extended to the fuzzy positive reciprocal matrices [224] and comparison values of each parameter was calculated as shown in eq. 2.

$$\tilde{r}_i = \left(\prod_{j=1}^{n} \tilde{d}_{ij}\right)^{1/n} \qquad (2)$$

Where,
i = 1, 2,… n; $\tilde{r}_i$: triangular values;
Later, replace the fuzzy triangular number by (-1) power of summation vector and finally making it in an increasing order.

Step 4: The normalized weights of criteria

The normalized weight (N_i) was estimated by the corresponding normalized row mean as shown in eq.3.

$$N_i = \frac{M_i}{\sum_{i=1}^{n} M_i} \quad (3)$$

Where,

$M_i = \frac{lw_i + mw_i + uw_i}{3}$; in which $\widetilde{w}_i = \tilde{r}_i \; x \; (\tilde{r}_1 + \tilde{r}_2 + \tilde{r}_3)$;

M_i: non-fuzzy number i, $\widetilde{w}_i$: the fuzzy weight of criterion i; $\tilde{r}_i$: reverse vector.

4.3.2Groundwater quality index (GWQI)

The estimation of GWQI was based on parameter weighting. A weighted value was used by using pair-wise comparison to each other and this assigned weighted value plays a major role in the calculation of the index value (Table 4.2). The limited threshold of quality values was based on the National technical regulation on groundwater quality of Vietnam (standard number 09-MT:2015/BTNMT) [225]. Due to the considered parameters have different units and ranges of values, all parameters must be turned into sub-indices expressed on a single scale. Thus, we calculated based on the following: relative weight (W_{rj}), quality rating scale (q_i), and GWQI.

Table 4.2 Groundwater quality parameters, units and limited threshold values [225]

Parameters	**Units**	**Limited threshold values**
As	mg/L	0.05
NO_3	mg/L	15
pH	-	5.5 - 8.5
NH_4	mg/L	1
$CaCO_3$	mg/L	500
Total Fe	mg/L	5

Relative weight calculation - It was calculated using eq. 4.

$$W_{rj} = \frac{W_j}{\sum_{j=1}^{n} W_j} \quad (4)$$

Where, W_i: the relative weight for the n^{th} parameters and $\sum W_i = 1$; w_i: the weight of each parameter, a number between 0 to 1; n: number of parameters.

The quality rating scale calculation- It was calculated using eq. 5.

$$q_j = \frac{c_{mj}}{c_{sj}} \; x \; 100 \qquad (5)$$

Where, q_i: the quality rating scale for the n^{th} variable ; c_m: the concentration of each parameter in each sample (mg/L), a groundwater threshold values specified by [225] for each parameter (mg/L).

4.3.3 Groundwater quality index calculation

In this study, we calculated GWQI based on the weighted arithmetic index method using eq. 6, which was applied in many previous studies [195,226,227] and classified groundwater quality based on rating values of GWQI in Table 4.3.

$$\mathbf{GWQI} = \sum_{\mathbf{j=1}}^{\mathbf{n}} (\mathbf{W_{rj}} \; \mathbf{x} \; \mathbf{q_j}) \qquad (6)$$

Where, GWQI: Groundwater quality index, a number between 0 to 300 units.

Table 4.3 Water quality classification based on GWQI for human consumption.

GWQI	**< 50**	**50-100**	**100-200**	**200-300**	**> 300**
Quality classification	Excellent	Good	Bad	Very bad	Unsuitable for drinking

4.4 Results

4.4.1 The Fuzzy- AHP with pair-wise comparison

To determine the weighted parameters, 20 experts in four groups were asked to enter into the pair-wise comparison matrix of AHP defined weighting parameters in four scenarios and Table 4.4 shows pair-wise comparison in scenario 3 in which As, $CaCO_3$, and Fe were of "Equal importance" while As was with "Moderate importance" of NH_4 and NO_3, and "Strong importance" with pH. Then four scenarios were defined to

estimate absolute group weights of different parameters obtained from pair-wise comparison as shown in

Table 4.5. Following it, optimal status of decision-making' powers were determined by sensitivity analysis. To reduce the uncertainty of expert's opinion, we have compared all the possible scenarios and calculated sensitivity values for all 6 paired scenarios. Table 4.6 shows the sensitivity comparison among six paired scenarios. It is clearly visible that scenario 3 performed best with the lowest SD (SD=0.007) in sensitivity analysis. Table 4.7 shows Relative weight factors of different **wa**ter quality parameters. As together with Fe concentrations and pH values were the most and least important parameters, respectively.

Table 4.4 Pair-wise comparison in scenarios 3.

Criteria	As	**NO_3**	**pH**	**NH_4**	**$CaCO_3$**	**Fe**
As	(1,1,1)	(2,3,4)	(4,5,6)	(2,3,4)	(1,1,1)	(1,1,1)
NO_3	(1/4,1/3,1/2)	(1,1,1)	(4,5,6)	(1,1,1)	(1/4,1/3,1/2)	(1/4,1/3,1/2)
pH	(1/6,1/5,1/4)	(1/6,1/5,1/4)	(1,1,1)	(1/6,1/5,1/4)	(1/6,1/5,1/4)	(1/6,1/5,1/4)
NH_4	(1/4,1/3,1/2)	(1,1,1)	(4,5,6)	(1,1,1)	(1,1,1)	(1/4,1/3,1/2)
$CaCO_3$	(1,1,1)	(2,3,4)	(4,5,6)	(1,1,1)	(1,1,1)	(1,1,1)
Fe	(1,1,1)	(2,3,4)	(4,5,6)	(2,3,4)	(1,1,1)	(1,1,1)

Table 4.5 Absolute group weights of parameters obtained from pair-wise comparison.

Parameters	**w_j**			
	S_1	**S_2**	**S_3**	**S_4**
As	0.396	0.431	0.265	0.253
NO_3^-	0.075	0.095	0.111	0.136
pH	0.024	0.030	0.038	0.048
NH_4^+	0.068	0.106	0.131	0.125
$CaCO_3$	0.163	0.166	0.219	0.190
Total Fe	0.319	0.241	0.265	0.275
Sum	**1.046**	**1.069**	**1.028**	**1.026**
Mean	**0.174**	**0.178**	**0.171**	**0.171**
SD	0.151	**0.143**	**0.093**	**0.085**

Table 4.6 Scenarios sensitivity analyses results.

Analysis	Compared scenarios			Mean	SD
1	S_1	to	S_2	0.0037	0.008
2	S_1	to	S_3	0.0031	0.058
3	S_1	to	S_4	0.0034	0.065
4	S_2	to	S_3	0.0068	0.050
5	S_2	to	S_4	0.0071	0.058
6	S_3	to	S_4	0.0003	**0.007**
			Min	0.0003	0.007

Table 4.7 Relative weight factors of different water quality parameters.

Parameters	w_j
As	0.258
NO_3^-	0.107
pH	0.037
NH_4^+	0.127
$CaCO_3$	0.214
Total Fe	0.258

4.4.2 Groundwater quality index (GWQI)

The temporal WQI values and percentage of the groundwater samples for different categories for the period of 2009-2018 were presented in Figure F1, 2 and Figure F6, 7. Figure 4.4 and Figure 4.5, respectively. Observed groundwater quality was better in the dry season as compared to the wet season except for NH_4 (Table F3, F4). Minh et al [206] also found NH_4 concentration in surface water in the wet season was higher than in the dry season in An Giang. However, we found that the improvement in water quality took place since the year 2009. The wide range of the GWQI values from 2009 to 2018 shows the best and the worst water quality observed at G_6 and G_4 in two seasons, respectively. In 2018, the GWQI values at G_6 were found to be 47 and 41 units in the dry and wet seasons respectively, while the GWQI at G_4 was detected to be 132 and 76 units in the dry season and the wet season, respectively. Net groundwater quality improvement occurred in most wells during the years 2009-2018 except G_1, G_3 and G_4 in the dry season. For example in the dry season, the "Very bad water" group of G_1, G_3, G_4 experienced 202, 176, 885 units, respectively in 2009, which more improved to be "Good" quality level in 2014 at G1 (GWQI = 67 units)

compared to G_3 and G_4, with WQI values of 102 and 161 units to be "Bad water" quality, respectively (Figure 4.4). However, G_3, G_4 became "Bad water" in 2016 and 2018 while G_1 became "Unsuitable water for drinking" in 2018. Water quality was a better improvement in the wet season as compared to the dry season at G_1, G_3, G_7, and G_8 from "Very bad water" quality level have improved significantly to the "Good water" and "Excellent water" quality level in 2016 and 2018. The water quality of G_4 had not been improved during 2009-2018 in both the seasons. However, G_4 in the wet season has less improved during 2015 and 2018. The water quality in well G_5 in the wet season first declined from 2009 to 2012 but it has not recovered to achieve "Good water" level in 2014 and in 2018. The well G_7 and G_8 improved significantly in quality during 2009 and 2018 in both the seasons (Table F3, F4). Figure 4.5 and Figure 4.6 show the percentage of wells with groundwater quality based on GWQI in the dry and wet seasons respectively. It is found that the percentage of wells in the "Unsuitable water for drinking" to "Very bad" groups was extremely high from 2009 to 2012, with about 39% of wells in the "Bad water" group. The only 25% of wells was considered as "Bad water" level in dry season in 2018.

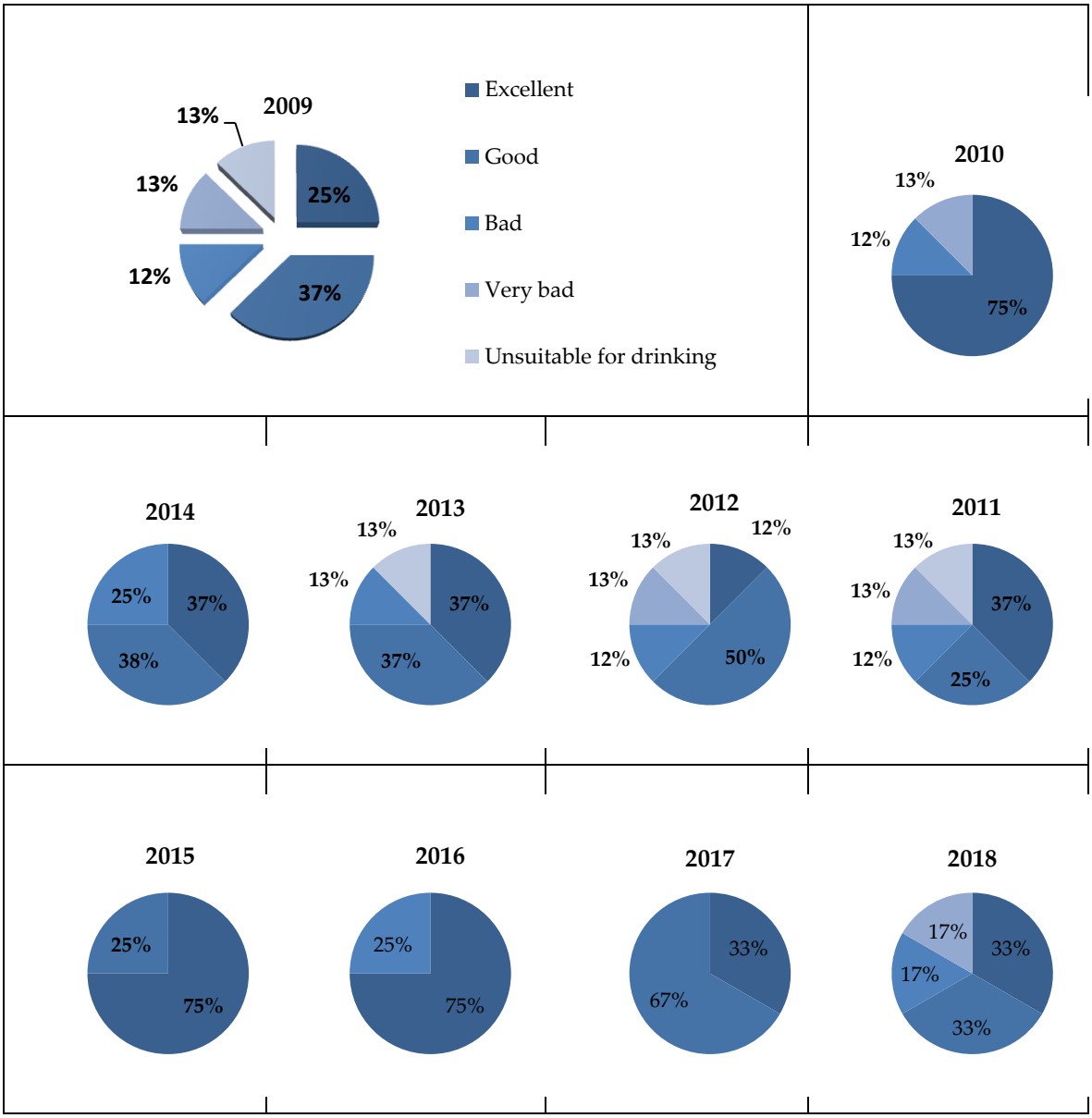

Figure 4.4 Percentage of groundwater quality at eight wells based on GWQI in the dry season during 2009-2018.

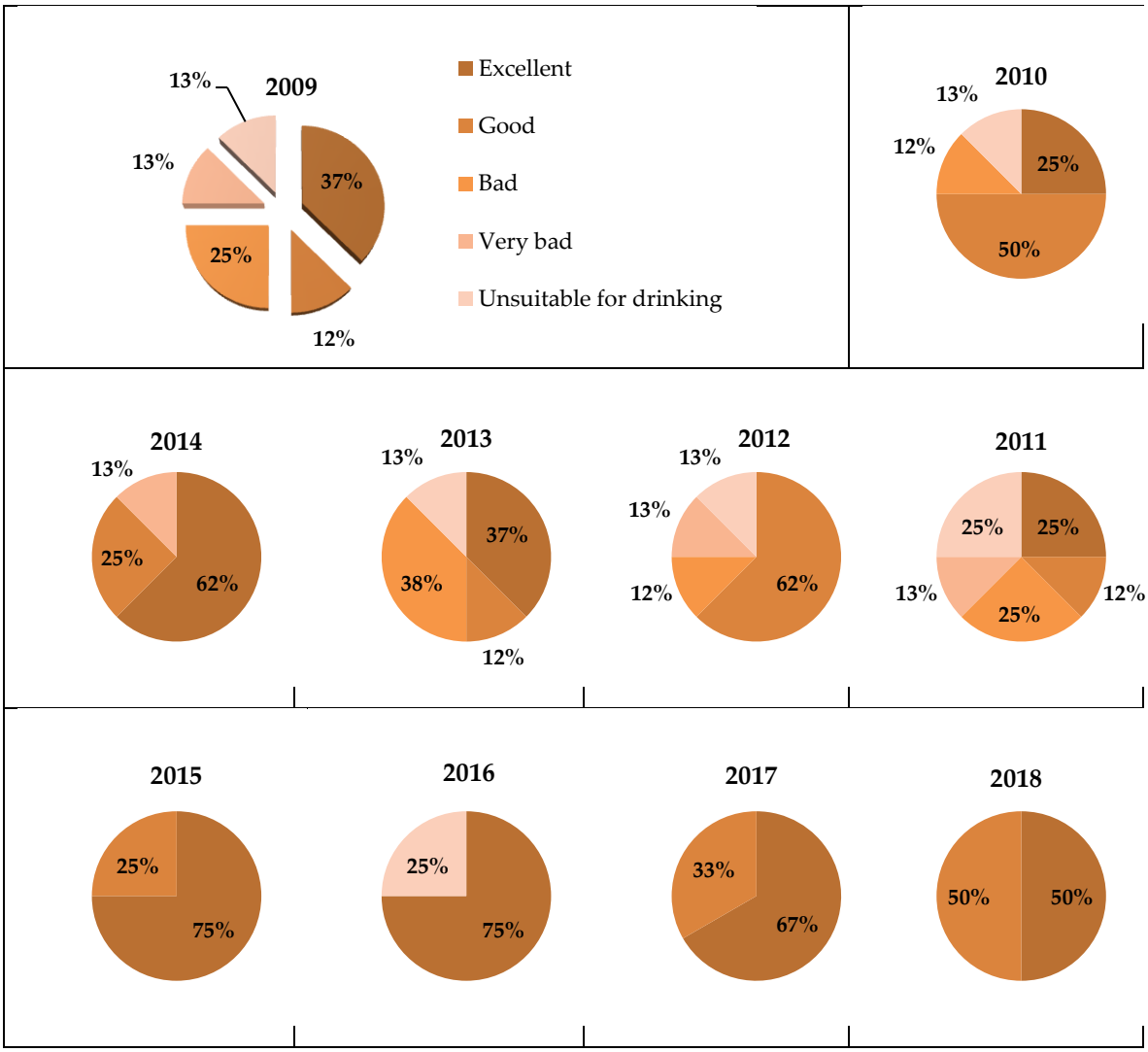

Figure 4.5 Percentage of groundwater quality at eight wells based on GWQI in the wet season, during 2009-2018.

4.4.3 Groundwater quality assessment

GWQI spatial distribution maps were prepared for the years of 2009, 2010 and 2016, and classified in accordance with GWQI rating system shown in Figure 4.6. The spatial distribution maps for As were displayed in Figure F7. It is found that the shallow wells (G_1, G_3, and G_4) had the lowest water quality in different years. However, the water quality of G_1 well has improved in the two seasons since 2014 and has decreased again in the dry season of 2018. The shallow wells G_1 and G_3 are located at the Northeastern part of An Giang, while G_4 is located in the Southeastern part of An Giang. The well G_1, G_3, and G_4 located between and

close to the Mekong and Bassac Rivers. It is well-reported that mobilization is prominent in the river flood plain [228]. Therefore, As concentration is the highest for well number G_1 and G_4, as they are located in the vicinity of river plain. Also, As has the highest weightage among all water quality parameters. High As concentration led to poor water quality.

In general, As values decreased during the period of 2009-2018. The extremely high As concentrations were detected during 2009 and 2010 in both seasons. The highest concentration of As was found in G_4 in 2009 at Cho Moi district located in the Southeast region. The second highest concentration levels of As were identified at well G_1 at An Phu district in the Northeast region. Recent studies by Thu et al. [214], [229] and Anh et al. [213] also showed a high concentration of As in the VMD such as An Giang, following Long An, and Dong Thap provinces. Arsenic above 0.01mg/L was typically found in wells with aquifer of Holocene rather than Pleistocene aquifer.

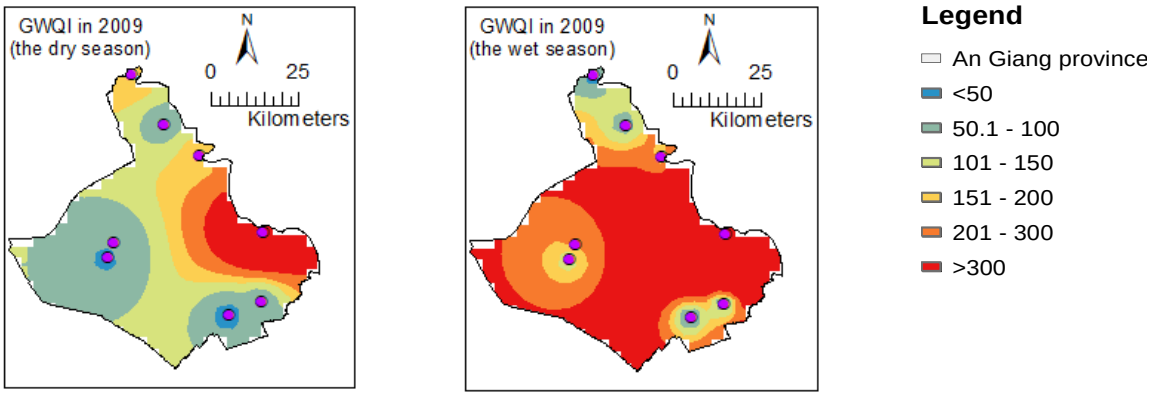

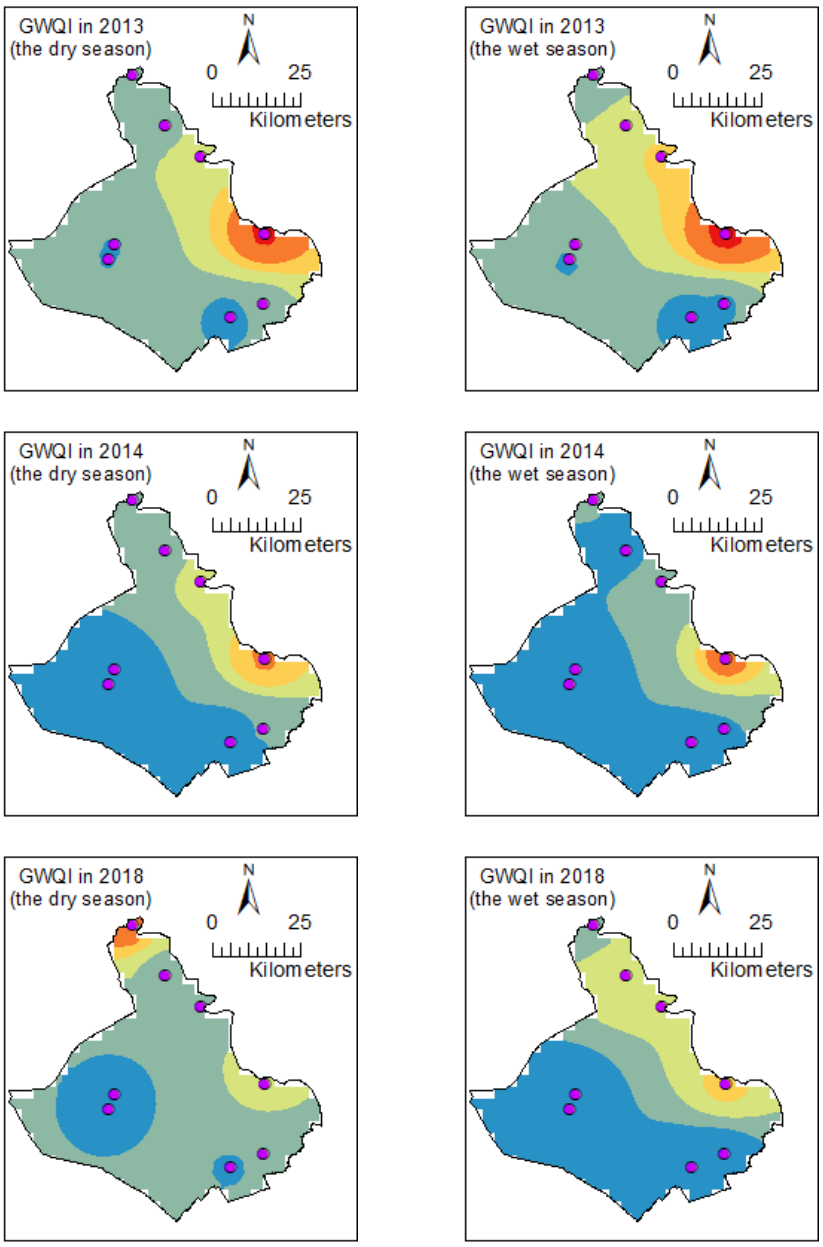

Figure 4.6 The groundwater quality index (GWQI) in An Giang. Notes: <50 (Excellent water), 50-100 (Good water), 100-200 (Bad water), 200-300 (Very bad water), and >300 (Unsuitable for drinking).

4.5 Discussion

The groundwater sources serve as the main supply for domestic use, and partially for irrigation purposes in areas with less river network. Understanding groundwater quality can help policymakers to protect and effectively manage the limited water resources available in the region. There are many water quality

parameters that contribute to groundwater pollution in the study area, each with its own important value. The Fuzzy-AHP technique, a systematic method is an effective tool to weigh multiple parameters in classifying the clear groundwater quality based on GWQI.

For this study, the Fuzzy-AHP considered As and total iron as the most important factors that affect the GWQI, with a weighted parameter of approximately $w_i = 0.258$. Temporal variation of GWQI suggests that the trend of groundwater quality at eight wells improved from 2009 to 2018 due to less sediment deposition and effective environmental management policies in An Giang. The construction of hydropower plants in the upper Mekong River basin caused a decrease in river discharge and sediment deposition in the study area [66,230]. Ngoc et al. [230] predicted the reduction of sediment at Tan Chau station in future due to the expansion of hydropower plant. Arsenic contaminant is often found in natural condition and human activities in Asia countries [231]. In a natural way, As concentration in groundwater resources is found in young Quaternary deltaic and alluvial sediments and As concentration also related to sediment concentration [231,232]. Moreover, Chuan et al. [232] also found the high relationship between sediment concentration and As in China. Figure 7 shows the decreasing trend of suspended solids in surface water from 2005 to 2017 at Long Xuyen station in An Giang which was consistent with the reduction of As concentration in the wet season. Besides the water resources law, decisions related to water and environmental protection was effectively implemented in An Giang. In decision 1566/QĐ-UBND of "Environmental protection planning of An Giang province up to 2020" was issued 2011, limitation of the usage of chemical fertilizers in agricultural activities and raising livestock and poultry

and aquatic products must have waste treatment systems up to standards and environmental sanitation".

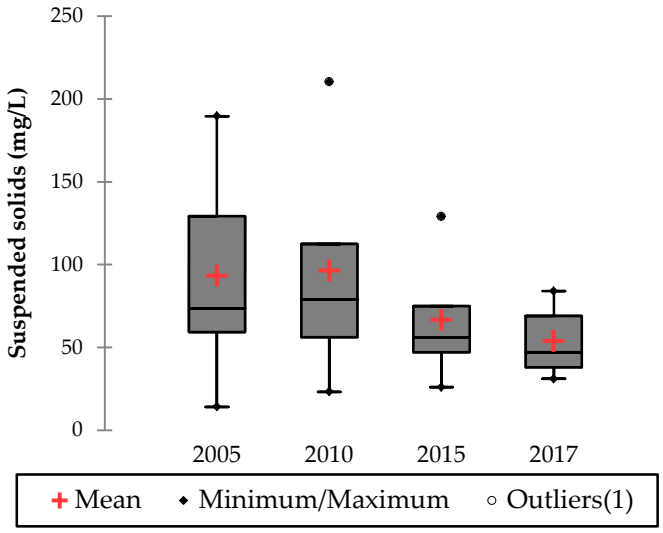

Figure 4.7 Box plot shows temporal changes in suspended solids in 2005, 2010, 2015, and 2017 at Long Xuyen station, An Giang. Data of suspended solids was obtained from the southern regional hydrometeorological center in Hochiminh city, Vietnam.

It should be noted that the quality of groundwater greatly improved from 2014 to 2018 as compared to 2009 to 2013. In 2009, four out of eight wells were identified as "Bad water" quality to "Unsuitable water for drinking" wet season. In 2013, 75% and 50% of wells achieved "Good water" to "Excellent water" levels in the dry season and wet season, respectively. In 2018, water quality of six wells in the dry season and seven wells in the wet season achieved "Good water" to "Excellent water" quality (accounts for 66% in the dry season and 100% in the wet season). However, groundwater quality at well G_4 at Cho Moi district was considered mostly "Unsuitable water for drinking" from 2009 to 2014 and became "Good water" in the wet season in 2018. The shallow wells such as G_1, G_2, G_3, and G_4 achieved a "Bad water" quality with high As concentration lies between Mekong and Bassac Rivers that have huge amounts of sediment deposition in monsoon season. This result agrees with other studies by Hoang et

al. [229] and Vongphuthone et al. [229,231]. Arsenic deposition might be caused by huge amounts of sediment deposition during the monsoon season [229,231,232]. The An Giang government recommends treating As in groundwater at the Holocene and the Upper Pleistocene aquifers before usage in the An Phu, Phu Tan, and Cho Moi districts.

The relationship between GWQI and agricultural intensification was not very clear. For example, high GWQI together with high As concentration was found in the Northeast and Southeast regions of An Giang province. However, the Southwestern side of An Giang province, which includes the Thoai Son, and Chau Phu districts located on the left bank of the Bassac River, has slightly higher GWQI but lower As concentration. These regions mentioned above are not using groundwater for irrigation while triple-rice cropping model is mostly applied. On the other hand, only the regions near mountainous areas such as Tri Ton and Tinh Bien districts, where single-rice was often applied extracted groundwater for irrigation. Furthermore, we detected the high values of GWQI links with high As concentration, where single- and double-rice crop were cultivated. In a nutshell, high As contamination in groundwater was found in agricultural land which used groundwater for irrigation. Findings from Thu et al. supported high As concentration in wells in the Northeast and Southeast regions of An Giang province that are mainly concentrated in the riverside areas with depths of 15 to 36m [214].

The groundwater quality improved in An Giang from 2009 to 2018 mainly due to the effective management of water resources by the An Giang government. Because of high groundwater pollution observed during the mid-2000s, policymakers ordered preventing the use of 1,460 wells during 2005-2009.

The effective implementation of decisions which were issued by An Giang government, such as 69/2010/QD-UBND (in article 8 of chapter 3) and an updated decision version 38/2015/QD-UBND that specified protection of the quality of groundwater by filling unused wells. The government has decided to fill the unused wells to prevent mixing of the pollutants from agricultural activities and human waste with the groundwater. Based on the preliminary data in An Giang, in 2017, less than 300 unused wells needed to be continuously filled.

The use of fuzzy logic seems to be the clearest innovation in the last decade, and its use is appropriate for an accurate GWQI. This approach allows evaluating the impact of each variable on the final index of the quality of the water. However, it remains to establish weighting factors for specific water use. These weighting factors must be locally determined. Also, the weighting partly affects the final index obtained and can change significantly when changing the expert's awareness and perspective. Therefore, the sensitivity assessment was conducted to reduce the uncertainty by comparison of parameters' weights in four scenarios based on mean values and SD. The least SD in the weight change was selected as the optimal relative weight. However, the disadvantage of pair-wise comparison is the need to repeat calculations as it follows the same step as the pair-wise comparison of each water quality parameters.

Although As concentration was under the permissible limits of the National technical regulation on groundwater quality (0.05mg/L). However, it still exceeds the World Health Organization (WHO) permissible limit i.e. 0.01 mg/L [233]. There is insufficient evidence to conclude whether agricultural activity affects the aquifer. However, we detected a high level of As in regions practicing agricultural production with the extraction of groundwater for irrigation. Many

types of setup time reduction problems can be solved by using Multiple Criteria Decision Making (MCDM) techniques such as Fuzzy-AHP, but they must be utilized according to the suitability of the problem in order to develop the best decision.

Chapter 5. Conclusions

We conducted the study to examine the effect of the dike system on rice cropping patterns and on surface and groundwater quality during 2017-2018. We successfully applied Sentinel-1A for monitoring rice phenology and mapping for rice cropping systems under water-control infrastructure by using radar backscattering. To examine the surface water quality parameters in terms of spatio-temporal variation, multivariate statistical analyses were used. Also, the Fuzzy-AHP and GWQI methods were conducted to an assessment of groundwater quality links to rice cropping system distribution.

Regarding rice phenology, the behavior of backscattering of Sentinel-1A SAR data showed a good relationship with rice phenology change in the three rice cropping systems. Sentinel-1A can detect rice growth stages and patterns which matched well with the crop calendar. Although the σ^{o}VH strongly correlated with the three rice growth stages compared σ^{o}VV, both of them are also strongly correlated in the reproductive stage because of the reduction in soil moisture and water drainage in the rice fields. Since we considered all the general rice patterns throughout the study, we found that the average maxima of VH polarization are higher than other crops in the winter-spring season. The mean of maximal values of VH polarization is also higher in the double-rice copping system than in other cropping patterns. We detected that the Sentinel-1A with dual polarization (VV and VH) is useful to distinguish various growth stages of rice cultivation and rice cropping patterns.

The above finding is associated with rice cropping pattern distribution under water infrastructure of An Giang province. Triple-rice crop is present in

the full-dike system and is close to the Bassac and Mekong Rivers with an abundant supply of irrigation water. Double-rice crop areas are located in semi dike, which is away from the main river compared to the triple-rice cropping system. However, the cultivation model of two rice crops per year was found next to the main rivers inside full-dike due to the three-three-two cropping cycle application in full-dike. The reason is the last year of three-three-two cropping cycle model; the double-rice pattern was applied in during study period.

The classification approach yielded an overall accuracy of 80.7% with 0.78 Kappa coefficient. The misclassification was mainly found in the triple-rice cropping system. The further work is needed regarding the use of TanDEM-X, RADARSAT-2, and PALSAR-2 which can be incorporated to improve identification of various growth stages and enhance accuracy for detection of rice cropping patterns. Polarimetric decomposition algorithm can also be used to detect various objects more accurately in the future.

The HCA and WQI al method was used to divide the sample sites into 4 clusters and cluster 1 showed “poor” water quality levels with reference to WQIal grades in both the dry and wet seasons. The most sample sites in the cluster 1 water samples inside the full-dike system and located in the secondary canal where triple-rice cropping system was dominant. Cluster 3a in wet season includes 7 out of 10 sites located in semi- and an outside dike was considered as “moderate” water quality level. Although water quality depends on other pollution sources besides rice cultivation, this study showed that the water quality in the full- dike area was more polluted than the semi-dike and outside of the dike system.

The concentrations of water quality parameters were generally lower in the wet season than during the dry season because of high runoff causing the dilution of water quality parameters. An extremely high concentration of PO_4^{3-} occurred during the dry season in the Northwest of An Giang, which is a tourist area with mainly lots of human waste since that time of rice sowing with less fertilizer usage. Moreover, the double-rice cropping system was applied in many rice plots in the Northwest while triple-rice cropping system was dominant at that time in the Southwest of An Giang. A high concentration of NO_3^- was found inside the full-dike area located in the Thoai Son district, in the Southwest region of the province, during the dry season. This district contains the largest triple-rice crop area in An Giang. However, the concentrations of COD and $NH4^+$ in the wet season were higher in value when compared with those in the dry season. The reason behind that might be partly affected by other sources of pollution upstream of the Mekong River basin, due to the trans-boundary nature of the river systems.

The limitation of the study was that the survey was done with 35 water sampling site for each season. Therefore, we only concluded surface water quality during the study as the first step of surface water quality assessment situation in An Giang. For the next step, we suggest that water quality in areas inside full dike-protected systems should be continuously monitored in both seasons especially PO_4^{3-} in Northeast An Giang and NO_3^- in Southwest An Giang during the dry season. With regard to the findings of high concentrations of NH_4^+ and COD in the Bassac River area during the wet season, we suggest monitoring water quality in the upper Mekong River basin. There is also a need to monitor water quality in the region using a real-time remote data acquisition system that is able to provide data in a timely fashion at a large scale.

The most important reasons for the poor groundwater quality were the combined effect of both natural and human activities. The lithological structure (sediment deposition) and leaching of chemicals from agricultural runoff might go to groundwater aquifers. The As contaminant from sediment concentration was often found in the shallow aquifer. In the recent year, less sediment deposition causing less As concentration. Besides, the An Giang government implemented the effective management of unused water wells by placing restrictions on filling the unused wells in these agricultural areas. Although enhancing the management of unused wells did not eliminate the contamination, but it can improve aquifer water quality. The effective management of no-longer-exploited wells is one of the factors that An Giang government can do to improve groundwater quality in the periods of 2009 to 2018. However, considering the shortcoming of this management plan, this study will be able to help policymakers to make some future plans such as conducting suitability analyses of all groundwater quality in different sectors. Another possible area of research is to look for the willingness of farmers to switch to different cropping patterns by growing crops with less water demand as mitigation measures in regions where groundwater has high As concentration.

The GWQI based on the Fuzzy-AHP was successfully applied to assess groundwater quality in An Giang, a province belonging to the VMD. The weighted parameters via a bottom-up approach provided a better understanding of water quality issues at the local level. Including more monitoring wells should be encouraged for diligent and regular monitoring. This will help in developing a more reliable GWQI in the future. Regarding the method of Fuzzy-AHP, to reduce uncertainty at the first stage in terms of pair-wise comparison, it should be noted that it is necessary to consider more scenarios. Furthermore, we need to

consider degrees of confidence and attitudes of experts. Also, we should compare the weighted arithmetic index method to other methods in terms of the weighted parameter values.

Dike protection systems have been useful in reducing flood hazards and supporting the intensification of rice cropping; however, they have adversely affected the maintenance of surface water quality within the region. We do not have enough evidence to show whether the dike system and the rice cropping system effect on groundwater quality because it depends on the characteristics of the aquifer. However, we found that the areas with underground waterfalls for irrigation, the groundwater quality was worse than other areas during the study period. In recent years, the area of triple-rice crops in full-dike in An Giang has reduced, which might help to restore surface water and soil quality. Interestingly, we noticed an increasing trend of traditional rice crop cultivation after 2013. This change has been detected in recent years; however, we expect that An Giang will be able to retrieve the single-rice crop to enhance the environment of water resources and keep traditional rice culture in the future.

References

1. Minh, N.T.H.; Kawaguchi, T. Overview of rice production system in the Mekong Delta-Vietnam. *Journal-Faculty of Agriculture Kyushu University* **2002**, *47*, 221–231.
2. Chea, R.; Grenouillet, G.; Lek, S. Evidence of Water Quality Degradation in Lower Mekong Basin Revealed by Self-Organizing Map. *PLOS ONE* **2016**, *11*, e0145527.
3. General Statistics Office Of Vietnam (GSO). *Statistical Yearbook of Viet Nam 2016*; General Statistics Office Of Vietnam (GSO), 2016;
4. Toan, T.Q. Climate Change and Sea Level Rise in the Mekong Delta: Flood, Tidal Inundation, Salinity Intrusion, and Irrigation Adaptation Methods. In *Coastal Disasters and Climate Change in Vietnam*; Thao, N.D., Takagi, H., Esteban, M., Eds.; Elsevier: Oxford, 2014; pp. 199–218 ISBN 978-0-12-800007-6.
5. Mekong delta Plan (MDP). *Long-term vision and strategy for a safe, prosperous and sustainable delta*; Amersfoort, Netherlands, Consortium Royal HaskoningDHV, WUR, Deltares, Rebel.; 2013;
6. Tuan, L.A.; Minh, H.V.T.; Tuan, D.D.A.; Thao, N.T.P. *Baseline study for community based water management project*; Mekong Water Governance Program Vietnam, 2015;
7. Can Tho University (CTU); DANIDA *Flood Forecasting and Damage Reduction Study in the Mekong Delta*; Can Tho University Viet Nam, 1996;
8. General Statistics Office Of Vietnam (GSO). *Statistical year book of Viet Nam 2014*; General Statistics Office Of Vietnam (GSO), 2014;
9. Minister of Agriculture and Rural Development (MARD) The action plan framework for adaptation to climate change in the agriculture and rural development sector period 2008-2020 2008.
10. Ministry of Planning and Investment (MPI). Decree 2006.
11. Liew, S.C.; Kam, S.P.; Tuong, T.P.; Chen, P.; Minh, V.Q.; Lim, H. Application of multitemporal ERS-2 synthetic aperture radar in delineating rice cropping systems in the Mekong River Delta, Vietnam. *IEEE Transactions on Geoscience and Remote Sensing* **1998**, *36*, 1412–1420.
12. Vietnamese Government National Strategy on Climate Change 2011.
13. General Statistics Office Of Vietnam (GSO). *Statistical Yearbook of Viet Nam 2014*; General Statistics Office Of Vietnam, 2014;
14. Ni, D.V.; Maltby, E.; Stafford, R.; Tuong, T.P.; Xuan, V.T. *Status of the Mekong Delta: Agricultural Development, Environmental Pollution and Farmer Differentiation*; Wetlands management in Vietnam: Issues and perspectives: Viet Nam, 2003;
15. Hung, N.N.; Delgado, J.M.; Güntner, A.; Merz, B.; Bárdossy, A.; Apel, H. Sedimentation in the floodplains of the Mekong Delta, Vietnam Part II: deposition and erosion. *Hydrological Processes* **2014**, *28*, 3145–3160.
16. Manh, N.V.; Dung, N.V.; Hung, N.N.; Merz, B.; Apel, H. Large-scale suspended sediment transport and sediment deposition in the Mekong Delta. *Hydrol. Earth Syst. Sci.* **2014**, *18*, 3033–3053.

17. Nguyen, Q.T. Outcomes of Vietnam's Agrarian policies after "Doi Moi": A case of attempted agricultural intensification in a village in Vietnam's Mekong Delta. *Global journal of human social science arts and humanities. Global journal* **2013**, *13*.
18. Pham, C.H. Planning and Implementation of the Dyke Systems in the Mekong Delta, Vietnam. Dissertation, Bonn University: Germany, 2011.
19. Miller, F. *Environmental risk in water resources management in the Mekong delta: A multiscale analysis*; I.B. Tauris: London, 2006; Vol. 1; ISBN 978-1-85043-445-0.
20. Kono, Y. Canal development and intensification of rice cultivation in the Mekong Delta: a case study in Cantho Province, Vietnam. *SoutheastAsian Studie* **2001**, *39*, 70–85.
21. Le Meur, P.Y.; Hauswirth, D.; Leurent, T.; Lienhard, T. *The local politics of land and water: Case studiesfrom the Mekong delta*; Groupe de Recherche et d' Echanges Technologiques, 2005;
22. Tran, V.H. Understanding farmer production strategies in context of policies for adaptation to floods in Vietnam Case study at two communes, An Giang province, Vietnam. Thesis, Swedish University of Agricultural Sciences: Swedish, 2011.
23. Sakamoto, T.; Phung, V.C.; Nhan, V.N.; Kotera, A.; Yokozawa, M. Agro-ecological interpretation of rice cropping systems in flood-prone areas using MODIS imagery. *Photogrammetric Engineering & Remote Sensing* **2009**, *75*, 413–424.
24. Matthias Garschagen; Diez, J.R.; Nhan, D.K.; Kraas, F. Socio-Economic Development in the Mekong Delta: Between the Prospects for Progress and the Realms of Reality. In *The Mekong Delta System: Interdisciplinary Analyses of a River Delta*; Renaud, F.G., Kuenzer, C., Eds.; Springer Netherlands: Dordrecht, 2012; pp. 83–132 ISBN 978-94-007-3962-8.
25. Berg, H.; Tam, N.T. Use of pesticides and attitude to pest management strategies among rice and rice-fish farmers intheMekong Delta, Vietnam. *International Journal of Pest Management* **2012**, *58*, 153–164.
26. Godfray, H.C.J.; Beddington, J.R.; Crute, I.R.; Haddad, L.; Lawrence, D.; Muir, J.F.; Pretty, J.; Robinson, S.; Thomas, S.M.; Toulmin, C. Food Security: The Challenge of Feeding 9 Billion People. *Science* **2010**, *327*, 812.
27. Dudgeon, D. River Rehabilitation for Conservation of Fish Biodiversity in Monsoonal Asia. *Resilience Alliance Inc.* **2005**, *10*, 15.
28. DONRE Water resource distribution in An Giang.
29. International Rice Research Institute (IRRI). *Bringing hope, improving lives: Strategic Plan 2007-2015*; International Rice Research Institute (IRRI): Manila, 2006;
30. Maclean, J.; Hardy, B.; Hettel, G. *Rice almanac*; 4th edition; International Rice Research Institute: Los Bahos (Philippines), 2013; ISBN 978-971-22-0300-8.
31. Hossain, M. Rice supply and demand in Asia: a socioeconomic and biophysical analysis. In; Springer Netherlands: Dordrecht, 1997; pp. 263–279 ISBN 978-94-011-5416-1.
32. Food and Agriculture Organization (FAO) *Save and grow: Maize, rice and wheat-A guide to sustainable crop production*; UN Food and Agriculture Organization: Rome, 2016; ISBN 978-92-5-108519-6.

33. Ndikumana, E.; Ho Tong Minh, D.; Dang Nguyen, T.H.; Baghdadi, N.; Courault, D.; Hossard, L.; El Moussawi, I. Estimation of Rice Height and Biomass Using Multitemporal SAR Sentinel-1 for Camargue, Southern France. *Remote Sensing* **2018**, *10*.
34. Bouman, B.A.M.; Tuong, T.P. Field water management to save water and increase its productivity in irrigated lowland rice. *Agricultural Water Management* **2001**, *49*, 11–30.
35. Intergovernmental Panel on Climate Change (IPCC). *Climate Change 2007: Impacts, Adaptation and Vulnerability. Contribution of Working Group II to the Fourth Assessment Report of the Intergovernmental Panel on Climate Change*; Cambridge University Press, Cambridge: UK, 2007;
36. Wassmann, R.; Jagadish, S.V.K.; Sumfleth, K.; Pathak, H.; Howell, G.; Ismail, A.; Serraj, R.; Redona, E.; Singh, R.K.; Heuer, S. Chapter 3 Regional Vulnerability of Climate Change Impacts on Asian Rice Production and Scope for Adaptation. In *Advances in Agronomy*; Academic Press, 2009; Vol. 102, pp. 91–133 ISBN 0065-2113.
37. Le, N.K.; Jha, K.M.; Jeong, J.; Gassman, W.P.; Reyes, R.M.; Doro, L.; Tran, Q.D.; Hok, L. Evaluation of Long-Term SOC and Crop Productivity within Conservation Systems Using GFDL CM2.1 and EPIC. *Sustainability* **2018**, *10*.
38. Van Ty, T.; Sunada, K.; Ichikawa, Y. Water resources management under future development and climate change impacts in the Upper Srepok River Basin, Central Highlands of Vietnam. *Water Policy* **2012**, *14*, 725–745.
39. Guan, X.; Huang, C.; Liu, G.; Meng, X.; Liu, Q. Mapping Rice Cropping Systems in Vietnam Using an NDVI-Based Time-Series Similarity Measurement Based on DTW Distance. *Remote Sensing* **2016**, *8*.
40. Bouvet, A.; Le Toan, T.; Lam-Dao, N. Monitoring of the Rice Cropping System in the Mekong Delta Using ENVISAT/ASAR Dual Polarization Data. *IEEE Transactions on Geoscience and Remote Sensing* **2009**, *47*, 517–526.
41. Avtar, R.; Suzuki, R.; Sawada, H. Natural Forest Biomass Estimation Based on Plantation Information Using PALSAR Data. *PLOS ONE* **2014**, *9*, e86121.
42. Avtar, R.; Herath, .; Saito, O.; Gera, W.; Singh, G.; Mishra, B.; Takeuchi, K. Application of remote sensing techniques toward the role of traditional water bodies with respect to vegetation conditions. *Environment, Development and Sustainability* **2014**, *16*, 995–1011.
43. Sakamoto, T.; Van Nguyen, N.; Ohno, H.; Ishitsuka, N.; Yokozawa, M. Spatio–temporal distribution of rice phenology and cropping systems in the Mekong Delta with special reference to the seasonal water flow of the Mekong and Bassac rivers. *Remote Sensing of Environment* **2006**, *100*, 1–16.
44. Vo, Q.M.; Huynh, T.T.H.; Nguyen, T.H.D.; Ho, V.C. Application of MODIS images to monitoring the progress of rice sowing and cropping calendar assisting in early warning rice brown hopper in the Mekong Delta, Vietnam. In Proceedings of the The 33rd Asian conference on remote sensing; Thailand, 2012.

45. Chen, C.F.; Son, N.T.; Chang, L.Y. Monitoring of rice cropping intensity in the upper Mekong Delta, Vietnam using time-series MODIS data. *Advances in Space Research* **2012**, *49*, 292–301.
46. Kontgis, C.; Schneider, A.; Ozdogan, M. Mapping rice paddy extent and intensification in the Vietnamese Mekong River Delta with dense time stacks of Landsat data. *Remote Sensing of Environment* **2015**, *169*, 255–269.
47. Dinesh Kumar, S.; Srinivasa Rao, S.; Sharma, J.R. Radar Vegetation Index as an Alternative to NDVI for Monitoring of Soyabean and Cotton. In Proceedings of the Indian Cartographer; 2013; Vol. XXXIII, pp. 91–96.
48. Xiao, X.; Boles, S.; Frolking, S.; Li, C.; Babu, J.Y.; Salas, W.; Moore, B. Mapping paddy rice agriculture in South and Southeast Asia using multi-temporal MODIS images. *Remote Sensing of Environment* **2006**, *100*, 95–113.
49. Peng, D.; Huete, A.R.; Huang, J.; Wang, F.; Sun, H. Detection and estimation of mixed paddy rice cropping patterns with MODIS data. *International Journal of Applied Earth Observation and Geoinformation* **2011**, *13*, 13–23.
50. Nguyen, D.B.; Gruber, A.; Wagner, W. Mapping rice extent and cropping scheme in the Mekong Delta using Sentinel-1A data. *Remote Sensing Letters* **2016**, *7*, 1209–1218.
51. Lasko, K.; Vadrevu, K.P.; Tran, V.T.; Justice, C. Mapping Double and Single Crop Paddy Rice With Sentinel-1A at Varying Spatial Scales and Polarizations in Hanoi, Vietnam. *IEEE Journal of Selected Topics in Applied Earth Observations and Remote Sensing* **2018**, *11*, 498–512.
52. Choudhury, I.; Chakraborty, M.; Santra, S.C.; Parihar, J.S. Methodology to classify rice cultural types based on water regimes using multi-temporal RADARSAT-1 data. *International Journal of Remote Sensing* **2012**, *33*, 4135–4160.
53. Nelson, A.; Setiyono, T.; Rala, B.A.; Quicho, D.E.; Raviz, V.J.; Abonete, J.P.; Maunahan, A.A.; Garcia, A.C.; Bhatti, Z.H.; Villano, S.L.; et al. Towards an Operational SAR-Based Rice Monitoring System in Asia: Examples from 13 Demonstration Sites across Asia in the RIICE Project. *Remote Sensing* **2014**, *6*.
54. Phan, H.; Le Toan, T.; Bouvet, A.; Nguyen, D.L.; Pham Duy, T.; Zribi, M. Mapping of Rice Varieties and Sowing Date Using X-Band SAR Data. *Sensors* **2018**, *18*.
55. Le Toan, T.; Ribbes, F.; Wang, L.-F.; Floury, N.; Ding, K.-H.; Jin Au Kong; M. Fujita; T. Kurosu Rice crop mapping and monitoring using ERS-1 data based on experiment and modeling results. *IEEE Transactions on Geoscience and Remote Sensing* **1997**, *35*, 41–56.
56. Mansaray, R.L.; Huang, W.; Zhang, D.; Huang, J.; Li, J. Mapping Rice Fields in Urban Shanghai, Southeast China, Using Sentinel-1A and Landsat 8 Datasets. *Remote Sensing* **2017**, *9*.
57. Torbick, N.; Chowdhury, D.; Salas, W.; Qi, J. Monitoring Rice Agriculture across Myanmar Using Time Series Sentinel-1 Assisted by Landsat-8 and PALSAR-2. *Remote Sensing* **2017**, *9*.
58. Ferrant, S.; Selles, A.; Le Page, M.; Herrault, P.-A.; Pelletier, C.; Al-Bitar, A.; Mermoz, S.; Gascoin, S.; Bouvet, A.; Saqalli, M.; et al. Detection of Irrigated Crops from

Sentinel-1 and Sentinel-2 Data to Estimate Seasonal Groundwater Use in South India. *Remote Sensing* **2017**, *9*.
59. Mandal, D.; Kumar, V.; Bhattacharya, A.; Rao, Y.S.; Siqueira, P.; Bera, S. Sen4Rice: A Processing Chain for Differentiating Early and Late Transplanted Rice Using Time-Series Sentinel-1 SAR Data With Google Earth Engine. *IEEE Geoscience and Remote Sensing Letters* **2018**, *15*, 1947–1951.
60. Wakamori, K.; Ichikawa, D. The Combined Use of Sentinel-1, Sentinel-2 and Landsat 7&8 Data for Estimating Heading Date of Paddy Rice. In Proceedings of the IGARSS 2018 - 2018 IEEE International Geoscience and Remote Sensing Symposium; 2018; pp. 7715–7718.
61. Aschbacher, J.; Milagro-Pérez, M.P. The European Earth monitoring (GMES) programme: Status and perspectives. *Remote Sensing of Environment* **2012**, *120*, 3–8.
62. Bacong, P.; Bargellini, P.; Laur, H.; Rosich, B.; Schmuck, S. Sentinel-1 mission operations concept. In Proceedings of the 2012 IEEE International Geoscience and Remote Sensing Symposium; 2012; pp. 1745–1748.
63. Clauss, K.; Ottinger, M.; Leinenkugel, P.; Kuenzer, C. Estimating rice production in the Mekong Delta, Vietnam, utilizing time series of Sentinel-1 SAR data. *International Journal of Applied Earth Observation and Geoinformation* **2018**, *73*, 574–585.
64. Ottinger, M.; Clauss, K.; Kuenzer, C. Opportunities and Challenges for the Estimation of Aquaculture Production Based on Earth Observation Data. *Remote Sensing* **2018**, *10*.
65. Arai, H.; Takeuchi, W.; Oyoshi, K.; Nguyen, D.L.; Inubushi, K. Estimation of Methane Emissions from Rice Paddies in the Mekong Delta Based on Land Surface Dynamics Characterization with Remote Sensing. *Remote Sensing* **2018**, *10*.
66. Dat, T.Q.; Kanchit, L.; Thares, S.; Trung, N.H. Modeling the Influence of River Discharge and Sea Level Rise on Salinity Intrusion in Mekong Delta. In Proceedings of the The 1st EnvironmentAsia International Conference; Thailand, 2011; Vol. 35, pp. 685–701.
67. Torres, R.; Snoeij, P.; Geudtner, D.; Bibby, D.; Davidson, M.; Attema, E.; Potin, P.; Rommen, B.; Floury, N.; Brown, M.; et al. GMES Sentinel-1 mission. *Remote Sensing of Environment* **2012**, *120*, 9–24.
68. Paul, S.; Dirk, G.; Ramón, T.; Malcolm, D.; David, B.; Svein, L. GMES Sentinel-1 System Overview. In Proceedings of the . POLinSAR 2013 Workshop Presentations; ESA ESRIN: Frascati, Italy, 2013; p. 21.
69. Kaplan, G.; Avdan, U. Monthly Analysis of Wetlands Dynamics Using Remote Sensing Data. *ISPRS International Journal of Geo-Information* **2018**, *7*.
70. Numbisi, F.N.; Van Coillie, F.M.B.; De Wulf, R. Delineation of Cocoa Agroforests Using Multiseason Sentinel-1 SAR Images: A Low Grey Level Range Reduces Uncertainties in GLCM Texture-Based Mapping. *ISPRS International Journal of Geo-Information* **2019**, *8*.
71. Zhu, J.; Wen, J.; Zhang, Y. A new algorithm for SAR image despeckling using an enhanced Lee filter and median filter. In Proceedings of the 2013 6th International Congress on Image and Signal Processing (CISP); 2013; Vol. 01, pp. 224–228.

72. Shamsoddini, A.; Trinder, J.C. Edge-detection-based filter for SAR speckle noise reduction. *International Journal of Remote Sensing* **2012**, *33*, 2296–2320.
73. Jonsson, P.; Eklundh, L. Seasonality extraction by function fitting to time-series of satellite sensor data. *IEEE Transactions on Geoscience and Remote Sensing* **2002**, *40*, 1824–1832.
74. Nguyen, D.B.; Wagner, W. European Rice Cropland Mapping with Sentinel-1 Data: The Mediterranean Region Case Study. *Water* **2017**, *9*.
75. International Rice Research Institute (IRRI). Rice knowledge bank 2015.
76. Xuan, V.T. Rice Cultivation in the Mekong Delta. *Japanese Journal of Southeast Asian Studies* **1975**, *13*, 88–111.
77. Tuong, T.P.; Bouman, B.; Mortimer, M. More rice, less waterintegrated approaches for increasing water productivity in irrigated rice-based systems in Asia. *Plant Prod. Sci.* **2005**, *8*, 231–241.
78. Thuy, P.T.; Van Geluwe, S.; Nguyen, V.-A.; Van der Bruggen, B. Current pesticide practices and environmental issues in Vietnam: management challenges for sustainable use of pesticides for tropical crops in (South-East) Asia to avoid environmental pollution. *Journal of Material Cycles and Waste Management* **2012**, *14*, 379–387.
79. Le Toan, T.; Beaudoin, A.; Riom, J.; Guyon, D. Relating forest biomass to SAR data. *IEEE Transactions on Geoscience and Remote Sensing* **1992**, *30*, 403–411.
80. Jiang, T.; Liu, X.; Wu, L. Method for Mapping Rice Fields in Complex Landscape Areas Based on Pre-Trained Convolutional Neural Network from HJ-1 A/B Data. *ISPRS International Journal of Geo-Information* **2018**, *7*.
81. Fukuda, S.; Hirosawa, H. Support vector machine classification of land cover: application to polarimetric SAR data. In Proceedings of the IGARSS 2001. Scanning the Present and Resolving the Future. Proceedings. IEEE 2001 International Geoscience and Remote Sensing Symposium (Cat. No.01CH37217); 2001; Vol. 1, pp. 187–189 vol.1.
82. Abdikan, S. LAND COVER MAPPING USING SENTINEL-1 SAR DATA. *ISPRS - International Archives of the Photogrammetry, Remote Sensing and Spatial Information Sciences* **2016**, *XLI-B7*, 757–761.
83. Son, N.-T.; Chen, C.-F.; Chen, C.-R.; Minh, V.-Q. Assessment of Sentinel-1A data for rice crop classification using random forests and support vector machines. *Geocarto International* **2018**, *33*, 587–601.
84. Küçük, Ç.; Taşkın, G.; Erten, E. Paddy-Rice Phenology Classification Based on Machine-Learning Methods Using Multitemporal Co-Polar X-Band SAR Images. *IEEE Journal of Selected Topics in Applied Earth Observations and Remote Sensing* **2016**, *9*, 2509–2519.
85. Kavzoglu, T.; Colkesen, I. A kernel functions analysis for support vector machines for land cover classification. *International Journal of Applied Earth Observation and Geoinformation* **2009**, *11*, 352–359.
86. Mountrakis, G.; Im, J.; Ogole, C. Support vector machines in remote sensing: A review. *ISPRS Journal of Photogrammetry and Remote Sensing* **2011**, *66*, 247–259.

87. Hsu, C.-W.; Chang, C.-C.; Lin, C.-J. *A Practical Guide to Support Vector Classification*; Department of Computer Science, National Taiwan University, 2016; p. 16;.
88. Achirul Nanda, M.; Boro Seminar, K.; Nandika, D.; Maddu, A. A Comparison Study of Kernel Functions in the Support Vector Machine and Its Application for Termite Detection. *Information* **2018**, *9*.
89. Cortes, C.; Vapnik, V. Support-vector networks. *Machine Learning* **1995**, *20*, 273–297.
90. Bayro-Corrochano, E.J.; Arana-Daniel, N. Clifford Support Vector Machines for Classification, Regression, and Recurrence. *Trans. Neur. Netw.* **2010**, *21*, 1731–1746.
91. Avtar, R.; Suzuki, R.; Takeuchi, W.; Sawada, H. PALSAR 50 m Mosaic Data Based National Level Biomass Estimation in Cambodia for Implementation of REDD+ Mechanism. *PLOS ONE* **2013**, *8*, e74807.
92. Avtar, R.; Takeuchi, W.; Sawada, H. Full polarimetric PALSAR-based land cover monitoring in Cambodia for implementation of REDD policies. *International Journal of Digital Earth* **2013**, *6*, 255–275.
93. Aronoff, S. The map accuracy report: A user's view. **1982**, *48*, 1309–1312.
94. Ginevan, M. Testing land-use map accuracy: another look. *Photogrammetric Engineering and Remote Sensing* **1979**, *45*, 1371–1377.
95. Congalton, R.G. A Review of Assessing the Accuracy of Classifications of Remotely Sensed Data. **1991**, *37*, 35–46.
96. Ashby, D. Practical statistics for medical research. Douglas G. Altman, Chapman and Hall, London, 1991. No. of pages: 611. Price: £32.00. *Statistics in Medicine* **1991**, *10*, 1635–1636.
97. Ludbrook, J. Statistical Techniques For Comparing Measurers And Methods Of Measurement: A Critical Review. *Clinical and Experimental Pharmacology and Physiology* **2002**, *29*, 527–536.
98. department of agriculture and rural development (DARD) *Ensuring production wins the Autumn-Winter season*; DARD website: Viet Nam, 2017;
99. He, Z.; Li, S.; Wang, Y.; Dai, L.; Lin, S. Monitoring Rice Phenology Based on Backscattering Characteristics of Multi-Temporal RADARSAT-2 Datasets. *Remote Sensing* **2018**, *10*.
100. Rose, J.B.; Epstein, P.R.; Lipp, E.K.; Sherman, B.H.; Bernard, S.M.; Patz, J.A. Climate variability and change in the United States: potential impacts on water- and foodborne diseases caused by microbiologic agents. *Environmental health perspectives* **2001**, *109 Suppl 2*, 211–221.
101. Oyoshi, K.; Tomiyama, N.; Okumura, T.; Sobue, S.; Sato, J. Mapping rice-planted areas using time-series synthetic aperture radar data for the Asia-RiCE activity. *Paddy and Water Environment* **2016**, *14*, 463–472.
102. Department of Natural Resources and Environment (DONRE). *The result survey of land degradation (complementary report)*; DONRE: An Giang, Viet Nam, 2016;
103. Banko, G. *A Review of Assessing the Accuracy of Classifications of Remotely Sensed Data and of Methods Including Remote Sensing Data in Forest Inventory*; 1998; p. 42;.

104. Koppe, W.; Gnyp, M.L.; Hütt, C.; Yao, Y.; Miao, Y.; Chen, X.; Bareth, G. Rice monitoring with multi-temporal and dual-polarimetric TerraSAR-X data. *International Journal of Applied Earth Observation and Geoinformation* **2013**, *21*, 568–576.
105. Qiu, B.; Li, W.; Tang, Z.; Chen, C.; Qi, W. Mapping paddy rice areas based on vegetation phenology and surface moisture conditions. *Ecological Indicators* **2015**, *56*, 79–86.
106. Dietz, T.; Stern, P.C.; Rycroft, R.W. Definitions of conflict and the legitimation of resources: The case of environmental risk. *Sociological Forum* **1989**, *4*, 47–70.
107. Vörösmarty, C.J.; McIntyre, P.B.; Gessner, M.O.; Dudgeon, D.; Prusevich, A.; Green, P.; Glidden, S.; Bunn, S.E.; Sullivan, C.A.; Liermann, C.R.; et al. Global threats to human water security and river biodiversity. *Nature* **2010**, *467*, 555.
108. Vörösmarty, C.J.; Green, P.; Salisbury, J.; Lammers, R.B. Global Water Resources: Vulnerability from Climate Change and Population Growth. *Science* **2000**, *289*, 284.
109. Woodhouse, P.; Muller, M. Water Governance—An Historical Perspective on Current Debates. *World Development* **2017**, *92*, 225–241.
110. Beaulac, M.N.; Reckhow, K.H. An examination of land use nutrient export relationships. *Water Resources Bulletin* **1982**, *18*, 1013–1024.
111. Carpenter, S.R.; Caraco, N.F.; Correll, D.L.; Howarth, R.W.; Sharpley, A.N.; Smith, V.H. Non-Point Pollution of Surface Waters With Phosphorus and Nitrogen. *Ecological Applications* **1998**, *8*, 559–568.
112. Chiwa, M.; Onikura, N.; Ide, J.; Kume, A. Impact of N-Saturated Upland Forests on Downstream N Pollution in the Tatara River Basin, Japan. *Ecosystems* **2012**, *15*, 230–241.
113. Forti, M.C.; Neal, C.; Jenkins, A. Modeling perspective of the deforestation impact in stream water quality of small preserved forested areas in the amazonian rainforest. *Water, Air, and Soil Pollution* **1995**, *79*, 325–337.
114. Mehdi, B.; Ludwig, R.; Lehner, B. Evaluating the impacts of climate change and crop land use change on streamflow, nitrates and phosphorus: A modeling study in Bavaria. *Journal of Hydrology: Regional Studies* **2015**, *4*, 60–90.
115. Miller, J.D.; Schoonover, J.E.; Williard, K.W.J.; Hwang, C.R. Whole Catchment Land Cover Effects on Water Quality in the Lower Kaskaskia River Watershed. *Water, Air, & Soil Pollution* **2011**, *221*, 337.
116. Tayyebi, A.; Pijanowski, B.C.; Pekin, B.K. Land use legacies of the Ohio River Basin: Using a spatially explicit land use change model to assess past and future impacts on aquatic resources. *Applied Geography* **2015**, *57*, 100–111.
117. USEPA *2004 National Water Quality Inventory: Report to Congress*; United States Environmental Protection Agency Office of Water, 2009; p. 43;.
118. Cooper, C.M. Biological Effects of Agriculturally Derived Surface Water Pollutants on Aquatic Systems—A Review. *Journal of Environmental Quality* **1993**, *22*, 402–408.
119. Ramankutty, N.; Mehrabi, Z.; Waha, K.; Jarvis, L.; Kremen, C.; Herrero, M.; Rieseberg, L.H. Trends in Global Agricultural Land Use: Implications for Environmental Health and Food Security. *Annu. Rev. Plant Biol.* **2018**, *69*, 789–815.

120. Shouqiang, L. The Smart Growth of Ulanhot and Arlington. In Proceedings of the 3rd International Conference on Management Science and Innovative Education (MSIE 2017); 2017.
121. Baker, A. Land use and water quality. *Encyclopedia of Hydrological Sciences* 2006.
122. Carvalho, L.; Solimini, A.; Phillips, G.; van den Berg, M.; Pietiläinen, O.-P.; Lyche Solheim, A.; Poikane, S.; Mischke, U. Chlorophyll reference conditions for European lake types used for intercalibration of ecological status. *Aquatic Ecology* **2008**, *42*, 203–211.
123. WWAP (United Nations World Water Assessment Programme *The United Nations. World Water Development Report 2016: Water and Jobs*; Paris, UNESCO, 2016; ISBN 978-92-3-100146-8.
124. Mutert, E.; Fairhurst, T.H. Developments in rice production in Southeast Asia. *Better Crops International* **2002**, *15*, 12–17.
125. Thakur, A.K.; Rath, S.; Mandal, K.G. Differential responses of system of rice intensification (SRI) and conventional flooded-rice management methods to applications of nitrogen fertilizer. *Plant and Soil* **2013**, *370*, 59–71.
126. General Statistics Office Of Vietnam (GSO). *Statistical Yearbook of An Giang 2012*; General Statistics Office Of Vietnam (GSO), 2013;
127. Department of Agriculture and Natural Development (DARD) *Annual report 2003*; An Giang Province, 2003;
128. Kontgis, C.; Schneider, A.; Ozdogan, M. Mapping rice paddy extent and intensification in the Vietnamese Mekong River Delta with dense time stacks of Landsat data. *Remote Sensing of Environment* **2015**, *169*, 255–269.
129. Bambaradeniya, C.N.B.; Amarasinghe, F.P. *Biodiversity Associated with the Rice Field Agroecosystem in Asian Countries: A Brief Review*; International Water Management Institute: Sri Lanka, 2003; p. 24;.
130. Center, E.M. Department of Natural Resources and Environment 2016.
131. (DONRE), D. of natural R. and E. National technical regulation on surface water quality 2015.
132. Monaghan, R.M.; Carey, P.L.; Wilcock, R.J.; Drewry, J.J.; Houlbrooke, D.J.; Quinn, J.M.; Thorrold, B.S. Linkages between land management activities and stream water quality in a border dyke-irrigated pastoral catchment. *Agriculture, Ecosystems & Environment* **2009**, *129*, 201–211.
133. Nguyen, V.K.T.; Nguyen, V.D.; Fujii, H.; Kummu, M.; Merz, B.; Apel, H. Has dyke development in the Vietnamese Mekong Delta shifted flood hazard downstream? *Hydrol. Earth Syst. Sci.* **2017**, *21*, 3991–4010.
134. Helena, B.; Pardo, R.; Vega, M.; Barrado, E.; Fernandez, J.M.; Fernandez, L. Temporal evolution of groundwater composition in an alluvial aquifer (Pisuerga River, Spain) by principal component analysis. *Water Research* **2000**, *34*, 807–816.
135. Avtar, R.; Kumar, P.; Singh, C.K.; Sahu, N.; Verma, R.L.; Thakur, J.K.; Mukherjee, S. Hydrogeochemical Assessment of Groundwater Quality of Bundelkhand, India Using Statistical Approach. *Water Quality, Exposure and Health* **2013**, *5*, 105–115.

136. Kido, M.; Yustiawati; Syawal, M.S.; Sulastri; Hosokawa, T.; Tanaka, S.; Saito, T.; Iwakuma, T.; Kurasaki, M. Comparison of general water quality of rivers in Indonesia and Japan. *Environmental Monitoring and Assessment* **2008**, *156*, 317.
137. Shammi, M.; Rahman, Md.M.; Islam, Md.A.; Bodrud-Doza, Md.; Zahid, A.; Akter, Y.; Quaiyum, S.; Kurasaki, M. Spatio-temporal assessment and trend analysis of surface water salinity in the coastal region of Bangladesh. *Environmental Science and Pollution Research* **2017**, *24*, 14273–14290.
138. Alberto, W.D.; María del Pilar, D.; María Valeria, A.; Fabiana, P.S.; Cecilia, H.A.; María de los Ángeles, B. Pattern Recognition Techniques for the Evaluation of Spatial and Temporal Variations in Water Quality. A Case Study:: Suquía River Basin (Córdoba–Argentina). *Water Research* **2001**, *35*, 2881–2894.
139. Johnson, R.A., (viaf)166780991; Wichern, D.W., (viaf)2713933 *Applied multivariate statistical analysis*; 3rd. ed.; Englewood Cliffs (N.J.) : Prentice-Hall, 1992; ISBN 0-13-041807-2.
140. Singh, K.P.; Malik, A.; Mohan, D.; Sinha, S. Multivariate statistical techniques for the evaluation of spatial and temporal variations in water quality of Gomti River (India)—a case study. *Water Research* **2004**, *38*, 3980–3992.
141. Singh, K.P.; Malik, A.; Sinha, S. Water quality assessment and apportionment of pollution sources of Gomti river (India) using multivariate statistical techniques—a case study. *Analytica Chimica Acta* **2005**, *538*, 355–374.
142. Shrestha, S.; Kazama, F. Assessment of surface water quality using multivariate statistical techniques: A case study of the Fuji river basin, Japan. *Environmental Modelling & Software* **2007**, *22*, 464–475.
143. Duan, W.; He, B.; Nover, D.; Yang, G.; Chen, W.; Meng, H.; Zou, S.; Liu, C. Water Quality Assessment and Pollution Source Identification of the Eastern Poyang Lake Basin Using Multivariate Statistical Methods. *Sustainability* **2016**, *8*.
144. Poulsen, J.; French, A. Discriminant function analysis 2008.
145. Chen, G.N. Assessment of environmental water with fuzzy cluster analysis and fuzzy recognition. *Analytica Chimica Acta* **1993**, *271*, 115–124.
146. Graça, M.A.S.; Coimbra, C.N. The elaboration of indices to assess biological water quality. A case study. *Water Research* **1998**, *32*, 380–392.
147. Vega, M.; Pardo, R.; Barrado, E.; Debán, L. Assessment of seasonal and polluting effects on the quality of river water by exploratory data analysis. *Water Research* **1998**, *32*, 3581–3592.
148. Adams, M.J. *The principles of multivariate data analysis. In: Analytical Methods of Food Authentication*; Blackie Academic & Professional: London, 1998;
149. McKenna, J.E. An enhanced cluster analysis program with bootstrap significance testing for ecological community analysis. *Environmental Modelling & Software* **2003**, *18*, 205–220.
150. Simeonov, V.; Stratis, J.A.; Samara, C.; Zachariadis, G.; Voutsa, D.; Anthemidis, A.; Sofoniou, M.; Kouimtzis, Th. Assessment of the surface water quality in Northern Greece. *Water Research* **2003**, *37*, 4119–4124.

151. Sridhar Kuma, A.; Shnakaraiah, K.; Raoc, P.L.K.M.; Sathyanarayana, M. Assessment of water quality in hussainsagar lake and its inlet channels using multivariate statistical techniques. In Proceedings of the international journal of scientific &engineering research; 2014; Vol. 5, pp. 327–333.
152. Massart, D.L.; Kaufman, L. *The Interpretation of Analytical Chemical Data by the Use of Cluster Analysis*; John Wiley & Sons: New York, 1983;
153. Willett, P. *Similarity and clustering in chemical information systems*; Chemometrics series ; 12; Letchworth, Hertfordshire, England : Research Studies Press: New York, 1987; ISBN 0-86380-050-5.
154. Bengraïne, K.; Marhaba, T.F. Using principal component analysis to monitor spatial and temporal changes in water quality. *Journal of Hazardous Materials* **2003**, *100*, 179–195.
155. Ouyang, Y. Evaluation of river water quality monitoring stations by principal component analysis. *Water Research* **2005**, *39*, 2621–2635.
156. Pop, H.F. Principal components analysis based on a fuzzy sets approach. *Studia Univ. Babes,-Bolyai, Informatica* **2001**, *XLVI*, 45–52.
157. Sârbu, C.; Pop, H.F. Principal component analysis versus fuzzy principal component analysis: A case study: the quality of danube water (1985–1996). *Talanta* **2005**, *65*, 1215–1220.
158. Shine, J.P.; Ika, R.V.; Ford, T.E. Multivariate statistical examination of spatial and temporal patterns of heavy metal contamination in New Bedford Harbor marine sediments. *Environ. Sci. Technot.* **1995**, *29*, 1781–1788.
159. Tauler, R.; Barcelo, D.; Thurman, E.M. Multivariate Correlation between Concentrations of Selected Herbicides and Derivatives in Outflows from Selected U.S. Midwestern Reservoirs. *Environ. Sci. Technol.* **2000**, *34*, 3307–3314.
160. Voutsa, D.; Manoli, E.; Samara, C.; Sofoniou, M.; Stratis, I. A Study of Surface Water Quality in Macedonia, Greece: Speciation of Nitrogen and Phosphorus. *Water, Air, and Soil Pollution* **2001**, *129*, 13–32.
161. Yu, C.-C.; Quinn, J.T.; Dufournaud, C.M.; Harrington, J.J.; Rogers, P.P.; Lohani, B.N. Effective dimensionality of environmental indicators: a principal component analysis with bootstrap confidence intervals. *Journal of Environmental Management* **1998**, *53*, 101–119.
162. Mekong River Commission (MRC) *Diagnostic study of water quality in the Lower Mekong Basin*; MRC Technical Paper No.15; Mekong River Commission: Vientiane, 2007; p. 57;.
163. Mekong River Commission (MRC) *An assessment of water quality in the Lower Mekong Basin*; Technical Paper No.19; Mekong River Commission: Vientiane, 2008; p. 70;.
164. Campbell, I. *Review of the MRC Water Quality Indices*; Mekong River Commission: Vientiane, 2014;
165. Yuan, L.; He, W.; Liao, Z.; Degefu, M.D.; An, M.; Zhang, Z.; Wu, X. Allocating Water in the Mekong River Basin during the Dry Season. *Water* **2019**, *11*.

166. Sikder, Md.; Tanaka, S.; Saito, T.; Hosokawa, T.; Gumiri, S.; Ardianor, A.; Uddin, Md.; Tareq, S.; Shammi, M.; Kamal, A.; et al. Vulnerability assessment of surface water quality with an innovative integrated multi-parameter water quality index (IMWQI). *Pollution* **2015**, *1*, 333–346.
167. Brian Oram Water research Center website. *Water reserach Center*.
168. Hamza Muhammad Arain Nitrogen-Ion Conversion Chart. *hamzasreef*.
169. Cattell, R.B.; Jaspers, J. A general plasmode (No. 30-15-5-2) for factor analytic excercises and research. *Mult Behave Res Monogr* **1967**, *67*, 1–212.
170. Kim, J.O.; Mueller, C.W. Factor Analysis: Statistical Methods and Practical Issues. *Beverly Hills* **1978**.
171. Wilbers, G.-J.; Sebesvari, Z.; Renaud, G.F. Piped-Water Supplies in Rural Areas of the Mekong Delta, Vietnam: Water Quality and Household Perceptions. *Water* **2014**, *6*.
172. FUJII, H.; FUJIHARA, Y.; HOSHIKAWA, K. Expansion of Full-dyke System and Its Impact in Flood-prone Rice Area in the Mekong Delta. *Transactions of The Japanese Society of Irrigation, Drainage and Rural Engineering* **2013**, *81*, 271–278.
173. Ty, T.V. Scenario-based Impact Assessment of Land Use/Cover and Climate Changes on Water Resources and Demand: A Case Study in the Srepok River Basin, Vietnam—Cambodia. *Water resources management* **2012**, *v. 26*, 1387–1407.
174. Dise, N.B.; Ashmore, M.; Belyazid, S.; Bleeker, A.; Bobbink, R.; Vries, W. de; Erisman, J.W.; Spranger, T.; Berg, C.J.S. and L. van den Nitrogen as a threat to European terrestrial biodiversity. **2011**, 463–494.
175. Al-Mukhtar, M.; Al-Yaseen, F. Modeling Water Quality Parameters Using Data-Driven Models, a Case Study Abu-Ziriq Marsh in South of Iraq. *Hydrology* **2019**, *6*.
176. Firat, M.; Güngör, M. Monthly total sediment forecasting using adaptive neuro fuzzy inference system. *Stochastic Environmental Research and Risk Assessment* **2010**, *24*, 259–270.
177. Wu, Z.; Zhang, D.; Cai, Y.; Wang, X.; Zhang, L.; Chen, Y. Water quality assessment based on the water quality index method in Lake Poyang: The largest freshwater lake in China. *Scientific Reports* **2017**, *7*, 17999.
178. Evtimova, V.V.; Donohue, I. Water-level fluctuations regulate the structure and functioning of natural lakes. *Freshwater Biology* **2016**, *61*, 251–264.
179. Wright, J.; Worrall, F. The effects of river flow on water quality in estuarine impoundments. *Physics and Chemistry of the Earth, Part B: Hydrology, Oceans and Atmosphere* **2001**, *26*, 741–746.
180. Pomerol, J.-C.; Sergio, B.-R. *Multicriterion Decision in Management: Principles and Practice.*; Kluwer Academic Publishers: Norwell, 2000; ISBN 9781461544593.
181. Zavadskas, E.; Turskis, Z. *Multiple Criteria Decision Making (MCDM) Methods in Economics: An Overview*; 2011; Vol. 17;.
182. Büyüközkan, G.; Feyzioğlu, O.; Nebol, E. Selection of the strategic alliance partner in logistics value chain. *International Journal of Production Economics* **2008**, *113*, 148–158.
183. Saaty, T.L. *The Analytic Hierarchy Process*; McGraw-Hill: New York, 1980;

184. Zadeh, L.A. Fuzzy sets. *Information and Control* **1965**, *8*, 338–353.
185. Karakuş, C.B. Evaluation of groundwater quality in Sivas province (Turkey) using water quality index and GIS-based analytic hierarchy process. *International Journal of Environmental Health Research* **2018**, 1–20.
186. Larimian, T.; Zarabadi, Z.S.S.; Sadeghi, A. Developing a fuzzy AHP model to evaluate environmental sustainability from the perspective of Secured by Design scheme—A case study. *Sustainable Cities and Society* **2013**, *7*, 25–36.
187. Petkovic, J.; Sevarac, Z.; Jaksic, M.L.; Marinkovic, S. Application of fuzzy AHP method for choosing a technology within service company. *Technics Technologies Education Management* **2012**, *7*, 332–341.
188. Bellman, R.E.; Zadeh, L.A. Decision making in a fuzzy environment. *Management Science* **1970**, *17*, 141–164.
189. Renigier-Bilozor, M.; Janowski, A.; Walacik, M. Geoscience Methods in Real Estate Market Analyses Subjectivity Decrease. *Geosciences* **2019**, *9*.
190. Lermontov, A.; Yokoyama, L.; Lermontov, M.; Machado, M.A.S. River quality analysis using fuzzy water quality index: Ribeira do Iguape river watershed, Brazil. *Ecological Indicators* **2009**, *9*, 1188–1197.
191. Casillas, J.; Francisco, J.M.-L. *Marketing Intelligent Systems Using Soft Computin: Manageral and Research Applications*; Springer, 2010;
192. Kahraman, C.; Kaya, İ. A fuzzy multicriteria methodology for selection among energy alternatives. *Expert Systems with Applications: An International Journal* **2010**, *37*, 6270–6281.
193. Ayhan, M.B. A Fuzzy AHP Approach for Supplier Selection Problem: A Case Study in a Gear Motor Company. *International Journal of Managing Value and Supply Chains (IJMVSC)* **2013**, *4*.
194. Baghapour, M.A.; Shooshtarian, M.R. Extending a Consensus-based Fuzzy Ordered Weighting Average (FOWA) Model in New Water Quality Indices. *Iranian Journal of Health, Safety and Environment; Vol 4, No 4 (2017)* **2017**.
195. Shooshtarian, M.R.; Dehghani, M.; Margherita, F.; Gea, O.C.; Mortezazadeh, S. Land use change and conversion effects on ground water quality trends: An integration of land change modeler in GIS and a new Ground Water Quality Index developed by fuzzy multi-criteria group decision-making models. *Food and Chemical Toxicology* **2018**, *114*, 204–214.
196. Mohammad, A.B.; Mohammad, R.S. Extending a Consensus-based Fuzzy Ordered Weighting Average (FOWA) Model in New Water Quality Indices. *Iranian Journal of Health, Safety and Environment* **2017**, *4*, :824-834.
197. Azarnivand, A.; Hashemi-Madani, F.S.; Banihabib, M.E. Extended fuzzy analytic hierarchy process approach in water and environmental management (case study: Lake Urmia Basin, Iran). *Environmental Earth Sciences* **2015**, *73*, 13–26.
198. Deng, H. Multicriteria analysis with fuzzy pairwise comparison. *International Journal of Approximate Reasoning* **1999**, *21*, 215–231.

199. Goyal, M.K.; Bharti, B.; Quilty, J.; Adamowski, J.; Pandey, A. Modeling of daily pan evaporation in sub tropical climates using ANN, LS-SVR, Fuzzy Logic, and ANFIS. *Expert Systems with Applications* **2014**, *41*, 5267–5276.
200. Moghaddamnia, A.; Ghafari Gousheh, M.; Piri, J.; Amin, S.; Han, D. Evaporation estimation using artificial neural networks and adaptive neuro-fuzzy inference system techniques. *Advances in Water Resources* **2009**, *32*, 88–97.
201. Ren Li; Xiang Xin-Yi; Ni Jian-Jun Forecast Modeling of Monthly Runoff with Adaptive Neural Fuzzy Inference System and Wavelet Analysis. *Journal of Hydrologic Engineering* **2013**, *18*, 1133–1139.
202. Wang Keh-Han; Altunkaynak Abdusselam Comparative Case Study of Rainfall-Runoff Modeling between SWMM and Fuzzy Logic Approach. *Journal of Hydrologic Engineering* **2012**, *17*, 283–291.
203. CASPER, M.; GEMMAR, P.; GRONZ, O.; JOHST, M.; STÜBER, M. Fuzzy logic-based rainfall—runoff modelling using soil moisture measurements to represent system state. *Hydrological Sciences Journal* **2007**, *52*, 478–490.
204. Aryafar, A.; Yousefi, S.; Doulati Ardejani, F. The weight of interaction of mining activities: groundwater in environmental impact assessment using fuzzy analytical hierarchy process (FAHP). *Environmental Earth Sciences* **2013**, *68*, 2313–2324.
205. Minh, H.V.T.; Ngoc, D.T.H.; Ngan, H.Y.; Men, H.V.; Van, T.N.; Ty, T.V. Assessment of Groundwater Level and Quality: A Case Study in O Mon and Binh Thuy Districts, Can Tho City, Vietnam. *Faculty of Engineering Naresuan University* **2016**, *11*, 25–33.
206. Minh, H.V.T.M.; Kurasaki, M.; Ty, T.V.; Dat, T.Q.; Kieu, L.N.; Avtar, R.; Osaki, M. Effects of Multi-Dike-Protection Systems on Surface Water Quality in the Vietnamese Mekong Delta 2019.
207. Singh, C.K.; Shashtri, S.; Mukherjee, S.; Kumari, R.; Avatar, R.; Singh, A.; Singh, R.P. Application of GWQI to Assess Effect of Land Use Change on Groundwater Quality in Lower Shiwaliks of Punjab: Remote Sensing and GIS Based Approach. *Water Resources Management* **2011**, *25*, 1881–1898.
208. Horton, R.K. An index number system for rating water quality. *J. Water Pollu. Cont. Fed.* **1965**, *37*, 300–305.
209. Tyagi, S.; Sharma, B.; Singh, P.; Dobhal, R. Water Quality Assessment in Terms of Water Quality Index. *American Journal of Water Resources* **2013**, *1*, 34–38.
210. Brown, R.M.; McClelland, N.I.; Deininger, R.A.; Tozer, R.G. A Water Quality Index: Do We Dare? *Water Sewage Works* **1970**, *117*, 339–343.
211. Bhargava, D.S.; Saxena, B.S.; Dewakar, R.W. A study of geo-pollutants in the Godavary river basin in India. *Asian Environ.* **1998**, *12*, 36–59.
212. Wilbers, G.-J.; Becker, M.; Nga, L.T.; Sebesvari, Z.; Renaud, F.G. Spatial and temporal variability of surface water pollution in the Mekong Delta, Vietnam. *Science of The Total Environment* **2014**, *485–486*, 653–665.
213. Anh, P.K.; Giao, N.T. Groundwater Quality and Human Health Risk Assessment Related to Groundwater Consumption in an Giang Province. *J Heavy Met Toxicity Dis* **2018**, *3*.

214. Thu, T.A.; Tinh, T.K.; Minh, V.Q. Investigating sources of arsenic contamination in groundwater in An Phu district, An Giang province. **2011**, *17a*, 118–123.
215. Asadi, S.S.; Vuppala, P.; Reddy, M.A. Remote sensing and GIS techniques for evaluation of groundwater quality in municipal corporation of Hyderabad (Zone-V), India. *Int J Environ Res Public Health* **2007**, *4*, 45–52.
216. Maheswaran, G.; Elangovan, K. Groundwater Quality Evaluation in Salem District, Tamil Nadu, Based on Water Quality Index. *An International Quarterly Scientific* **2014**, *13*, 547–552.
217. Chang, D.-Y. Applications of the extent analysis method on fuzzy AHP. *European Journal of Operational Research* **1996**, *95*, 649–655.
218. Zarghami, M.; Szidarovszky, F. Group decision support system for ranking of water resources projects. *The 3rd International Conference on Water Resources and Arid Environments (2008) and the 1st Arab Water Forum* **2008**.
219. Minh, H.V.T.; Avtar, R.; Mohan, G.; Misra, P.; Kurasaki, M. Monitoring and Mapping of Rice Cropping Pattern in Flooding Area in the Vietnamese Mekong Delta Using Sentinel-1A Data: A Case of An Giang Province. *ISPRS International Journal of Geo-Information* **2019**, *8*.
220. South Vietnam geological mapping division Project of Impact assessment of climate change to land water resources in the Mekong Delta proposal of response solutions. *South Vietnam geological mapping division. Tp Ho Chi Minh, Vietnam* **2013**.
221. Department of Natural resources and Environment (DONRE). *Report on environmental status in An Giang province, 2005 - 2009*; 2010;
222. General Statistical Office of Viet Nam (GSO). *Statistical Yearbook of An Giang 2012*; General Statistical Office of Viet Nam (GSO), 2013;
223. Soberi, M.S.F.; Ahmad, R. Application of fuzzy AHP for setup reduction in manufacturing industry. *Journal of Engineering Research and Education* **2016**, *8*, 73–84.
224. Buckley, J.J. Fuzzy hierarchical analysis. *Fuzzy Sets and Systems* **1985**, *17*, 233–247.
225. Ministry of Natural Resources and Environment (DONRE). National technical regulation on ground water quality. *Ha Noi, Vietnam* **2015**.
226. Ashiyani, N.; Suryanarayana, T.M.V. Assessment of groundwater quality using GWQI method – a case study of nadiad taluka, Gujarat, India. *ter quality using GWQI method – a case study of nadiad taluka, Gujarat, India. In: 20th International Conference on Hydraulics, Water Resources and River Engineering - Hudro 2015 International, India* **2015**.
227. Rupal, M.; Tanushree, B.; Sukalyan2, C. Quality Characterization of Groundwater using Water Quality Index in Surat city, Gujarat, India. *International Research Journal of Environment Sciences* **2012**, *1*, 14–23.
228. Chakraborti, D.; Singh, K.S.; Rahman, M.M.; Dutta, N.R.; Mukherjee, C.S.; Pati, S.; Kar, B.P. Groundwater Arsenic Contamination in the Ganga River Basin: A Future Health Danger. *International Journal of Environmental Research and Public Health* **2018**, *15*.

229. Hoang, T.H.; Bang, S.; Kim, K.-W.; Nguyen, M.H.; Dang, D.M. Arsenic in groundwater and sediment in the Mekong River delta, Vietnam. *Environmental Pollution* **2010**, *158*, 2648–2658.
230. Anh Ngoc, T. *Assessing the Effects of Upstream Dam Developments on Sediment Distribution in the Lower Mekong Delta, Vietnam*; 2017; Vol. 9;.
231. Vongphuthone, B.; Kobayashi, M.; Igarashi, T. Factors affecting arsenic content of unconsolidated sediments and its mobilization in the Ishikari Plain, Hokkaido, Japan. *Environmental Earth Sciences* **2017**, *76*, 645.
232. CHUAN-DE, G.; ZHI-MIN, W. Analysis of the source of arsenic in the Yellow River and its relation to sediment. *IAHS-AISH publication* **1986**, 249–255.
233. World Health Organization (WHO) (2006) Guidelines for Drinking-water Quality. Third Edition. 1st Addendum to Vol. 1. WHO, Geneva. (http://www.who.int/water_sanitation_health/dwq/gdwq0506.pdf).

Annexures

Annexure A1: Multi-temporal Sentinel-1A data - The display of An Giang province in composite image R:G:B by bands (VV:VH:VV/VH) - scale: 1/3.000.000.

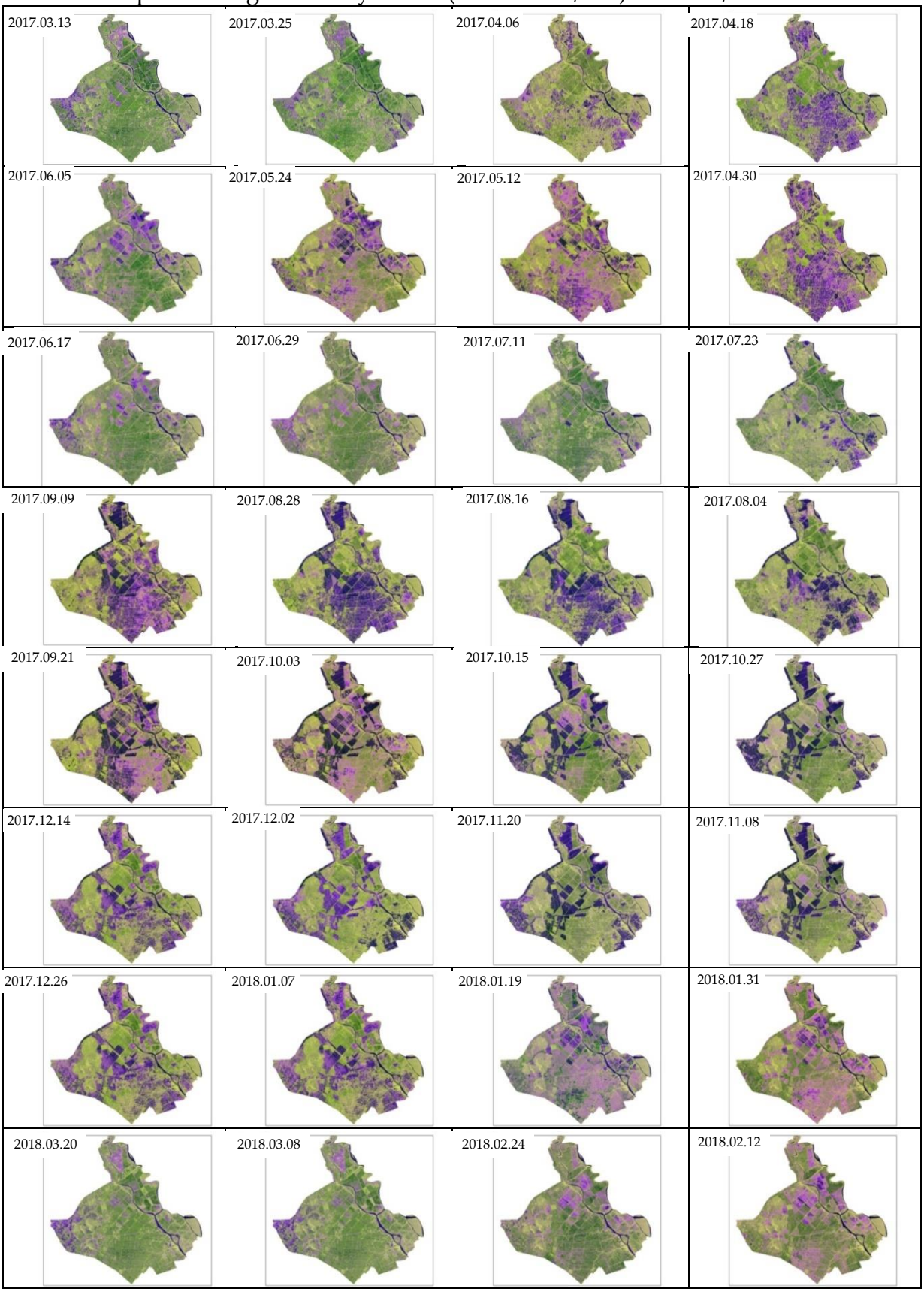

Annexure B

Table B1. Min, Max, Standard Deviation of water quality parameters at dry and wet season 2017.

Variables	dry season				wet season			
	Min	**Max**	**Mean**	**SD**	**Min**	**Max**	**Mean**	**SD**
DO	4.98	8.24	6.39	1.07	6.59	9	7.22	0.55
pH	6.8	9.4	7.72	0.62	7	8.7	7.79	0.41
EC	190	810	287	166.8	70	430	166	89.32
Turbidity	3.34	56	19.43	14.2	4.34	80	34.59	16.46
COD	4.5	30	14.04	5.61	9	55	24.53	11.97
NH_4^+	0.05	0.8	0.25	0.15	0.08	2	0.52	0.52
NO_2^-	0.01	0.4	0.08	0.09	0.001	0.75	0.09	0.2
NO_3^-	0.001	6	1.48	1.82	0.01	3	0.55	0.65
PO_4^{3-}	0.01	1.8	0.25	0.35	0.02	1	0.16	0.22
TC	144	1200	558	217	150	850	479	197

Table B2. Classification matrix for DA of seasonal change.

From\to	Dry season	Wet season	Total	% correct
		Standard mode		
Dry season	33	1	34	97.14%
Wet season	2	32	34	93.94%
Total	**35**	**33**	**68**	**95.54%**
		Backward stepwise mode		
Dry season	31	3	34	91.43%
Wet season	2	32	34	93.94%
Total	**33**	**35**	**68**	**92.68%**
		Forward stepwise mode		
Dry season	31	3	34	91.43%
Wet season	2	32	34	93.94%
Total	**33**	**35**	**68**	**92.68%**

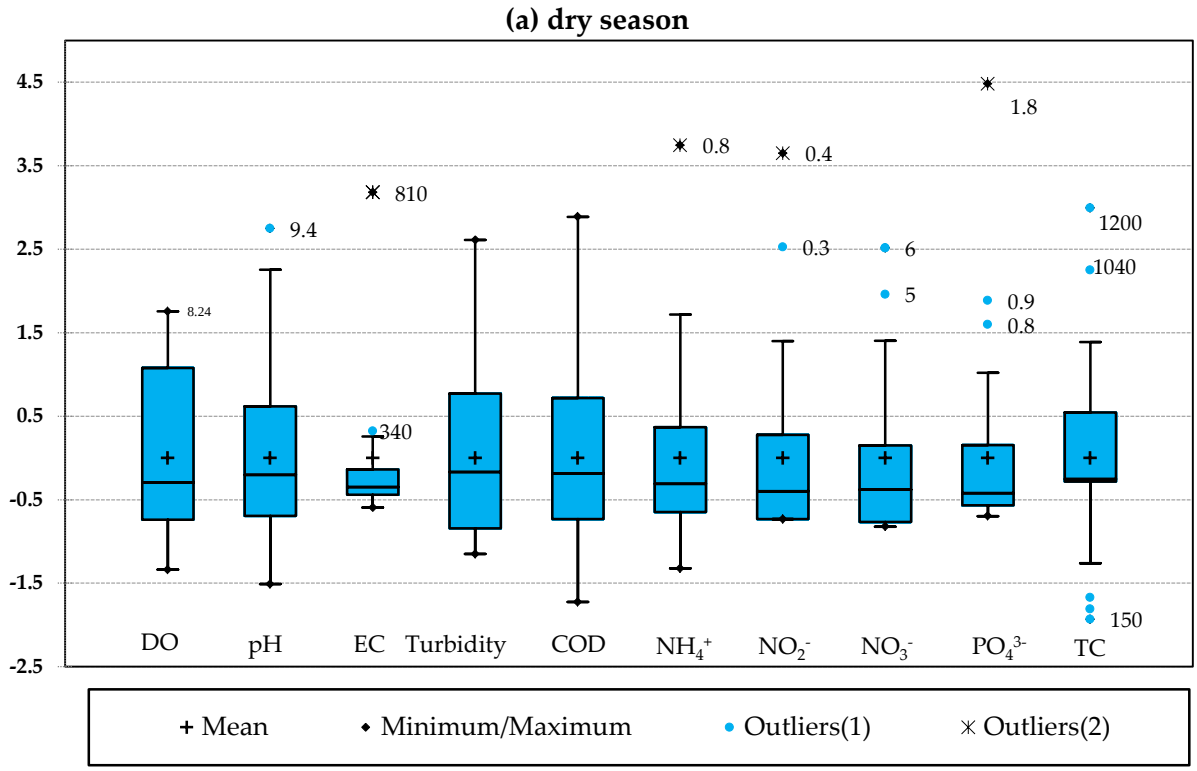

Figure B1. Box and whisker plot in 10 discriminant parameters in dry season.

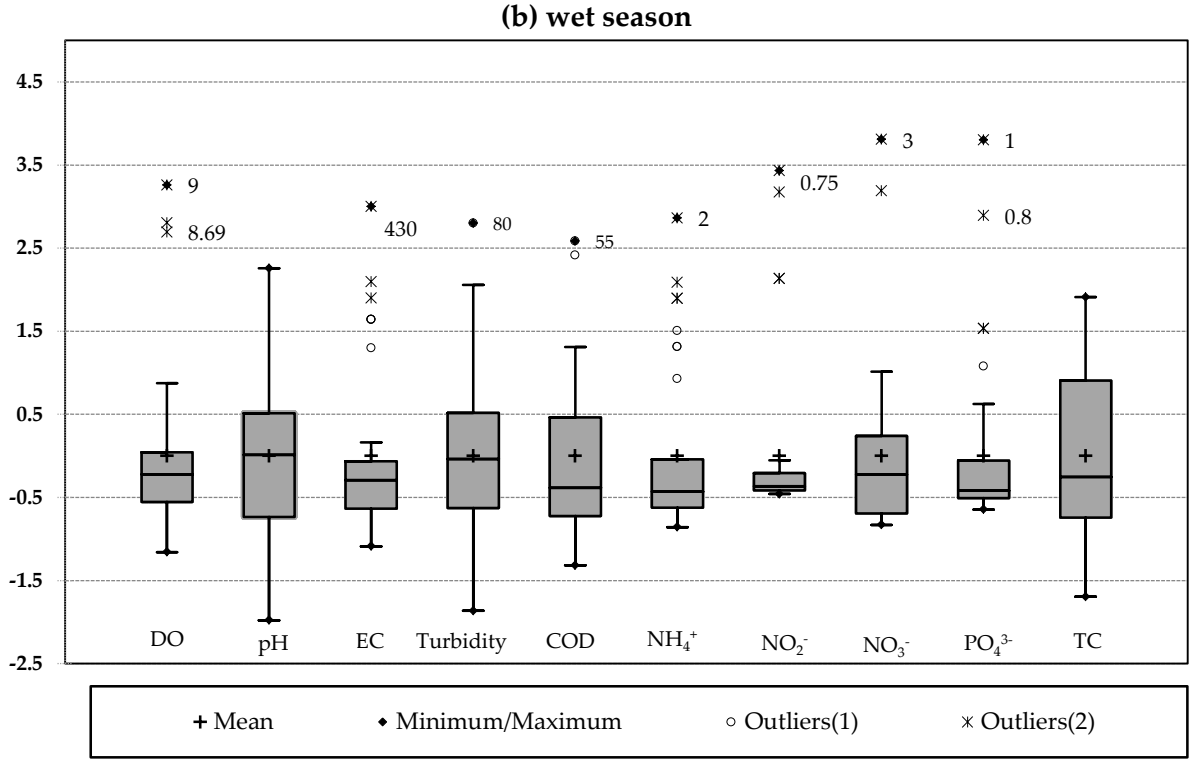

Figure B2. Box and whisker plot in 10 discriminant parameters in wet season.

Annexure C. Different spatial distribution of water quality between dry and wet seasons.

Figure C1. Different spatial distribution of water quality between dry and wet seasons.

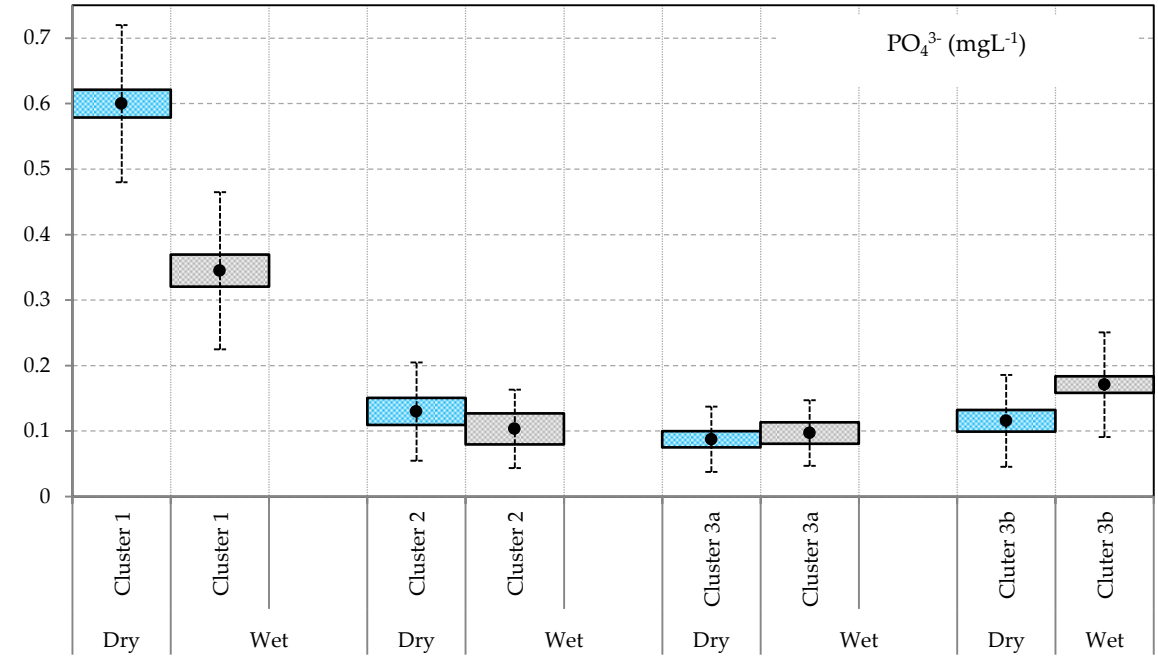

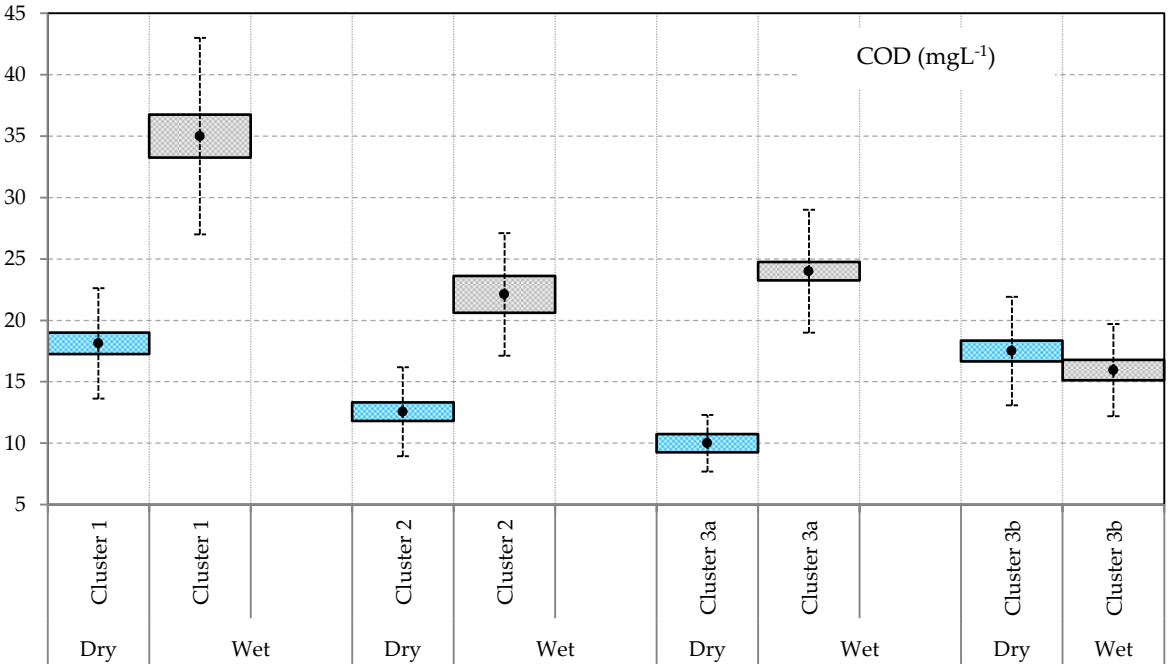

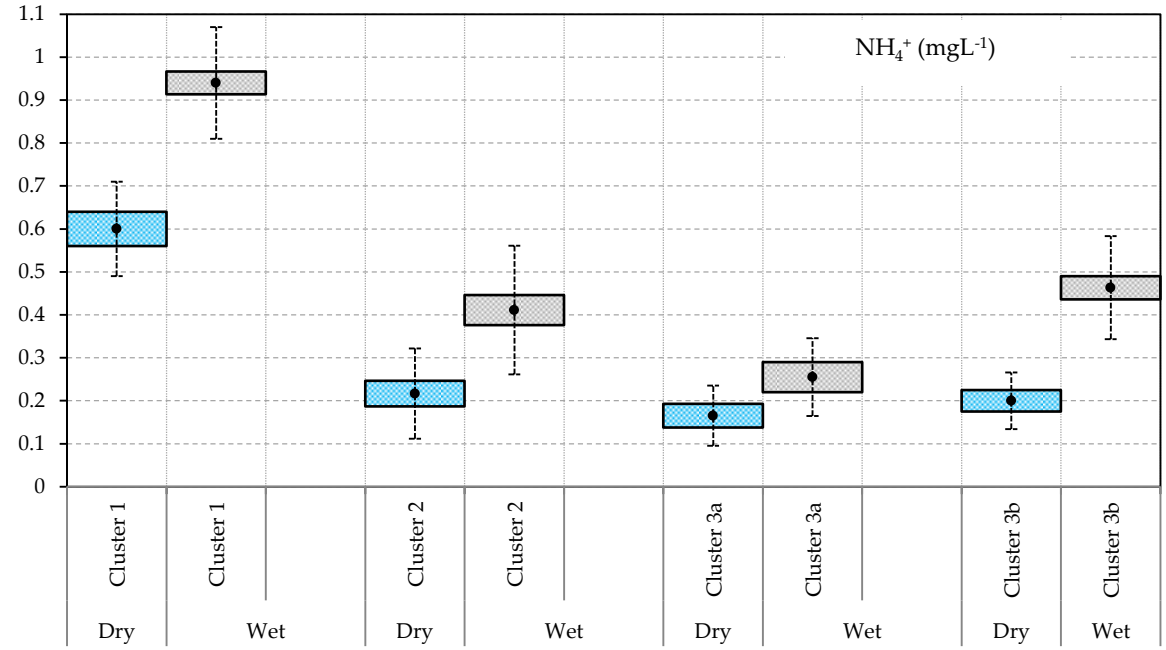
NH_4^+ (mgL^{-1})
1.1
1
0.9
0.8
0.7
0.6
0.5
0.4
0.3
0.2
0.1
0
Cluster 1
Cluster 1
Cluster 2
Cluster 2
Cluster 3a
Cluster 3a
Cluster 3b
Cluster 3b
Dry
Wet
Dry
Wet
Dry
Wet
Dry
Wet

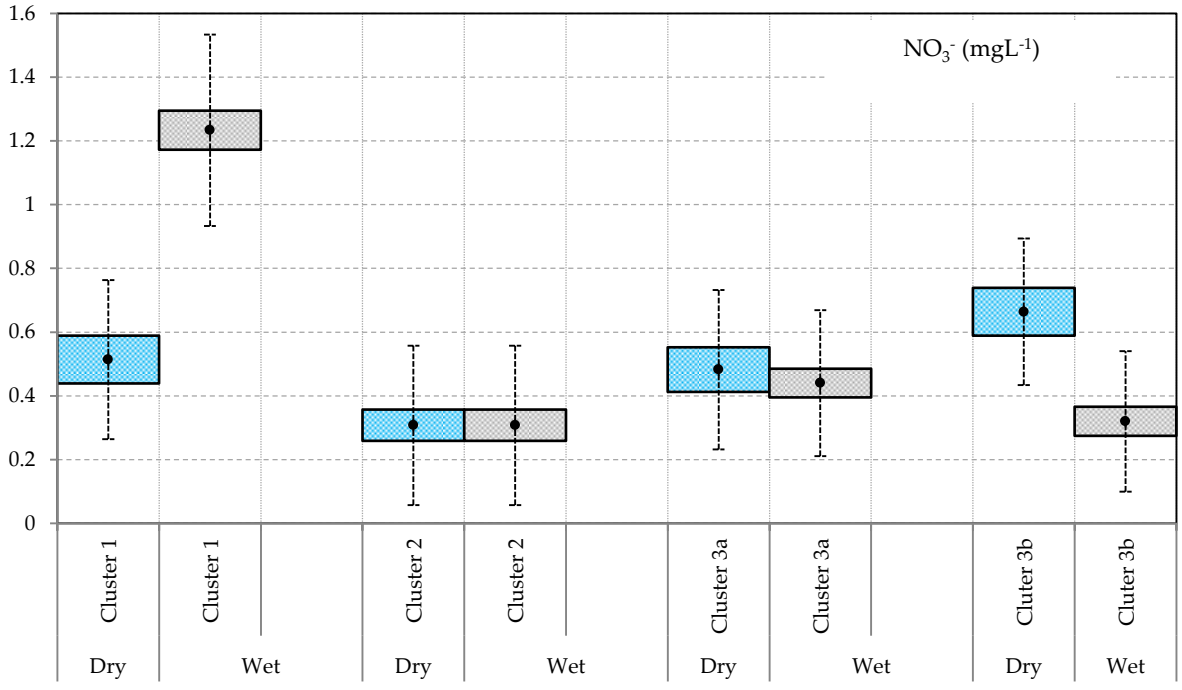
NO_3^- (mgL^{-1})
1.6
1.4
1.2
1
0.8
0.6
0.4
0.2
0
Cluster 1
Cluster 1
Cluster 2
Cluster 2
Cluster 3a
Cluster 3a
Cluter 3b
Cluter 3b
Dry
Wet
Dry
Wet
Dry
Wet
Dry
Wet

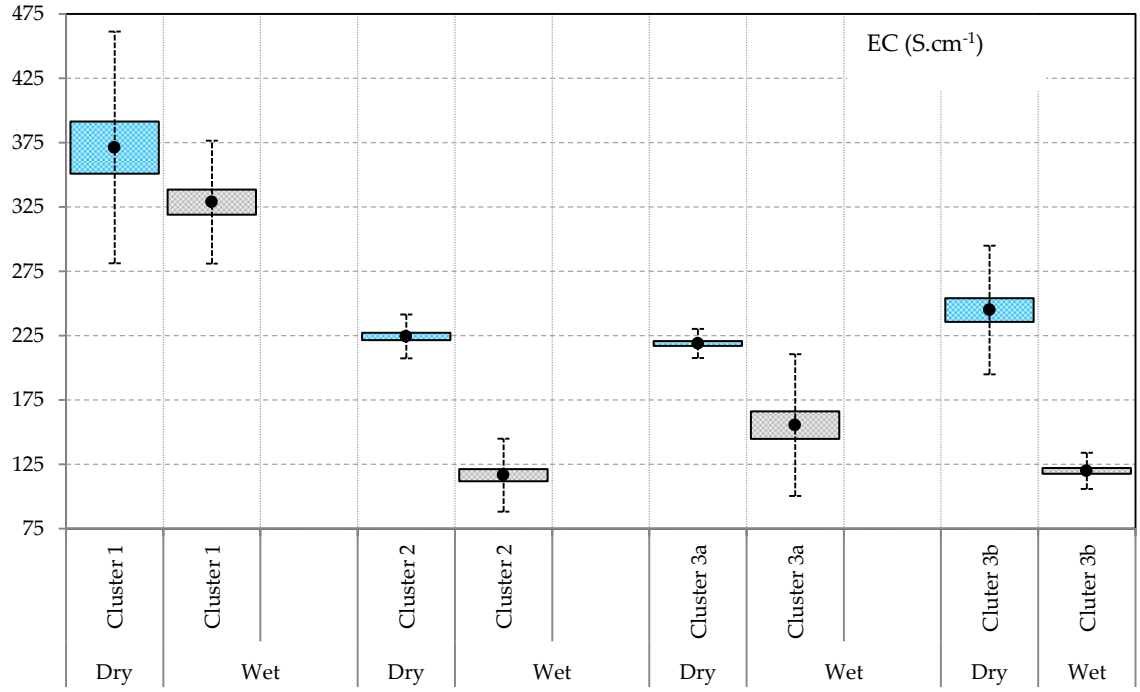
EC (S.cm-1)
475
425
375
325
275
225
175
125
75
Cluster 1
Cluster 1
Cluster 2
Cluster 2
Cluster 3a
Cluster 3a
Cluter 3b
Cluter 3b
Dry
Wet
Dry
Wet
Dry
Wet
Dry
Wet

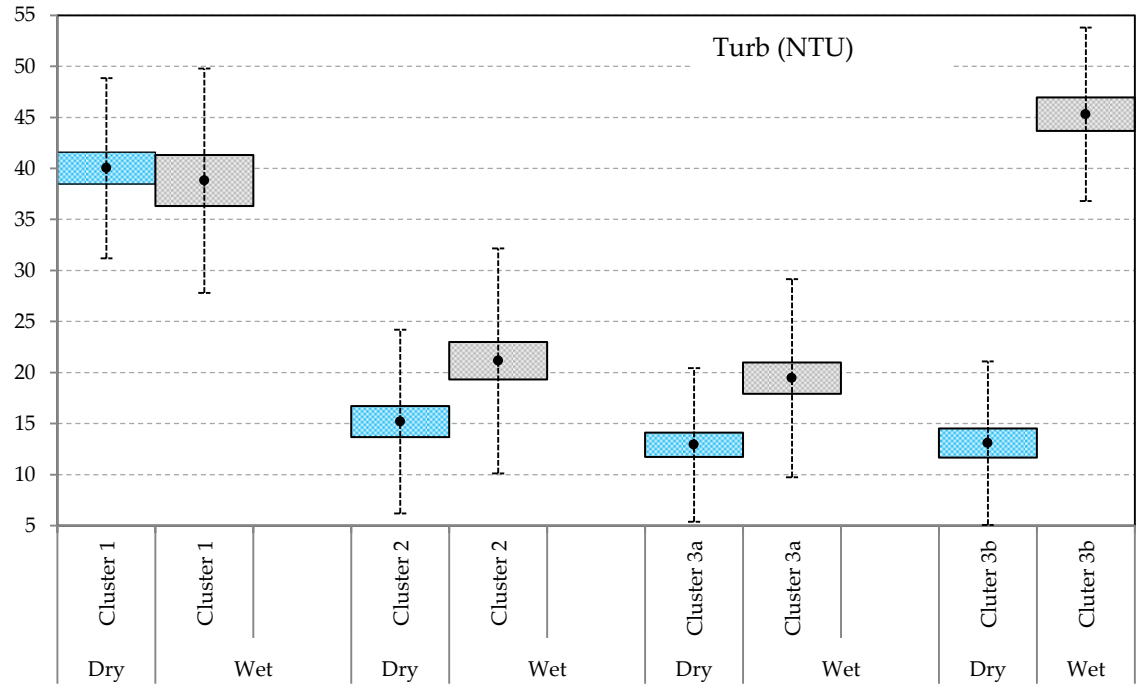
Turb (NTU)
55
50
45
40
35
30
25
20
15
10
5
Cluster 1
Cluster 1
Cluster 2
Cluster 2
Cluster 3a
Cluster 3a
Cluter 3b
Cluter 3b
Dry
Wet
Dry
Wet
Dry
Wet
Dry
Wet

Annexure D

Figure D1. Scree plot of the eigenvalues of principal components in Dry (a) and Wet (b) seasons.

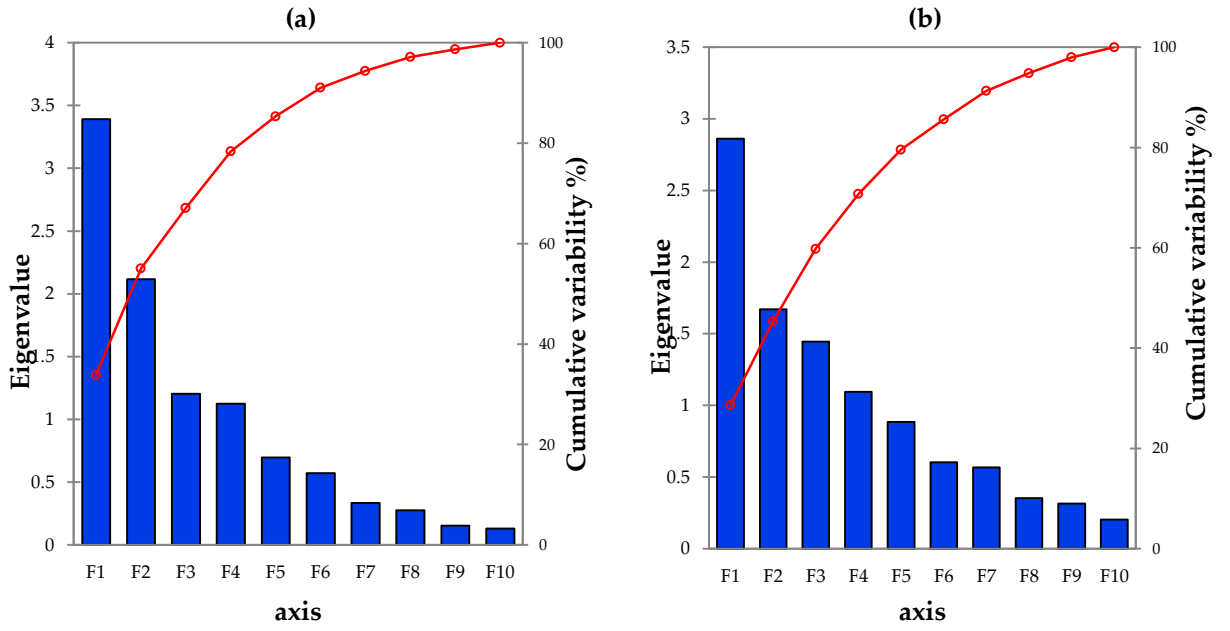

Table D1. Correlations between variables and factors for each season.

Parameters	**dry season**		**wet season**	
	F1	**F2**	**F1**	**F2**
DO	-0.191	0.184	-0.097	-0.336
pH	-0.746	0.415	-0.670	-0.046
EC	**0.907***	0.164	**0.907***	-0.278
Turb	**0.870***	0.091	-0.293	0.086
COD	0.534	0.339	0.691	-0.119
$NH_4^{(+)}$	0.642	0.290	0.695	-0.182
$NO_2^{(-)}$	-0.105	**0.915***	0.499	0.582
$NO_3^{(-)}$	-0.287	**0.884***	0.378	0.741
$PO_4^{(3-)}$	0.705	0.145	0.460	-0.635
TC	0.025	0.190	0.321	0.364

Note: * value is different from 0 at a significant level of 0.05.

Annexure E

Table E1. Min, Max, Mean and Standard Deviation of water quality parameters at three clusters in the dry season.

Variables	Cluster 1				Cluster 2				Cluster 3a				Cluster 3b			
	Min	Max	Mean	SD	Min	Max	Mean	SD	Min	Max	Mean	SD	Min	Max	Mean	SD
DO	4.98	7.83	5.93	0.93	5.11	7.96	6.67	1.06	4.98	7.55	5.66	0.78	5.66	8.24	7.38	0.78
pH	6.8	8	7.21	0.43	7.8	8.5	8.17	0.25	7.30	8.60	7.69	0.39	7.20	9.4	7.84	0.89
EC	220	810	486	270	190	250	224	18.10	200	330	228	37.06	200	320	245	48.70
Turbidity	30	56	40	9	3.75	30	14	9.63	3.64	46.72	14.38	12.13	3.34	28.31	13	8.66
COD	12	30	18	5.25	9	20	12.56	3.84	4.50	18	10.35	4.67	13	28	17.5	4.72
$NH_4^{(+)}$	0.2	0.8	0.43	0.18	0.1	0.5	0.22	0.11	0.05	0.30	0.17	0.09	0.1	0.3	0.2	0.07
$NO_2^{(-)}$	0.01	0.2	0.07	0.06	0.05	0.4	0.18	0.11	0.01	0.10	0.02	0.03	0.01	0.1	0.03	0.03
$NO_3^{(-)}$	0.01	1.5	0.58	0.65	1.5	6	4.17	1.41	0.01	1.5	0.36	0.53	0.00	2.00	0.66	0.75
$PO_4^{(3-)}$	0.2	1.8	0.7	0.51	0.02	0.4	0.13	0.13	0.01	0.80	0.14	0.24	0.02	0.30	0.13	0.10
TC	170	856	490	218	200	1040	573	233	144	856	587	195	300	1200	634	257

Table E2. Min, Max, Mean and Standard Deviation of water quality parameters at three clusters in the wet season.

Variables	Cluster 1				Cluster 2				Cluster 3a				Cluster 3b			
	Min	Max	Mean	SD	Min	Max	Mean	SD	Min	Max	Mean	SD	Min	Max	Mean	SD
DO	6.59	7.25	6.92	0.25	6.60	7.42	7.04	0.25	6.85	9.00	7.75	0.78	6.85	7.24	7.04	0.14
pH	7	7.60	7.37	0.22	7.50	8.70	7.94	0.38	7.20	8.00	7.60	0.27	7.60	8.60	8.06	0.28
EC	280	430	329	52.35	70	160	116.6	30	110	350	158	71.15	100	140	117.7	13.94
Turbidity	13.5	80	38.8	23.80	4.34	45.38	21.14	14.26	22.40	48.20	33.47	9.31	33.8	68	45.89	11.44
COD	20	55	39.67	13.37	9	40	22.11	11.91	13	35	26.20	7.51	11	20	15.17	3.28
$NH_4^{(+)}$	0.50	2	1.23	0.5	0.1	1.3	0.41	0.35	0.10	0.40	0.26	0.10	0.08	1.5	0.34	0.46
$NO_2^{(-)}$	0.01	0.75	0.32	0.31	0.00	0.05	0.02	0.02	0.01	0.05	0.02	0.01	0.01	0.70	0.09	0.23
$NO_3^{(-)}$	0.02	3	1.45	1.13	0.01	1	0.31	0.31	0.10	0.80	0.44	0.24	0.02	1	0.32	0.32
$PO_4^{(3-)}$	0.07	0.80	0.35	0.26	0.02	0.50	0.10	0.15	0.03	0.40	0.10	0.11	0.02	1	0.18	0.31
TC	320	740	567	173	430	850	702	143	250	520	391	76	150	480	319	116

Annexure F

Table F1. Statistical summary of physico-chemical parameters for groundwater samples in the dry season in An Giang, during 2009-2018.

Well	As		NO_3^-		pH		NH_4+		$CaCO_3$		Fe	
	Ave ± SD	Range	Ave ± SD	Range	Ave ± SD	Range	Ave ± SD	Range	Ave ± SD	Range	Ave ± SD	Range
G1	0.06±0.09	0-0.25	0.43±1.01	0-3.3	7±0.51	6.6-8.4	2.01±2.63	0-8.37	671±316	83-975	1.53±3.04	0-9.73
G2	0.01±0.02	0-0.05	0.1±0.11	0-0.25	6.9±0.5	6.3-8.3	2.09±1.96	0-4.80	279±352	132-1,265	0.34±0.44	0-1.42
G3	0.02±0.02	0-0.05	0.38±0.52	0-1.45	7.1±0.54	6.4-8.2	3.17±2.7	0-6.28	958±823	15-1788	0.19±0.31	0-0.91
G4	0.01±0.02	0-0.05	0.45±0.79	0-2.5	6.7±0.28	6.3-7.1	2.65±2.53	0-7	851±460	173-1,485	0.55±0.49	0-1.24
G5	0.01±0.01	0-0.03	0.09±0.19	0-0.62	7±0.47	6.3-7.8	0.86±0.67	0-2.13	648±309	166-1,063	0.28±0.50	0-1.58
G6	0.01±0.01	0-0.02	0.08±0.17	0-0.56	7.1±0.34	6.5-7.6	0.75±0.63	0-1.8	284±277	14-820	1.37±2.62	0-8.31
G7	0.02±0.01	0-0.03	3.96±5.44	0-14.1	7.2±0.25	6.5-7.5	0.43±0.57	0-1.5	424±201	172-722	0.09±0.14	0-0.44
G8	0.01±0.01	0-0.02	0.67±1.17	0-3.47	7±0.32	6.4-7.3	1.72±1.67	0-4.43	234±66	146-320	0.31±0.38	0-0.94

Table F2. Statistical summary of physico-chemical parameters for groundwater samples in the wet season in An Giang, during 2009-2018.

Well	As		NO_3^-		pH		NH4+		$CaCO_3$		Fe	
	Ave ± SD	Range	Ave ± SD	Range	Ave ± SD	Range	Ave ± SD	Range	Ave ± SD	Range	Ave ± SD	Range
G1	0.26±0.82	0-2.6	0.3±0.38	0-1.08	6.9±0.2	6.5-7.2	0.70±0.88	0-2.86	788±216	426-1,056	0.22±0.41	0-1.4
G2	0.54±1.67	0-5.29	0.16±0.31	0-1.06	6.9±0.3	6.1-7.3	2.39±2.66	0-7.08	365±417	152-1,504	0.14±0.14	0-0.4
G3	0.01±0.01	0-0.02	0.19±0.26	0-0.81	6.6±0.2	6.2-6.9	1.71±2.22	0-5.25	1,763±1,116	171-3,966	0.16±0.13	0-0.34
G4	0.84±2.6	0-8.35	0.28±0.43	0-1.29	6.5±0.3	6.1-6.9	2.83±3.01	0-10	1,496±1,685	129-5,996	0.52±0.58	0-1.48
G5	0.55±1.72	0-5.44	0.03±0.04	0-0.11	6.7±0.4	6.1-7.3	0.64±0.95	0-2.7	651±308	83-918	0.62±0.94	0-2.41
G6	0.002±0.003	0-0.01	0.08±0.14	0-0.46	6.79±0.3	6.2-7.2	0.23±0.24	0-0.7	366±280	66-808	1.17±2.26	0-7.31
G7	0.006±0.008	0-0.02	10±14.78	0-38.5	6.9±0.2	6.6-7.4	1.15±1.93	0-4.7	521±294	208-1,228	0.42±0.995	0-3.23
G8	0.005±0.005	0-0.01	1.04±2.14	0-6.26	6.8±0.3	6.5-7.2	0.66±0.88	0-2.32	270±193	116-730	2.28±4.99	0-14.6

Table F3. Annual Groundwater classification based on WQI in the dry season.

	2009	**2010**	**2011**	**2012**	**2013**	**2014**	**2015**	**2016**	**2017**	**2018**
G_1	Very bad	Very bad	Unsuitable for drinking	Good	Good	Good	Good	Excellent	Excellent	Very bad
G2	Good	Excellent	Very bad	Good	Good	Good	Excellent	Excellent	Good	Good
G3	Bad	Excellent	Excellent	Bad	Bad	Bad	Excellent	Bad	N/A	N/A
G4	Unsuitable for drinking	Bad	Excellent	Unsuitable for drinking	Unsuitable for drinking	Bad	Excellent	Bad	Good	Bad
G5	Good	Excellent	Good	Excellent	Good	Good	Excellent	Excellent	Good	Good
G6	Excellent	Excellent	Excellent	Good	Excellent	Excellent	Excellent	Excellent	Good	Excellent
G7	Good	Excellent	Bad	Very bad	Excellent	Excellent	Excellent	Excellent	Excellent	Excellent
G8	Excellent	Excellent	Good	Good	Excellent	Excellent	Good	Excellent	N/A	N/A

TableF4. Annual Groundwater classification based on WQI in the wet season.

	2009	2010	2011	2012	2013	2014	2015	2016	2017	2018
G1	Excellent	Unsuitable for drinking	Good	Good	Good	Good	Good	Excellent	Excellent	Good
G2	Good	Good	Bad	Good	Bad	Excellent	Excellent	Unsuitable for drinking	Good	Good
G3	Bad	Good	Very bad	Bad	Bad	Good	Excellent	Excellent	N/A	N/A
G4	Unsuitable for drinking	Bad	Unsuitable for drinking	Unsuitable for drinking	Unsuitable for drinking	Very bad	Good	Excellent	Good	Good
G5	Excellent	Good	Unsuitable for drinking	Very bad	Excellent	Excellent	Excellent	Unsuitable for drinking	Excellent	Excellent
G6	Excellent	Excellent	Excellent	Good	Excellent	Excellent	Excellent	Excellent	Excellent	Excellent
G7	Very bad	Good	Bad	Good	Bad	Excellent	Excellent	Excellent	Excellent	Excellent
G8	Bad	Excellent	Excellent	Good	Excellent	Excellent	Excellent	Excellent	N/A	N/A

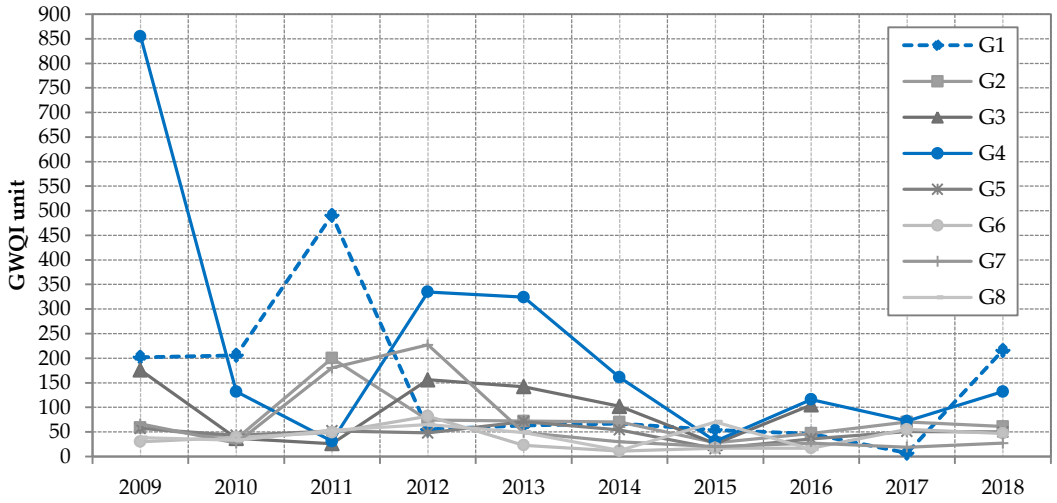

Figure F5. Annual Groundwater quality index (WQI) in the wet season in An Giang.

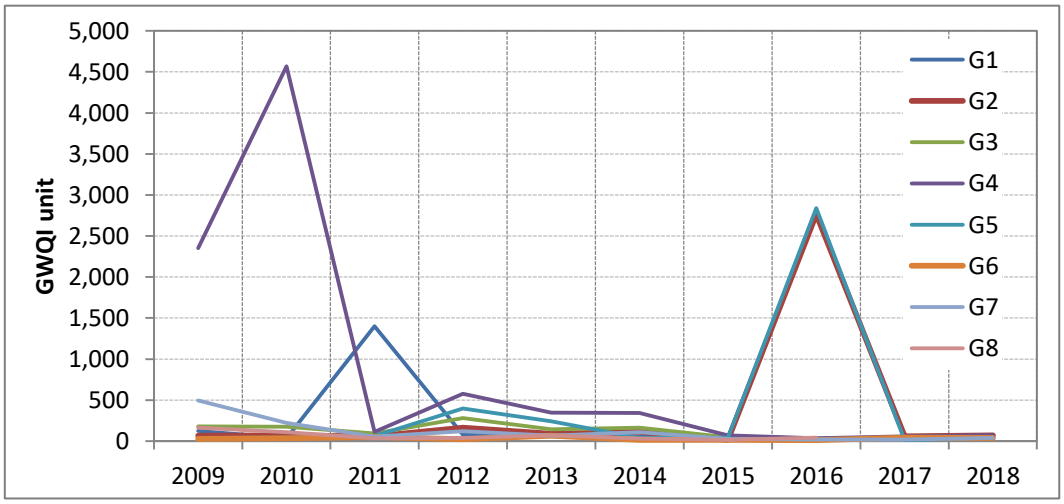

Figure F6. Annual Groundwater quality index (WQI) in the wet season in An Giang.

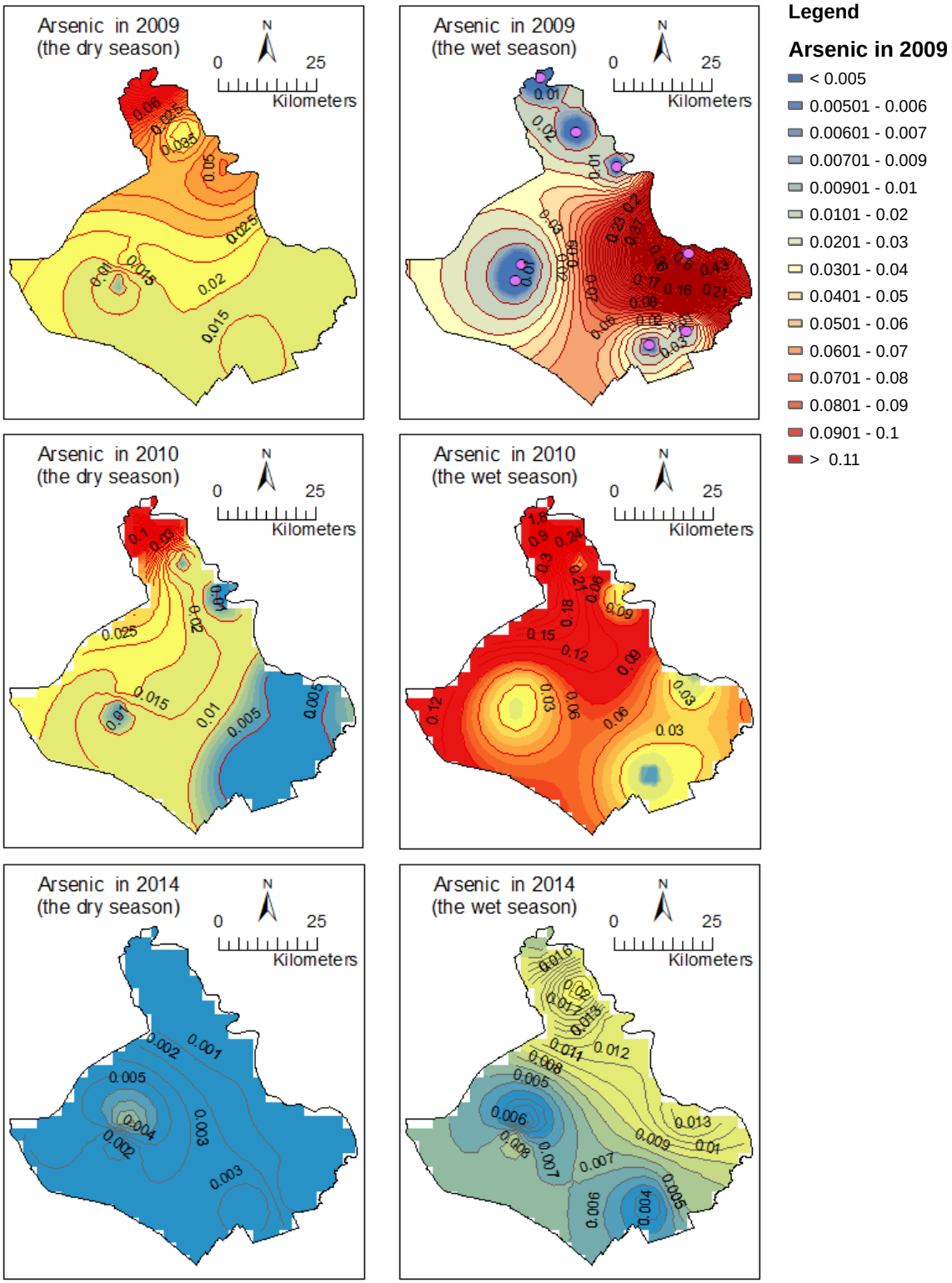

Figure F7. Concentrations of As (mg/L) were displayed by IDW in An Giang province.